STRESS CONCENTRATION FACTORS FOR CIRCULAR, REINFORCED PENETRATIONS IN PRESSURIZED CYLINDRICAL SHELLS

A Dissertation

Presented to

the Faculty of the School of Engineering and Applied Science

University of Virginia

In Partial Fulfillment

of the Requirements for the Degree

Doctor of Philosophy (Civil Engineering)

By

James W. Ramsey, Jr.

May 1975

(NASA-TM-X-68733) STRESS CONCENTRATION FACTORS FOR CIRCULAR, REINFORCED PENETRATIONS IN PRESSURIZED CYLINDRICAL SHELLS Ph.D. Thesis - Virginia Univ. (NASA) 205 p HC $7.25 CSCL 20K G3/39

N75-22813

Unclas

21172

204

APPROVAL SHEET

This dissertation is submitted in partial fulfillment of the requirements for the degree of Doctor of Philosophy (Civil Engineering)

James W. Ramsey, Jr.
Author

Approved:

Faculty Advisor

Dean, School of Engineering and Applied Science

May 1975

ACKNOWLEDGMENTS

The author wishes to gratefully acknowledge the following in making this dissertation possible:

The National Aeronautics and Space Administration for sponsoring this research;

Professor Furman W. Barton of the University of Virginia for his patience, encouragement, and constructive criticism throughout the preparation of this paper and my total Ph.D. program;

Dr. Ross L. Goble, Chief of Research Facilities Engineering Division, for his motivational push, moral support, and constructive criticism;

My management and fellow workers, especially Mr. John E. Doyle, for the opportunity to work and encouragement to finish;

Mr. Carl E. Gray, Jr. for helpful discussions, computer programming and figure preparation; Mr. Peter F. Jacobs, for programming; Mr. John T. Taylor for constructive ctiticism; and Miss Mary Morgan Cox and Mrs. Theresa C. Walker for help in preparing this manuscript.

And last, but certainly not least, the author also wishes to thank his wife, Jane, for her total encouragement and support before and during the course of the research and Jennifer, Todd, and Leslie - who make it all worthwhile.

ABSTRACT

The effect on stresses in a cylindrical shell with a circular penetration subject to internal pressure has been investigated. The research is limited to thin, shallow, linearly elastic cylindrical shells; however, some comparisons are made to thick shell experimental measurements. Results provide numerical predictions of peak stress concentration factors around nonreinforced and reinforced penetrations in pressurized cylindrical shells. Analytical results are correlated with published formulas, as well as theoretical and experimental results. An accuracy study is made of the finite element program for each of the configurations considered important in pressure vessel technology.

A formula is developed to predict the peak stress concentration factor (SCF) for analysis and/or design in conjunction with the ASME Boiler and Pressure Vessel Code, Section VIII, Divisions 1 and 2. The formula is rationally derived to include all of the parameters that are required to define the various penetration configurations used in pressure vessel analysis, design, and construction. The accuracy of the empirical formula is determined by comparing to numerical, theoretical, and experimental data. In most cases, it is shown that the ASME Pressure Vessel Code SCF of 3.3 is extremely conservative.

TABLE OF CONTENTS

LIST OF TABLES

TABLE PAGE

TABLE PAGE

LIST OF FIGURES

FIGURE PAGE

LIST OF SYMBOLS

A_j	multipoint constraint coefficient
A_{hole}, A_{pad}, $A_{reinf.}$	cross sectional areas
D	$ET^3/12\ (1 - \nu^2)$
E	modulus of elasticity
F	force vector
j	degree of freedom
K	stiffness matrix
M_y, M_{xy}, M_x	moments in plate element
P, p	pressure
R	cylindrical shell mid radius
t, t_p, T, TH	pipe, pad, shell, and shell or pipe thicknesses
u	system displacement vector
V_x, V_y	shears in plate element
w	radial shell deflection
X, Y, Z	rectangular coordinates
Z	longitudinal cylindrical coordinate
α	transformation matrix
β^4	$3(1 - \nu^2)/(16)R^2T^2$
β_1^4	$3(1 - \nu_p^2)/(16)R^2T^2$
Δ	deflection

δ	element displacement vector
λ	coefficient in force formula
ν_1, ν_p	Poisson's ratio of shell and pipe
ϕ	rotation angle to locate grid point
ρ	distance to locate grid point
ρ_a	hole radius
ρ_o	pipe mid radius
ρ_p	pad outside radius
σ_m	membrane stress
σ_x, σ_y, τ_{xy}	stresses in plate element
θ	rotational cylindrical coordinate
Σ	summation symbol

CHAPTER I

INTRODUCTION

1.1 Statement of the Problem

In a cylindrical shell weakened by a hole, the stress distribution caused by an internal pressure load applied to the shell will differ considerably from that in an unweakened shell. The maximum stress will be much larger if there is a circular hole in the shell than in the case where there is no penetration. This conjecture is suggested immediately by the case of a flat plate weakened by a hole with the plate stretched per unit length in one direction and with one-half of this stretch per unit length in the other direction. The maximum stress is 2.5 times the maximum stress in the solid plate. This factor (2.5) is known as the stress concentration factor (SCF). There is no reason to expect that the SCF is 2.5 for the shell. It depends on the geometry of the shell and the penetration: the curvature parameter of the shell, $\frac{\rho_a^2}{RT}$ (ρ_a being the radius of the hole, which is a circle in the projected shell surface, R is the radius of the middle surface of the cylinder, and T, the shell wall thickness); the ratio of the diameter of the hole or pipe to the radius of the shell; and the ratio of the thickness of the pipe to that of the shell.(1) The most important feature of the stress state in the shell near the hole is that bending stresses occur, whereas in the unweakened shell only membrane stresses ($\frac{PR}{T}$ and $\frac{PR}{2T}$) are present.

The loaded hole boundary condition in a pressurized cylindrical shell with a membrane or diaphragm over the hole to contain pressure only has been investigated by many authors.[1,2,3,4,5,6] Another type of loaded hole boundary is the perpendicular intersection of two cylinders - shell and pipe. There are a few isolated numerical solutions [7,8,9,10] and some theoretical investigations.[1,2,11,12] There are many experimental results for both thin and thick shells containing nonreinforced penetrations (pipe only) [13 through 21] and very few for reinforced penetrations - pipe and pad [14,15,17,22,24] and pipe and pads.[23,24]

Also, the ASME Pressure Vessel Code[25] requires in a stress or fatigue analysis the stress concentration factor (SCF) to be not less than 3.3 for a "<u>well designed penetration</u>" in a cylindrical shell unless positive evidence is available to the contrary. This evidence usually means a separate analysis to confirm the peak SCF. This factor is primarily needed to obtain peak stresses to perform a fatigue analysis to predict the remaining life at a penetration in the shell or to assure that the peak stress around a penetration does not exceed allowable stresses. The need for a more refined and/or a more clearly defined stress concentration factor became apparent in validating the useful life of 91 penetrations in a cylindrical shell[38] located in a work/residential area of NASA - Langley Research Center. These penetrations in the shell range in size from 1-inch to 60-inches in diameter. There are a few formulas in the published literature[2,4,26,27] for a membrane over the hole or a very thin penetration (pipe), but none are applicable for reinforced penetrations in pressurized cylindrical shells.

The author and others were unsuccessful in obtaining any computer answers to an analytical finite element approach to the actual intersection curve of the shell, pipe, and pads boundaries. The compatibility equations for this actual curve, rather than a projected circular curve (uncovered during this study), were not acceptable to the computer program. Also, different coordinate systems for the shell and pipe input descriptions, solution vectors, and output notations were unsuccessful. Therefore, it was decided to abandon the analytical work and to magnetic particle examine and/or rework these penetrations rather than perform the analyses to obtain the refined stress concentration factors. This type of verification (field work in lieu of analysis) is not practical in all cases since this shell which contains 91 penetrations is one of 1,600 pressure vessels (6000 pressure components) for which the structural integrity must be verified or validated in a five-year program at NASA - Langley Research Center. Thus, there is a need for a positive and clear definition of a well designed penetration to allow use of the 3.3 SCF or to obtain the appropriate SCF. A "proven" formula to approximate the peak SCF and/or a finite element program to obtain a refined SCF would be invaluable in validating shells, pipes and/or pad(s) configurations.

1.2 Object and Scope

The objective of this study is to determine the effect on stresses in a cylindrical shell with a circular penetration subject to internal pressure. The research is limited to thin, shallow, linearly elastic cylindrical shells; however, some comparisons are made to thick shell experimental measurements. Results from this study provide numerical predictions of the peak stresses around nonreinforced and reinforced penetrations in cylindrical shells. Analytical results are correlated with published formulas, theoretical and experimental results.

The present research also investigates the convergence and accuracy of different finite elements and mesh sizes. Finally, an approximate formula is developed to predict the peak stress concentration factor for analysis and/or design in conjunction with the ASME Boiler and Pressure Vessel Code, Section VIII, Division 1 and 2.[25] The formula is rationally derived to include all of the parameters that are required to define the penetrations used in pressure vessel technology. The accuracy of the empirical formula is determined by comparing to numerical, theoretical, and experimental data. Since limited data is available for reinforced penetrations, many different configurations are pursued to supplement the published data to provide the restrictions to the formula. These configurations are modeled utilizing finite elements where compatibility between the cylindrical shell and the pipe/pad(s) are introduced through enforced constraint equations. The configurations investigated are for force and/or pipe around both nonreinforced and reinforced circular penetrations in cylindrical shells subject to internal pressure. For the force case, the penetration is considered to be covered by a diaphragm or membrane that allows the hole edge to deflect and rotate. It also transmits the pressure force to the shell in the form of a uniform transverse shear stress at the hole edge. An automation computer program which punches cards for these configurations for input to a finite element computer program (NASA STRUCTURAL ANALYSIS PROGRAM - NASTRAN[28]) is utilized.

CHAPTER II

ANALYSIS

2.1 Matrix Analysis by Finite Element Methods

In the finite element method, it is necessary to obtain a characterization of the stiffness properties of each element in the structure and to relate end nodal displacements to the corresponding forces. This is expressed in the following form:

$$[K]\{u\} = \{F\} \tag{1}$$

where: $[K]$ is the stiffness matrix

$\{u\}$ is the displacement vector

$\{F\}$ is the force vector

The process for generating a computer program of any structure that is composed of many finite elements is to first pick a set of local coordinates convenient for a typical element. The generalized element displacements are $\{\delta\}$ and forces are $\{F\}$. The displacements $\{\delta\}$ and stiffness matrix $[K]$ are partitioned corresponding to ends i and j:

$$\begin{bmatrix} K_{ii} & K_{ij} \\ K_{ji} & K_{jj} \end{bmatrix} \begin{Bmatrix} \delta_i \\ \delta_j \end{Bmatrix} = \begin{Bmatrix} F_i \\ F_j \end{Bmatrix} \tag{2}$$

In the process of connecting elements, it is found that one element's local coordinates are not the same as those for another element. Therefore, a set of system coordinates is chosen that is convenient for a system of elements and the local coordinate points are numbered (points 1, 2, 3, ...).

A systematic numbering process for the node points and members is chosen. The stiffness K_{ij} for each element is calculated in local coordinates where i and j refer to the end points of each element.

If the system coordinates or displacements are called $\{u\}$, the transformation from an element's coordinates to a system's coordinates is accomplished by a transformation matrix, $[\alpha]$. That is:

$$\{\delta\} = [\alpha]\ \{u\} \tag{3}$$

The stiffness of the element is transformed to system coordinates by use of Equations (3), (2), and (1).

$$[\bar{K}] = [\alpha]^T\ [K]\ \ [\alpha] \tag{4}$$

Consider several elements that are connected. The next step is to generate the master stiffness matrix $[K_{ij}]_M$ by summing all member stiffnesses in system coordinates.[29]

The compatibility equations for required coordinate points are introduced through multipoint constraint (MPC) equations of the form:

$$\Sigma A_j u_j = 0 \tag{5}$$

where: A is the coefficient

u is the point

j is the degree of freedom

Thus, the stiffness matrix, force, and displacement vectors are modified by this degree of freedom link for each MPC Equation (5) at each grid point.[30]

After the compatibility equations are satisfied, the boundary conditions (displacements of the structure) are enforced through single-point constraints (SPC). Finally, the system applied external forces $\{F\}$ are identified and the equation:

$$[K]_R \{u\}_R = \{F\}_R \tag{6}$$

is solved.

2.2 Formulation of the Problem

Consider a flat rectangular plate of thickness T containing a circular hole of radius ρ_a with its edges parallel to axes Y', Z' of the circular hole. A material point or finite element grid point within the plate may be located through cylindrical coordinates (ρ, ϕ, X) defined through

$$Y' = \rho \sin \phi, \ Z' = \rho \cos \phi \tag{7}$$

Suppose that the plane Y' Z' is now rolled into a circular cylindrical shell in such a way that the Z'-axis becomes a generator of the cylinder and Y' a circular arc denoted by Y (see Figure 2.2.1). If R is the radius of the middle surface of the shell and θ the angle in any normal cross section of the cylinder measured from the Y=0 plane in the positive direction of the Y-axis, then the following relationships are obtained to define the finite elements and grid points (see Figure 2.2.2):

$$\begin{aligned} Y' &= Y = R\theta \\ R &= R \\ \theta &= \text{Arc sin } \left(\frac{\rho \sin \phi}{R} \right) \\ Z' &= Z = \rho \cos \phi \end{aligned} \tag{8}$$

Consider that this same configuration - main (lower) shell (shown in Figure 2.2.1) with mid-surface radius R - is intersected by a branch (upper) shell with mid-surface radius ρ_o and thickness t, ($\rho_o = \rho_a + t/2$), see Figure 2.2.3. The axis of the branch shell is normal to the axis of the main shell. Both shells are considered to be infinite in length and capped at their ends. Finally, consider that these two circular cylindrical

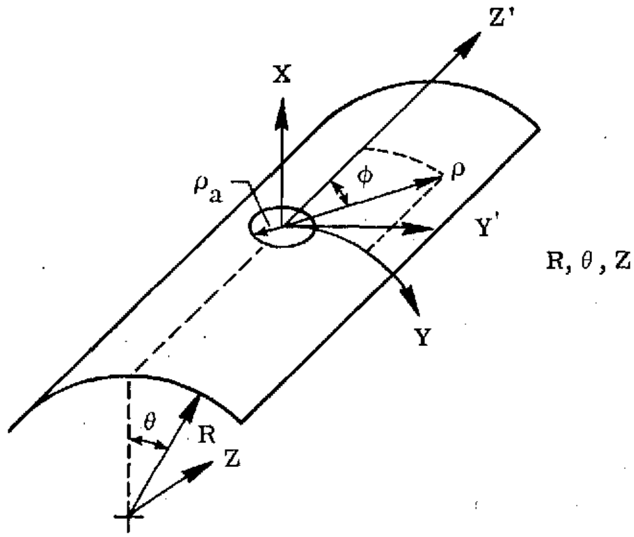

Figure 2.2.1.- Coordinate system for a cylindrical shell with hole.

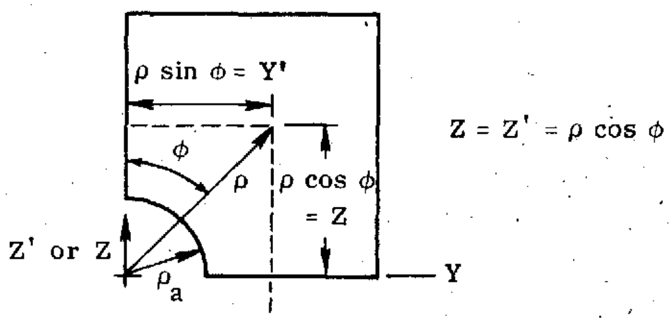

(a) Plan view

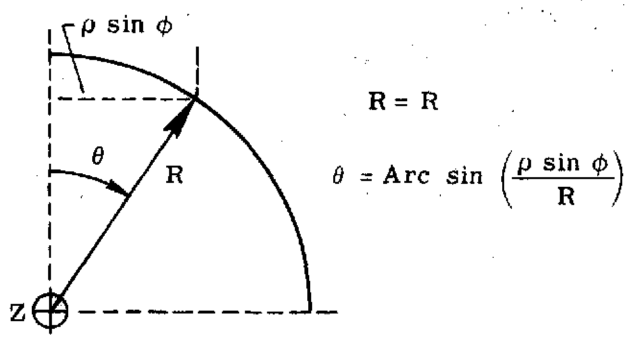

(b) Elevation view

Figure 2.2.2.- Relationships used to define finite elements.

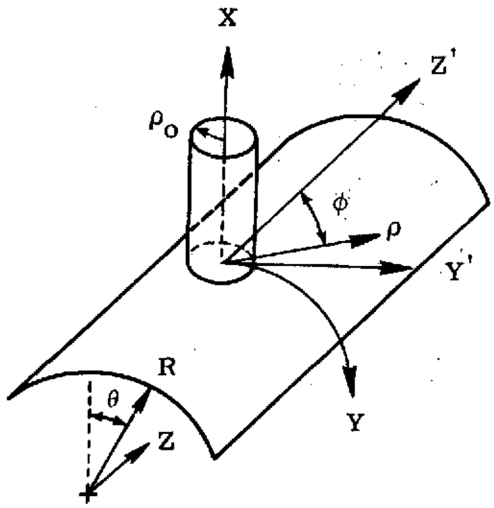

Figure 2.2.3.- Intersecting circular cylinders (pipe and shell).

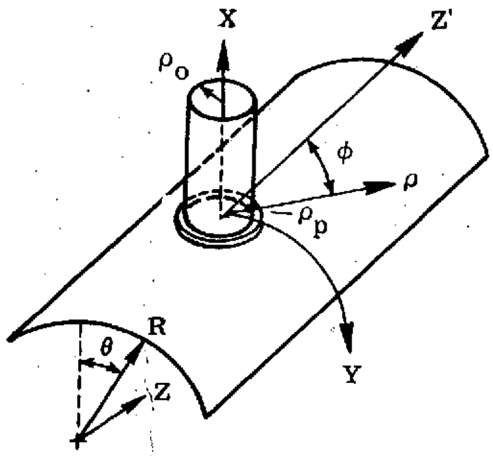

Figure 2.2.4.- Intersecting circular cylinders with reinforcing pad(s).

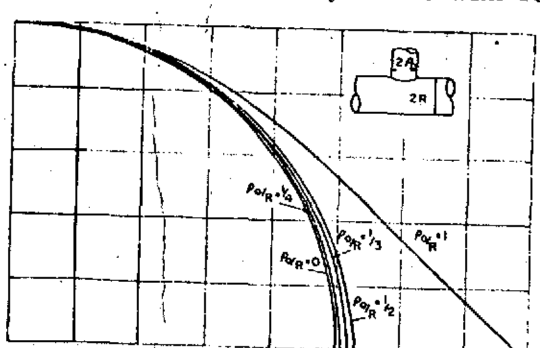

Figure 2.3.1.- Intersection curve of small cylinder with large cylinder when rolled out flat for various values of ρ_o/R.

shells with mid-surface radii ρ_o and R are complicated by the addition of one or two reinforcing pads with outside radius ρ_p and thickness t_p (see Figure 2.2.4). The location of the finite elements through grid points for a projected circular hole in a cylindrical shell with a pipe and pad(s) is governed by Equations (8).

2.3 Introduction of Compatibility Equations

The solution of these problems requires the matching of certain physical quantities (compatibility equations) along the intersection curve of the two shells and pad(s). When expressed in the cylindrical coordinate system, the intersection curve is of a very complex nature. Due to the difficulty of solving boundary value problems in which the boundaries are not situated on constant coordinate curves, the intersection curve can be approximated by ρ_a, ρ_o, and ρ_p equal to some constants, whenever ρ_o/R is small. Figure 2.3.1, indicates the error involved in this approximation when the lower shell surface is developed onto a plane.[11] It can be seen that the actual intersection curve does not differ appreciably from a circle, providing

$$\frac{\rho_o}{R} \leq 1/2 \quad . \tag{9}$$

Therefore, the actual hole boundary is assumed to be circular, identical to that of a projected view of the penetration.

The compatibility equations for a pipe and shell configuration (Figure 2.2.3) are introduced through MPC Equations (5). The six equations for each grid point for both the shell and the pipe at the pipe and shell juncture at ρ_o are as follows (Δ is deflection and θ is rotation):

$$
\begin{aligned}
&\Delta_R^{pipe} - \Delta_R^{shell} = 0 \\
&\Delta_\theta^{pipe} - \Delta_\theta^{shell} - \frac{T}{2}\,\theta_Z^{shell} = 0 \\
&\Delta_Z^{pipe} - \Delta_Z^{shell} - \frac{T}{2}\,(-\theta_\theta^{shell}) = 0 \\
&\theta_R^{pipe} - \theta_R^{shell} = 0 \\
&\theta_\theta^{pipe} - \theta_\theta^{shell} = 0 \\
&\theta_Z^{pipe} - \theta_Z^{shell} = 0
\end{aligned}
\qquad (10)
$$

where the subscript is the degree of freedom of the grid point. For the finite element analysis, the independent degrees of freedom are those for the shell, and the dependent degrees of freedom are those for the pipe. The superscript in Equations (10) denotes whether the degree of freedom represents the pipe or shell.

The compatibility equations for a "pipe-shell-inner pad" configuration (Figure 2.2.4) are as follows:

1. Pipe-to-shell juncture (ρ_o): Equations (10)
2. Inner pad (ip) to shell junctures for each grid point at both ρ_a and ρ_p:

$$
\begin{aligned}
&\Delta_R^{ip} - \Delta_R^{shell} = 0 \\
&\Delta_\theta^{ip} - \Delta_\theta^{shell} - \frac{(T+t_{ip})}{2} (-\theta_Z^{shell}) = 0 \\
&\Delta_Z^{ip} - \Delta_Z^{shell} - \frac{(T+t_{ip})}{2} \theta_\theta^{shell} = 0 \\
&\theta_R^{ip} - \theta_R^{shell} = 0 \\
&\theta_\theta^{ip} - \theta_\theta^{shell} = 0 \\
&\theta_Z^{ip} - \theta_Z^{shell} = 0
\end{aligned}
\tag{11}
$$

The compatibility equations for a "pipe-shell-outer pad(op)" configuration for each grid point at locations ρ_o for the pipe and ρ_a and ρ_p for outer pad are as follows:

$$
\begin{aligned}
&\Delta_R^{pipe} - \Delta_R^{shell} = 0 \\
&\Delta_\theta^{pipe} - \Delta_\theta^{shell} - (\tfrac{T}{2} + t_{op}) \theta_Z^{shell} = 0 \\
&\Delta_Z^{pipe} - \Delta_Z^{shell} + (\tfrac{T}{2} + t_{op}) \theta_\theta^{shell} = 0
\end{aligned}
\tag{12a}
$$

$$\theta_R^{pipe} - \theta_R^{shell} = 0$$

$$\theta_\theta^{pipe} - \theta_\theta^{shell} = 0 \qquad (12a)$$

$$\theta_Z^{pipe} - \theta_Z^{shell} = 0$$

$$\Delta_R^{op} - \Delta_R^{shell} = 0$$

$$\Delta_\theta^{op} - \Delta_\theta^{shell} - \left(\frac{T+t_{op}}{2}\right) \theta_Z^{shell} = 0$$

$$\Delta_Z^{op} - \Delta_Z^{shell} + \left(\frac{T+t_{op}}{2}\right) \theta_\theta^{shell} = 0 \qquad (12b)$$

$$\theta_R^{op} - \theta_R^{shell} = 0$$

$$\theta_\theta^{op} - \theta_\theta^{shell} = 0$$

$$\theta_Z^{op} - \theta_Z^{shell} = 0$$

The compatibility equations for a "pipe-shell-outer and inner pads" configuration are identical to Equations (11) and (12). Each of these equations is provided as enforced constraints to every shell, pipe, and pad(s) connecting grid point.

2.4 Structural Analysis Computer Program

The finite element method is a modern, computer-oriented approach to the analysis of structures. One of its principal advantages is its complete generality. This versatility makes it possible to consider arbitrary geometries, support conditions, loadings, and variations of material properties within the structures. The principal limitation is the cost of operation. The cost is incurred both in the time required to prepare the input data describing the finite idealization of the structure and its loading, and in the computer time required to obtain the solution. The process for generating the complete finite element computer program is described in Chapter II, Section 2.1.

The finite element computer program utilized in this study is the latest NASA STRUCTURAL ANALYSIS (NASTRAN) version - level 15.5.1. Structural elements are provided for specific representation of more common types of construction including rods, beams, shear panels, and plates. The range of analyses that can be solved include static, elastic stability, and dynamic structural problems. NASTRAN has been specifically designed to treat large problems with many degrees of freedom. Computation procedures in NASTRAN were selected to provide the maximum obtainable efficiency for large problems. NASTRAN uses a finite element model, wherein the distributed physical properties of a structure are represented by the elements interconnecting at the grid points. Loads are applied either at grid points or on the elements for which displacements are calculated.[30]

The system displacements {u} in Equations (1), (3), (5), and (6) locate individual grid or node points which schematically represent the structure. The structure is approximated by connecting these grid points with the proper elements (rods, bars, beams, and plates) which best describe the individual shapes and the overall configuration to be analyzed. In the process of connecting the elements to the grids, material and geometrical properties (areas, moments of inertia, modulus of elasticity, Poisson's ratio) for each element can be identified. By organizing all of the grids, elements, and properties in the form acceptable to NASTRAN, or other general purpose finite element computer programs, the stiffness matrix [K] in Equations (1), (2), (4) and (6) can be generated in the computation process. The loads {F} that apply to each element and/or discrete grid points can be identified, and the cards generated.

Triangular and quadrilateral elements with both inplane and bending stiffness are used in this study. The NASTRAN (level 15) numerical results were calculated using Langley Research Center's CDC-6000 series computers. Also, HP-9810 programmable desk top calculator was used to assist in interpreting the data and to automate the empirical formula developed. The approximate number of degrees of freedom required to model the different configurations in this study are as follows: shell, 1500; pipe, 300; and pad, 300. Once the displacements {u}, Equation (6), are determined, internal element stresses are obtained. Finally, inside and outside surface stresses for each element in the structure are computed by NASTRAN from these internal stresses (membrane stress $\pm$ bending stress). A shell, pipe, and two pad configuration (modeled with 2400 degrees of freedom) is presented in Appendix A.

With regard to the cost of preparing the finite element program input data previously described, it is quite likely that this will exceed the cost of the computer operation in most cases. In any numerical computer method, the characterization process of a structure can be tedious and time-consuming. A major part of the cost of data preparation is spent in eliminating errors in the extensive tables of numbers required to describe the idealization. The extent of the input process can only be minimized by the use of automation. In order that the finite element method may be used effectively as a research, analysis, or design tool, it is essential that automatic mesh generation programs be developed which will define the idealizations of arbitrary shell geometries. Of similar importance to the practical use of such programs is automatic plotting to present the configuration and results in a readily usable format.

A computer program to "automatically" punch input cards in the format acceptable to NASTRAN was developed. This program generates the input for shell, pipe, and pads: grid, element, load, compatibility, and boundary condition cards. The cards punched from this program are input to NASTRAN for solving the inside and outside surface element stresses. Many configurations were solved (presented in Chapter V) in order to obtain trend data and comparative results. As a spin-off of the NASTRAN program, plots can be obtained for pictorial or presentation purposes and as a debugging tool. Sample plots are shown in Figures 2.4.1, 2.4.2, and 2.4.3.

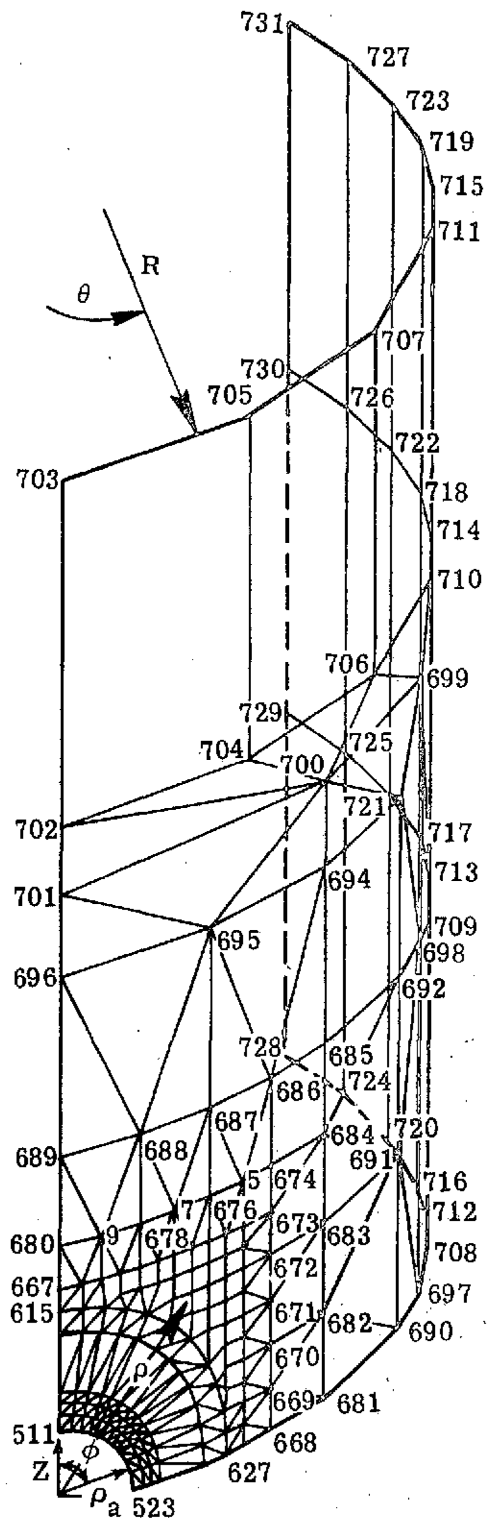

Figure 2.4.1.- Nonreinforced hole in cylindrical shell.

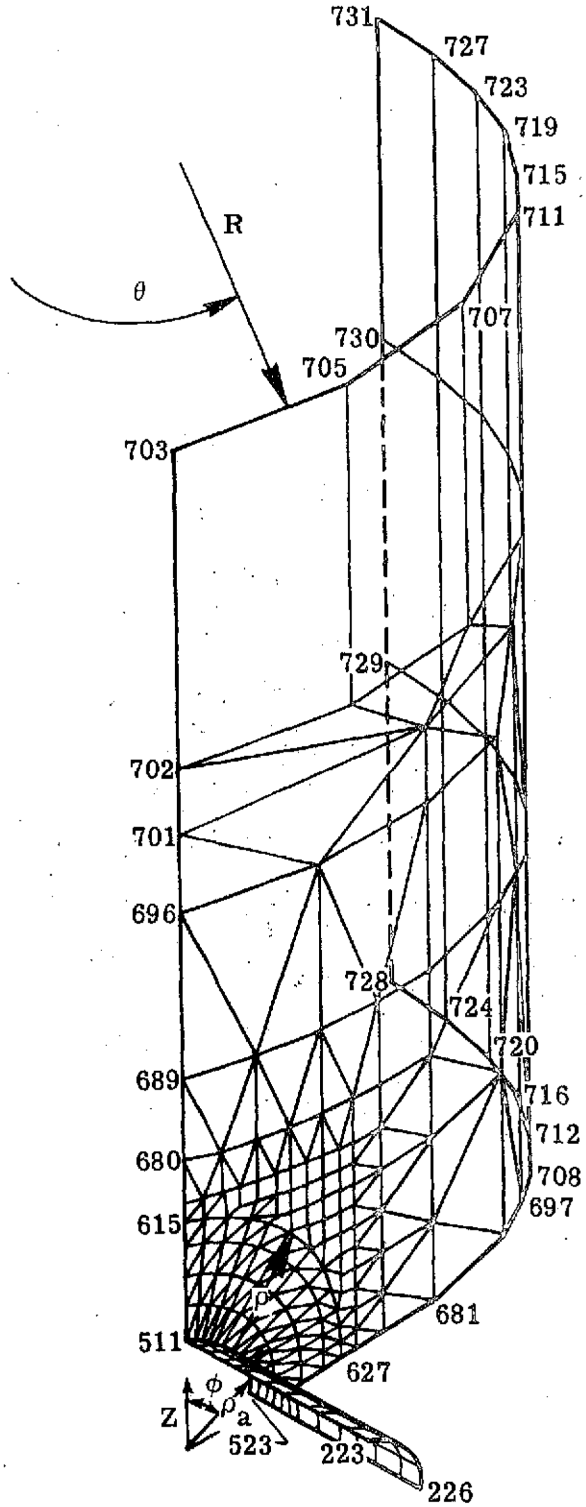

Figure 2.4.2.- Nonreinforced hole in cylindrical shells.

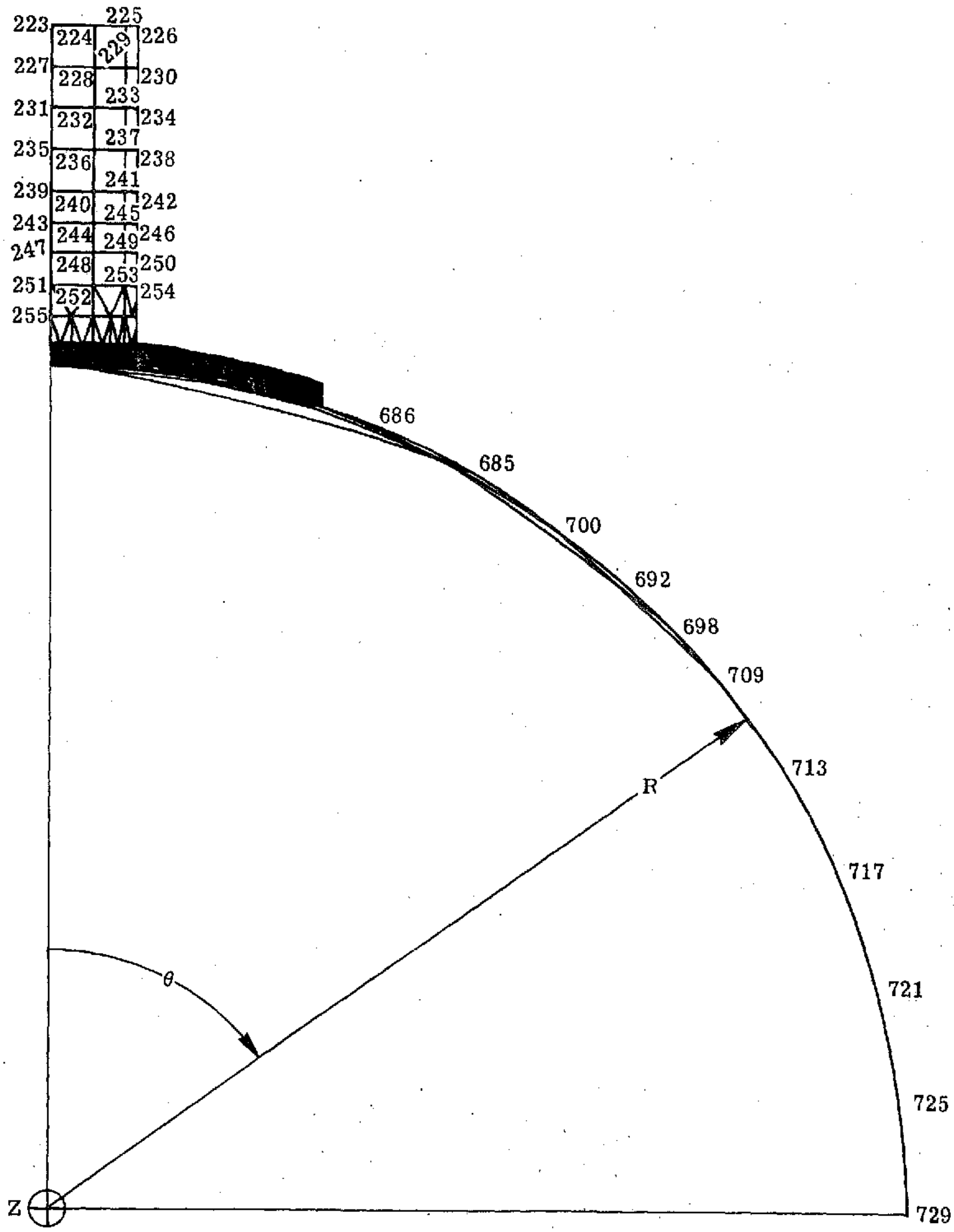

Figure 2.4.3.- Pipe and bottom pad reinforced hole in cylindrical shell.

CHAPTER III

ACCURACY STUDY

3.1 Introduction

In the finite element analysis of any structure, a first requirement is the idealization of the structure. For example, a shell surface (shown in Figure 3.1.1) is divided into a system of appropriately shaped pieces. The individual pieces must be standardized as simple shapes such as triangles, rectangles, or quadrilaterals in order that their stiffness properties may be defined. This requirement imposes a certain degree of approximation in idealizing the geometry of shells: a curved boundary will usually be represented as a series of straight line segments. In general, this boundary approximation is not severe, and it can be reduced to any desired error limit by reducing the size of the elements.

The most important approximation is in the shell behavior assumption itself. If the shell is treated as a two-dimensional surface rather than as a three-dimensional solid, this implies certain assumptions and limitations. For example, in the Kirchhoff theory, it is assumed that stresses in the direction normal to the shell surface are small compared to membrane stresses, and lines normal to the surface are assumed to remain normal and unstrained

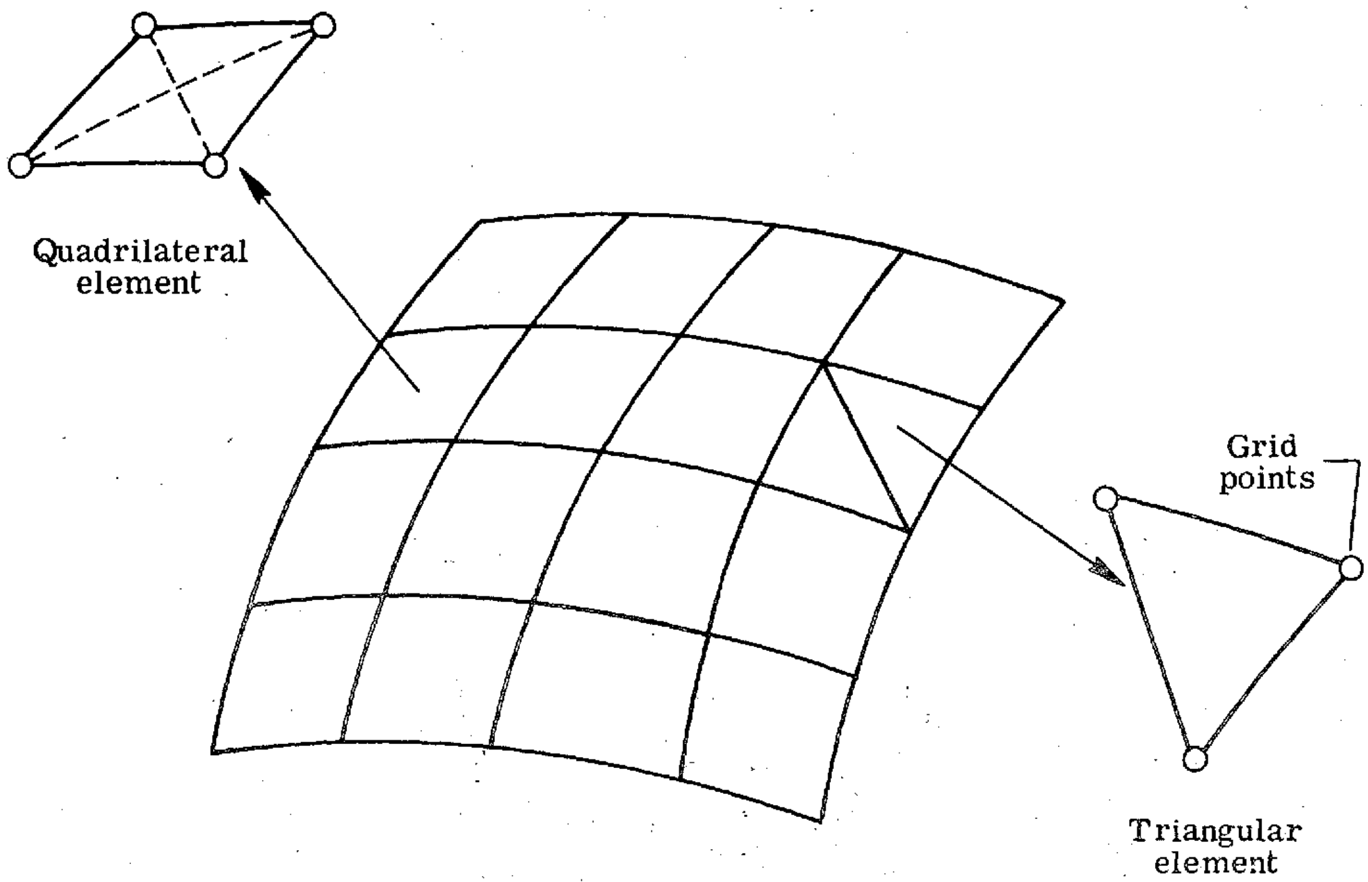

Figure 3.1.1.- Discretized shell.

during deformation. Approximations of this type are not a special feature of the finite element solution but are inherent in any shell theory. Another common approximation, in addition to the straight line segment representation of boundaries, is that the elements connecting grid points are flat surfaces or a group of several flat surfaces. The great advantage of this assumption is that the membrane and bending stiffness properties of the individual flat plates are uncoupled. The coupling, which is characteristic of shell behavior, is developed only in the assemblage of the flat plates into an approximation of the curved shell surface.[31]

3.2 Types of Finite Elements

The nature of the finite element approximation is such that the analytical results generally converge toward the true solution as the finite element mesh size is refined. Other factors in the convergence criteria are the number of grid points specified for each element, type of elements, and primarily, the number of degrees of freedom (DOF) at each grid. The Kirchhoff theory takes account of five DOF (3 translations and 2 rotations about axes tangent to the shell surface). Most shell elements make use of these same 5 DOF at each grid.

The finite elements employed in the discretized shell in Figure 3.1.1 are both planar triangles and quadrilaterals assembled from 4 planar triangles. The forces and stresses on these elements are shown in Figure 3.2.1[30] The membrane stiffness of the triangular element is represented by the well-known constant strain triangle and shown in Figure 3.2.2. The components of displacement, u and v, are parallel to the local coordinate system (element X and Y axes). The bending property based on cubic displacement patterns is given by a fully compatible plate bending element, a Clough bending triangle.[32] This triangle is formed by subdividing it into three basic bending triangles as shown in Figure 3.2.3. The X-axis of each sub-triangle corresponds with an exterior edge, so that continuity of slope and deflection with surrounding Clough triangles is assured. The added grid point in the center is like the other grid points in that equilibrium of forces and compatibility of displacements are required at the center point. In addition, the rotations parallel to the internal boundaries at their midpoints, points 5, 6 and 7, are constrained to be continuous across the boundaries. The equations for slopes in the basic triangles contain quadratic and lower order terms, and since the normal slopes along interior boundaries are constrained to be equal at three points (both ends and the middle), it follows that slope continuity is satisfied along the whole boundary. Displacement continuity on all

Structural modeling

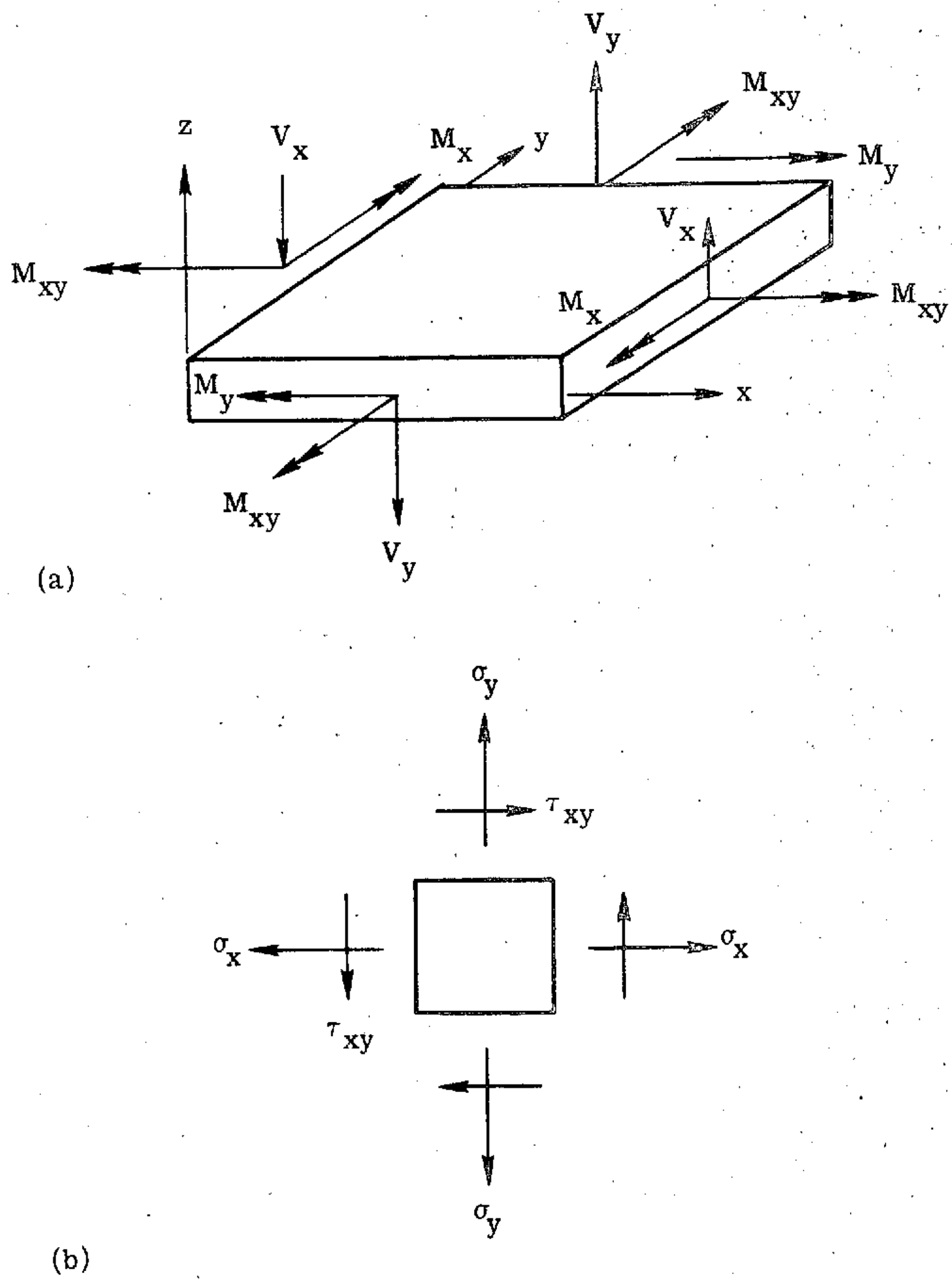

Figure 3.2.1.- Forces and stresses in plate elements.

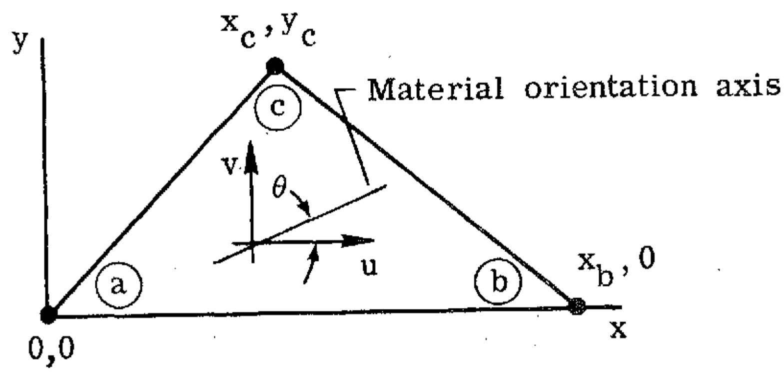

Figure 3.2.2.- Triangular membrane element.

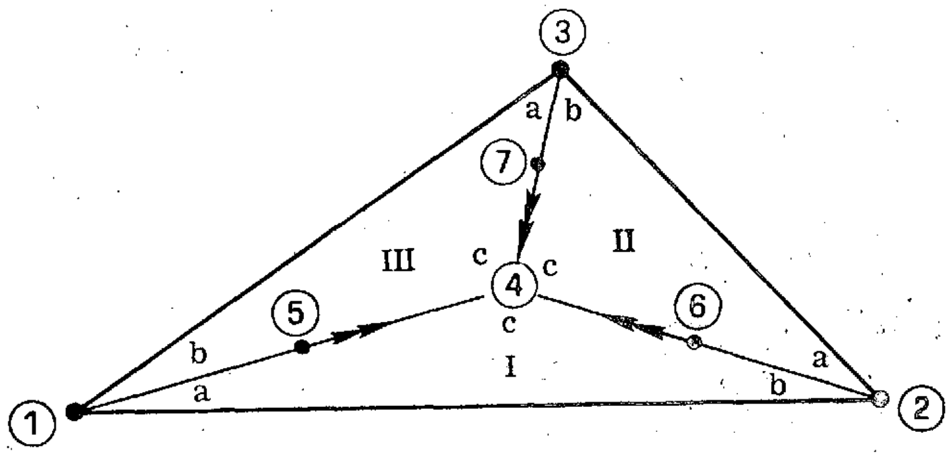

Figure 3.2.3.- Clough bending triangle.

boundaries is automatically satisfied when the displacement function contains only cubic and lower order terms. Thus, complete continuity of slope and displacement on all interior and exterior boundaries is assured for the Clough triangle.

The Clough triangle is superimposed with a membrane triangle to form triangular elements with both membrane and bending stiffness. Therefore, this triangular element has 5 DOF at each corner, 2 deriving from membrane displacements and 3 from the bending. The quadrilateral plate was developed to provide improved membrane strain behavior while retaining the basic 5 DOF per grid system. It is formed as 4 planar triangles as shown in Figure 3.2.4 plus 3.2.5, with the grids modeling the shell midsurface. Each triangle has one-half of the bending, stiffness or one-half of the thickness (membrane) assigned to the quadrilateral element. Since four points, in general, do not lie in a plane, care must be taken to ensure equilibrium and compatibility. Rather than try to define a warped surface, an averaging process is used on the noncoplanar membrane triangles. The bending element uses two sets of overlapping basic bending triangles. Since coupling between membrane stiffness and bending stiffness is not, at present, included in NASTRAN, quadrilateral elements with both membrane and bending properties are treated by simple superposition of their

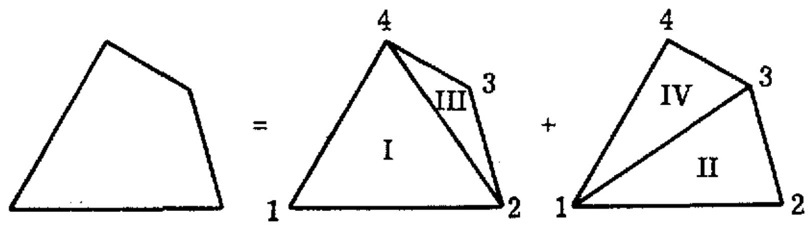

Figure 3.2.4.- Quadrilateral membrane element.

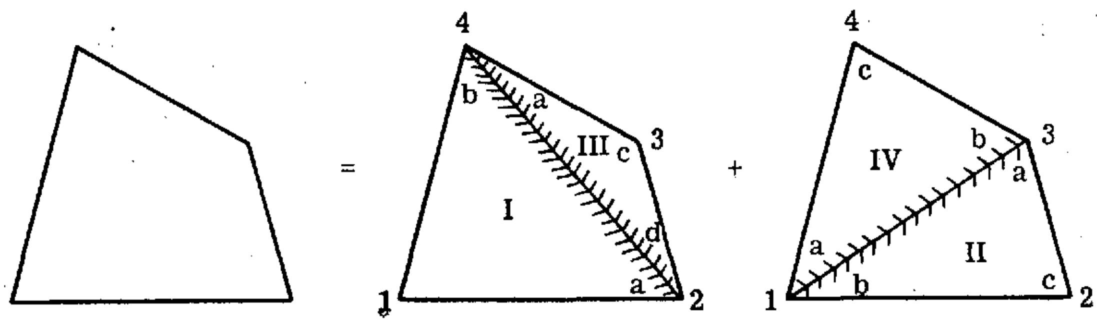

Figure 3.2.5.- Quadrilateral bending element.

membrane and bending stiffness matrices. The following NASTRAN elements are the ones used in this research:

1. TRIA 2 - The triangular element with both inplane and bending stiffness.
2. QUAD 2 - A quadrilateral element similar to TRIA 2.

3.3 Shell

In this section, consideration is given to the accuracy obtained with different mesh sizes and the two types of elements (TRIA 2 and QUAD 2) used to obtain the peak stress concentration factor for a pressurized cylindrical shell with a circular hole, Figure 2.2.1. A quarter of the shell is chosen as the model: shell radius, R; length, $\geq$ 2R; and the hole radius, ρ_a. A typical finite element model is shown in Figure 3.3.1. If the element size or general mesh geometry is too large at discontinuities (such as a penetration), the structure will be "too stiff". The finite element approximations to peak stress concentration factors will be below the correct answer. This model provides a gradual transition of large to small elements as the hole opening is approached. Since the "radial" section is the easiest to generate or modify, different mesh arrangements and elements will be used to compare the accuracy of peak stress concentration factors (SCF) to "exact" solutions.

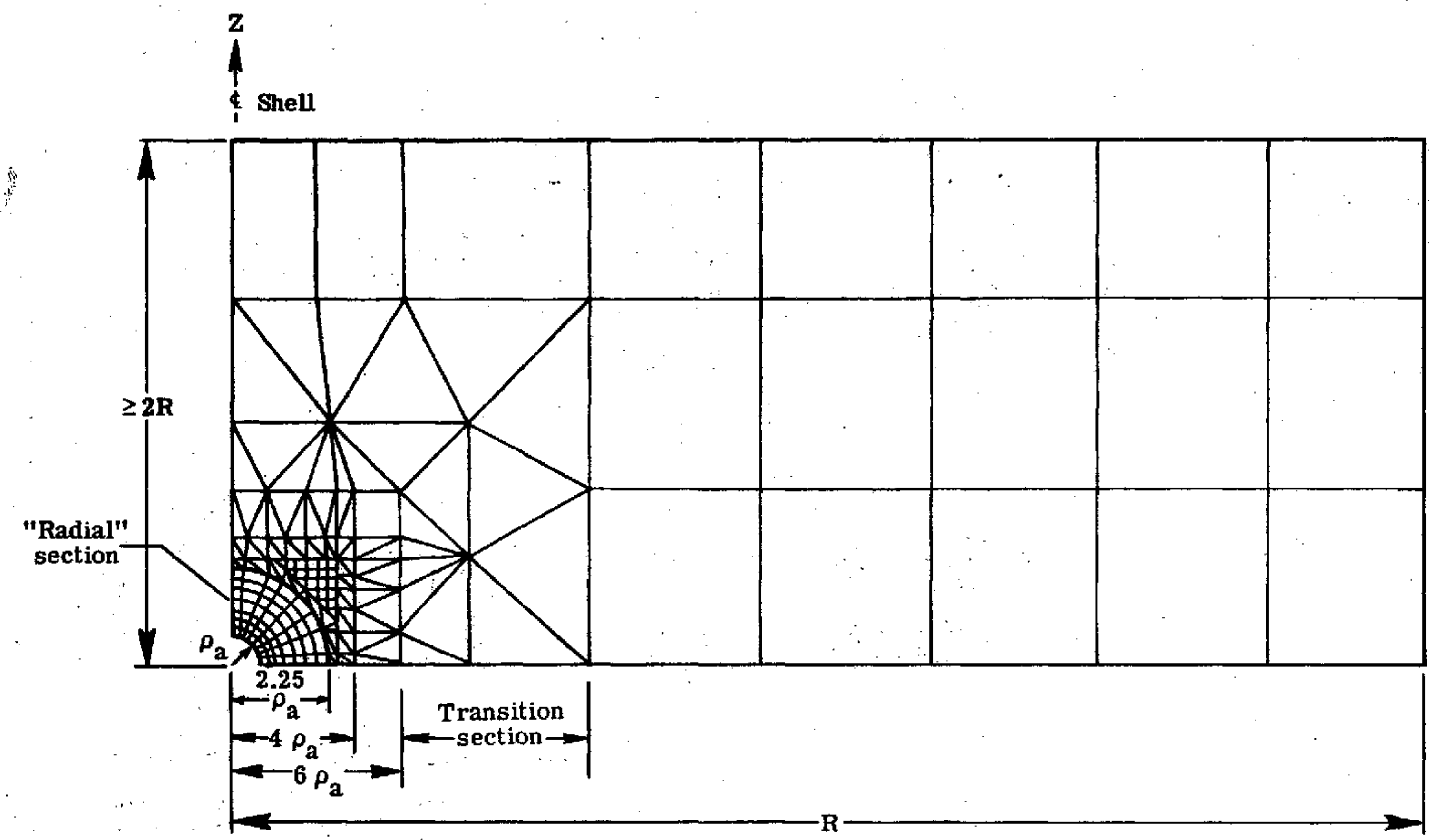

Figure 3.3.1.- Typical plan view of a finite element model of a cylindrical shell with a circular hole.

The rectangular arrangement of quadrilateral (RQ) elements of the "radial" section is shown to a larger scale in Figure 3.3.2. The right (RDT) and left (LDT) diagonal arrangements of triangular elements for the "radial" section are shown in Figures 3.3.3 and 3.3.4, respectively. A refined version (additional grid points) of left diagonal triangular (RLDT) elements is shown in Figure 3.3.5. The triangularizing of only the first element in the rectangular arrangement of quadrilateral (1TRQ) elements is shown in Figure 3.3.6. These code names for identifying the articulation arrangements are similar to those used by Melosh.[31] It should be noted that efforts were pursued in refining these configurations by grouping the same number of grid points very near the hole (see Figure 3.3.7) - all to no avail. Also, results for refining of the RLDT, regardless of the local transition, were in error. This idea of too much local refining is known.[31] When the elements were smaller than one-half of the shell thickness, the peak SCF oscillated about the "exact" solution.

A summary of the computer runs for peak stress concentration factors for a pressurized cylindrical shell with force around the hole is presented in Table 3.3.1. The units used in this table and throughout this study are in the English or American System (inches and pounds). The RQ radial section model approximates the peak inside SCF to within -11% (below) of the theoretical or "exact" solution obtained in Reference (3). The approximations for the triangular arrangements (RDT, 1TRQ, LDT) are converging to the theoretical solution without local refining (RLDT). Many authors have reported the mid-surface (average) SCF. (1,2,3) Since this is not the peak value, the largest SCF (inside) will be the gauge in the accuracy comparisons to determine the arrangement to use for all other shell/force problems. The LDT (which is much easier to generate) peak inside SCF is slightly more accurate (-1.05% difference) than the RLDT (+1.14% difference). Therefore, the LDT arrangement is the one chosen to obtain the peak SCF results for shell configurations with just a force around the hole.

Table 3.3.1 - Peak SCF For Finite Element Models For A Pressurized Cylindrical Shell With Force Around The Hole: ρ_a=13.0, R=112.0, ν=0.3.

RADIAL SECTION DESCRIPTION	T	Peak SCF @ $\phi = 0$ and ρ_a					
		INSIDE		OUTSIDE		AVG.	
		NASTRAN	% DIFF	NASTRAN	% DIFF	NASTRAN	% DIFF
RQ	1.25	4.997	-10.99	3.108	-16.83	4.053	-13.31
RDT	1.25	5.405	- 3.72	3.395	- 9.15	4.400	- 5.88
ITRQ	1.25	5.479	- 2.41	3.477	- 6.96	4.478	- 4.21
LDT	1.25	5.555	- 1.05	3.554	- 4.90	4.555	- 2.57
RLDT	1.25	5.678	+ 1.14	3.680	- 1.53	4.679	+ 0.09
	"EXACT" REF. (3)		5.614	"EXACT" REF. (3)	3.737	"EXACT" REFERENCES (1,2,3)	4.675

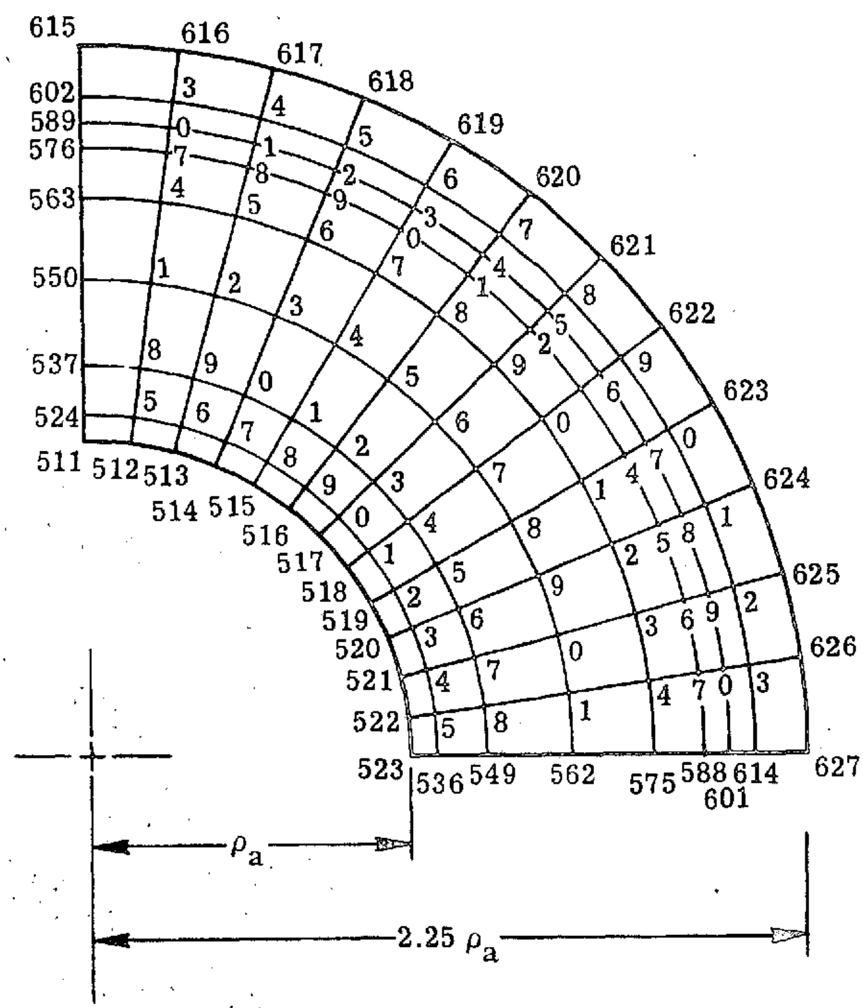

Figure 3.3.2.- Rectangular arrangement of quadrilateral (RQ) elements for "radial" section.

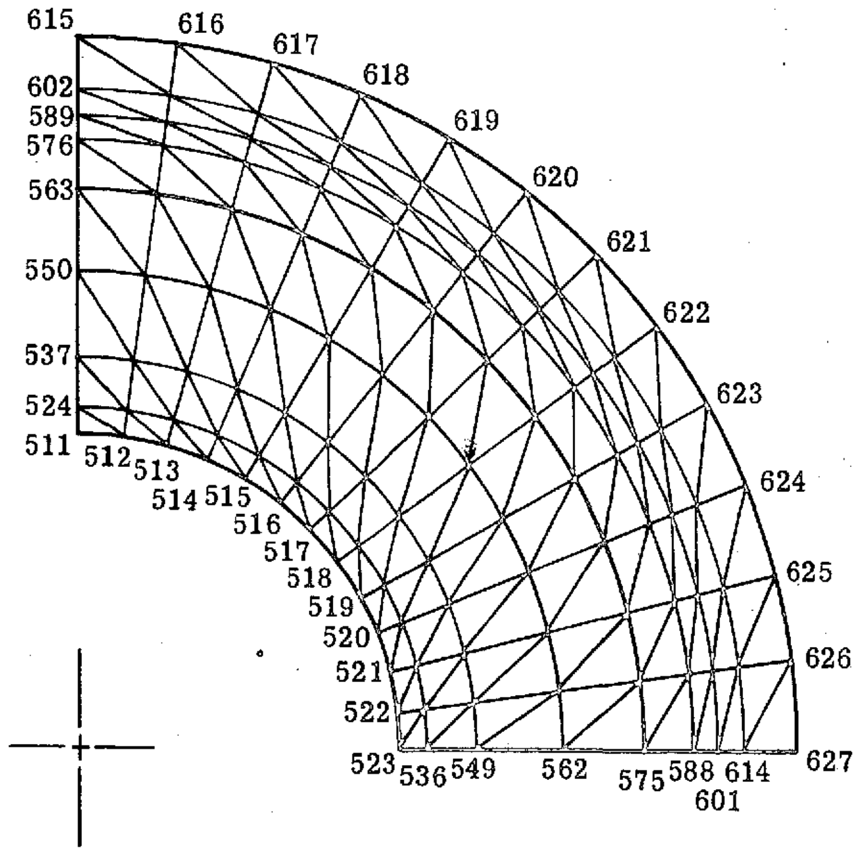

Figure 3.3.3.- Right diagonal arrangement of triangular (RDT) elements for "radial" section.

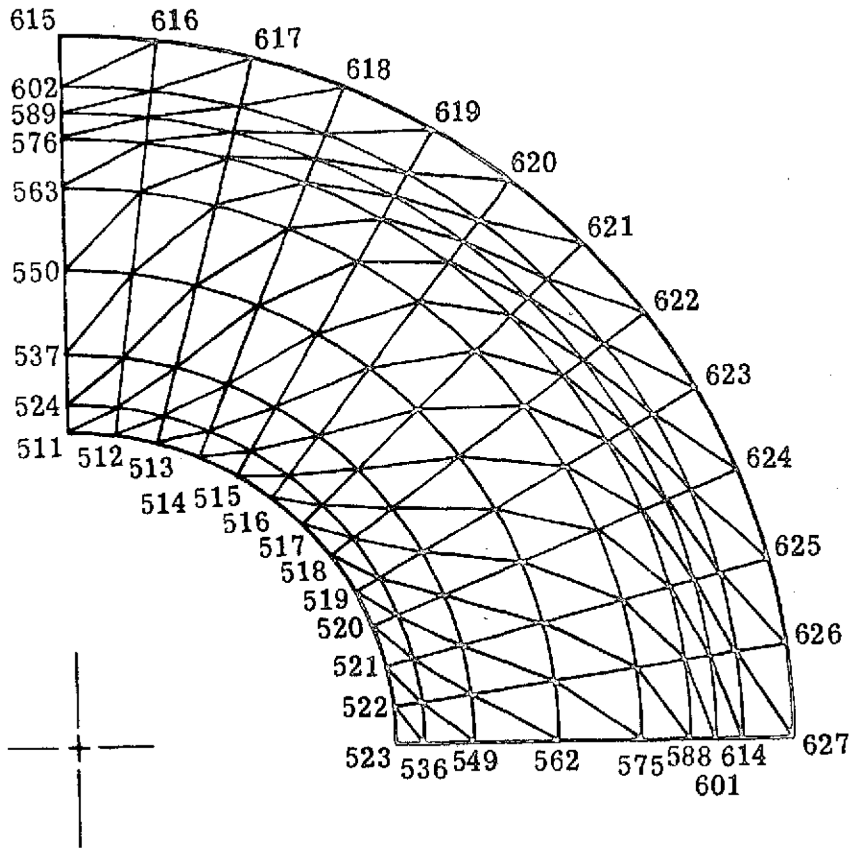

Figure 3.3.4.- Left diagonal arrangement of triangular (LDT) elements for "radial" section.

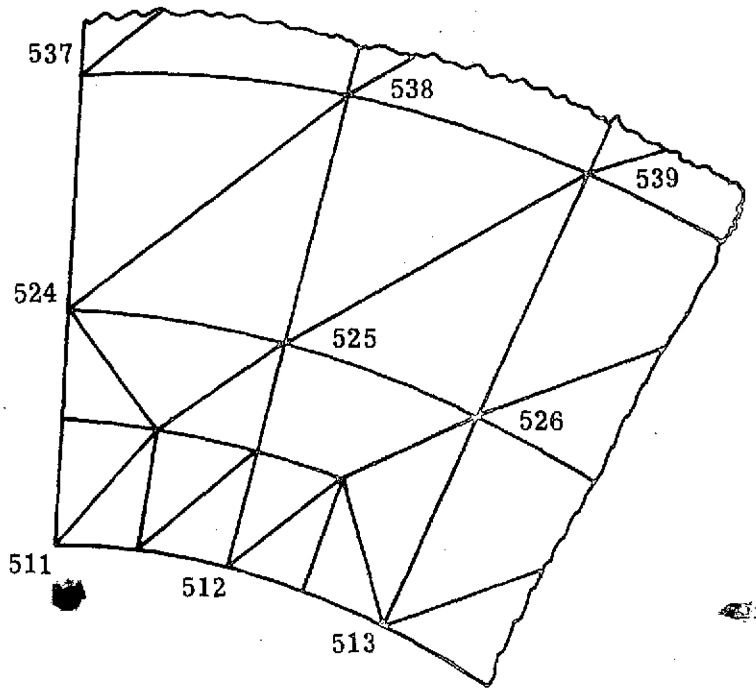

Figure 3.3.5.- Refined left diagonal arrangement of triangular (RLDT) elements.

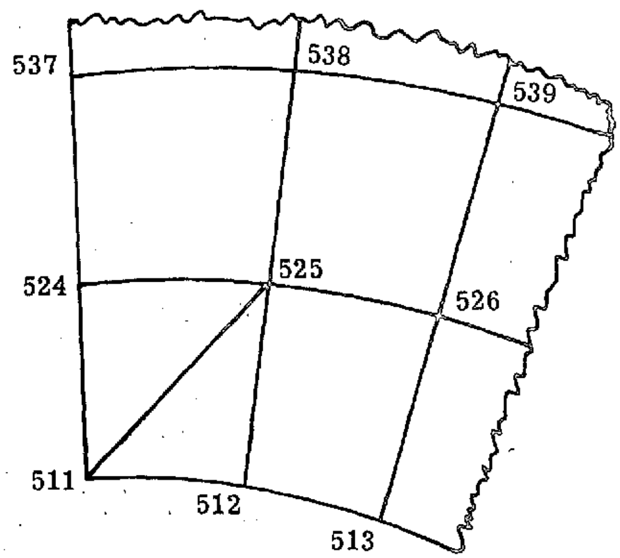

Figure 3.3.6.- First element triangularized in RQ arrangement (ITRQ).

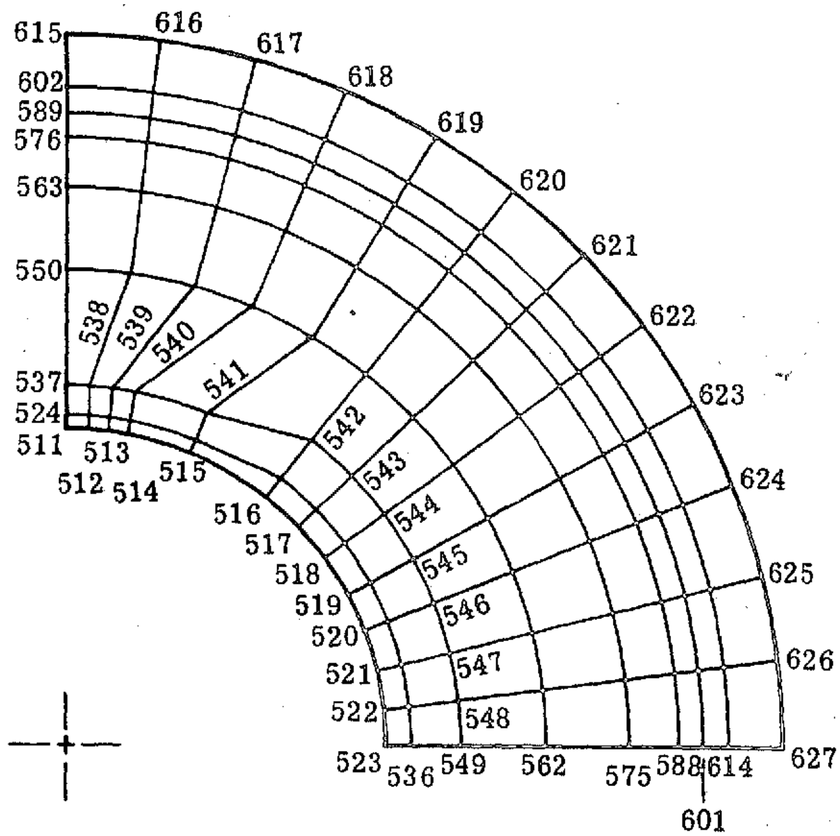

Figure 3.3.7.- Poor approach to refining of "radial" or pad(s) sections.

3.4 Shell and Pipe

The next configuration to be considered is two intersecting circular cylinders (shell and pipe) as shown in Figure 2.2.3. The same shell models in Section 3.3 are used; therefore, a quarter of the pipe is modeled: hole radius, ρ_a; pipe radius, ρ_o; pipe thickness, t; pipe length, $\geq 2\ \rho_a$, and all of the shell parameters previously described. Typical finite element models for a pipe are arranged and shown as follows: rectangular quadrilateral (RQ), Figure 3.4.1; right diagonal triangles (RDT), Figure 3.4.2; and left diagonal triangles (LDT), Figure 3.4.3. The successful implementation of the compatibility equations for the pipe/shell juncture was accomplished by using the following:

1. The θ relationship in Equations (8) and <u>not</u>

   $$\theta = 2 \text{ Arc sin } \left(\frac{\rho \sin \phi}{2R}\right) \quad \text{or}$$

   $$\theta = 2 \text{ Arc sin } \left(\frac{\rho_o \sin \phi}{2R}\right),$$

2. The same coordinate system for both the shell and the pipe, and

3. The same coordinate system for input, solution, and output.

A summary of the peak SCF computer solutions for shell and pipe is presented in Table 3.4.1. The finite element approximations are converging to the theoretical solutions.[1,3] For T = 1.084, the convergence is as good as the shell problem. For the same reasons, the left diagonal triangular shell and the right diagonal pipe is the configuration used in the numerical NASTRAN results. For comparison purposes, computer results for two other shell thicknesses (T = 1.25 and 2.167) for the "simplest" and the chosen configurations are also shown.

Figures 3.4.4 through 3.4.7 show the comparison of the NASTRAN results with experimental and analytical data. The difference between the chosen NASTRAN configuration and the experimental data from that in Cranch [14] is only 8.38%, see Figure 3.4.4. Another example of trend and accuracy is the nozzle-to-cylinder intersection model in Figure 3.4.5. The analysis was performed by Prince and the experimental investigation by the Oak Ridge National Laboratory.[7] Remarkable accuracy is achieved (-3.95% difference) with a direct trend comparison, see Figures 3.4.6 and 3.4.7. Other examples of experimental data and numerical/analytical findings are presented in the results, Chapter V.

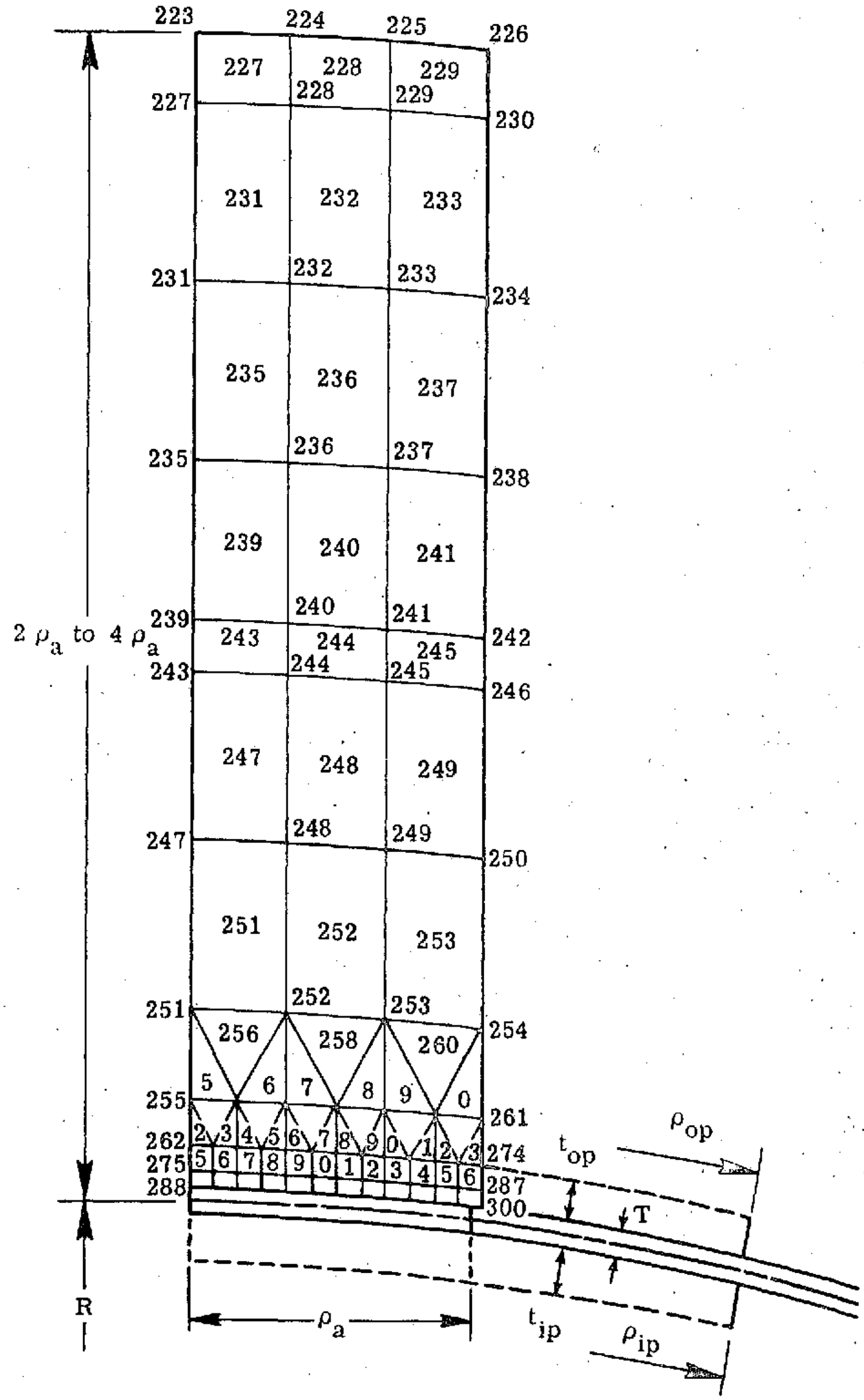

Figure 3.4.1.- Rectangular arrangement of quadrilateral (RQ) elements for pipe.

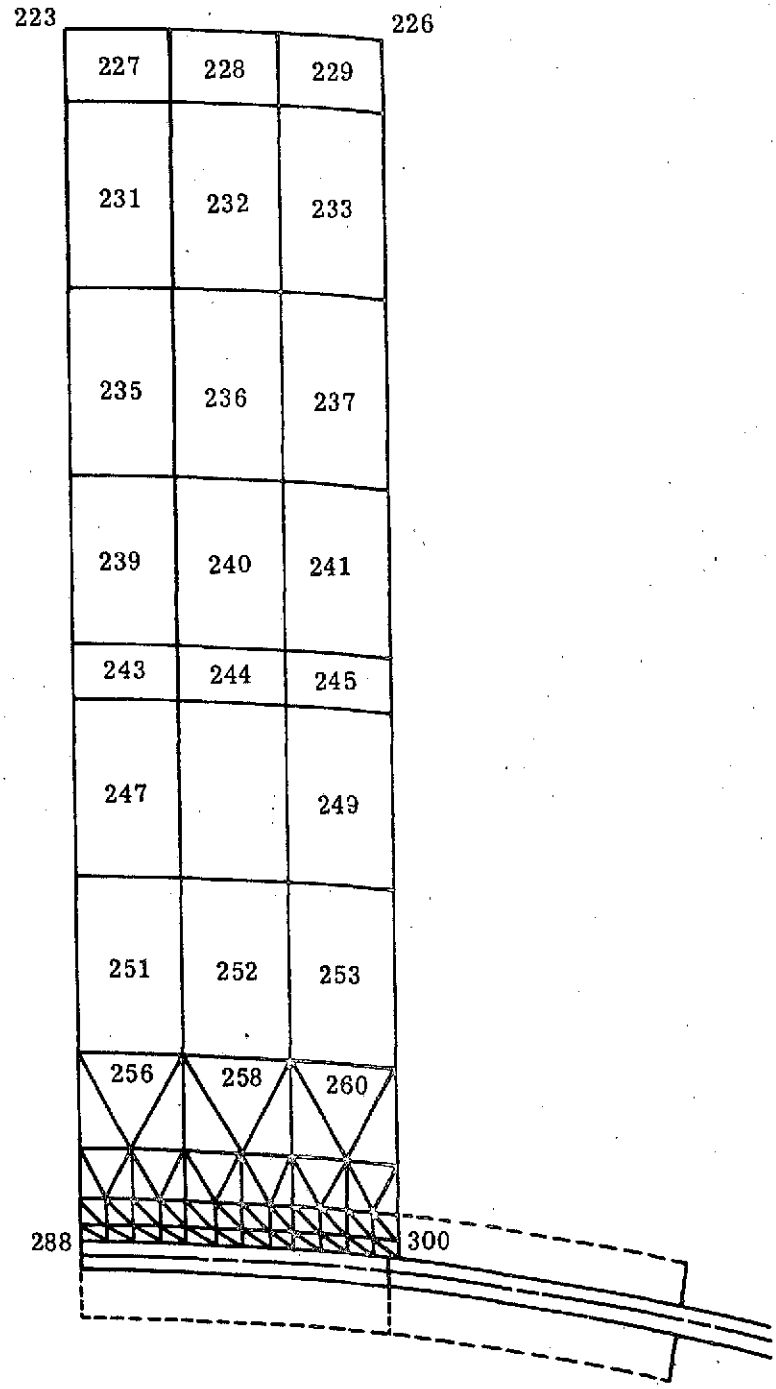

Figure 3.4.2.- Right diagonal arrangement of triangular (RDT) elements for pipe.

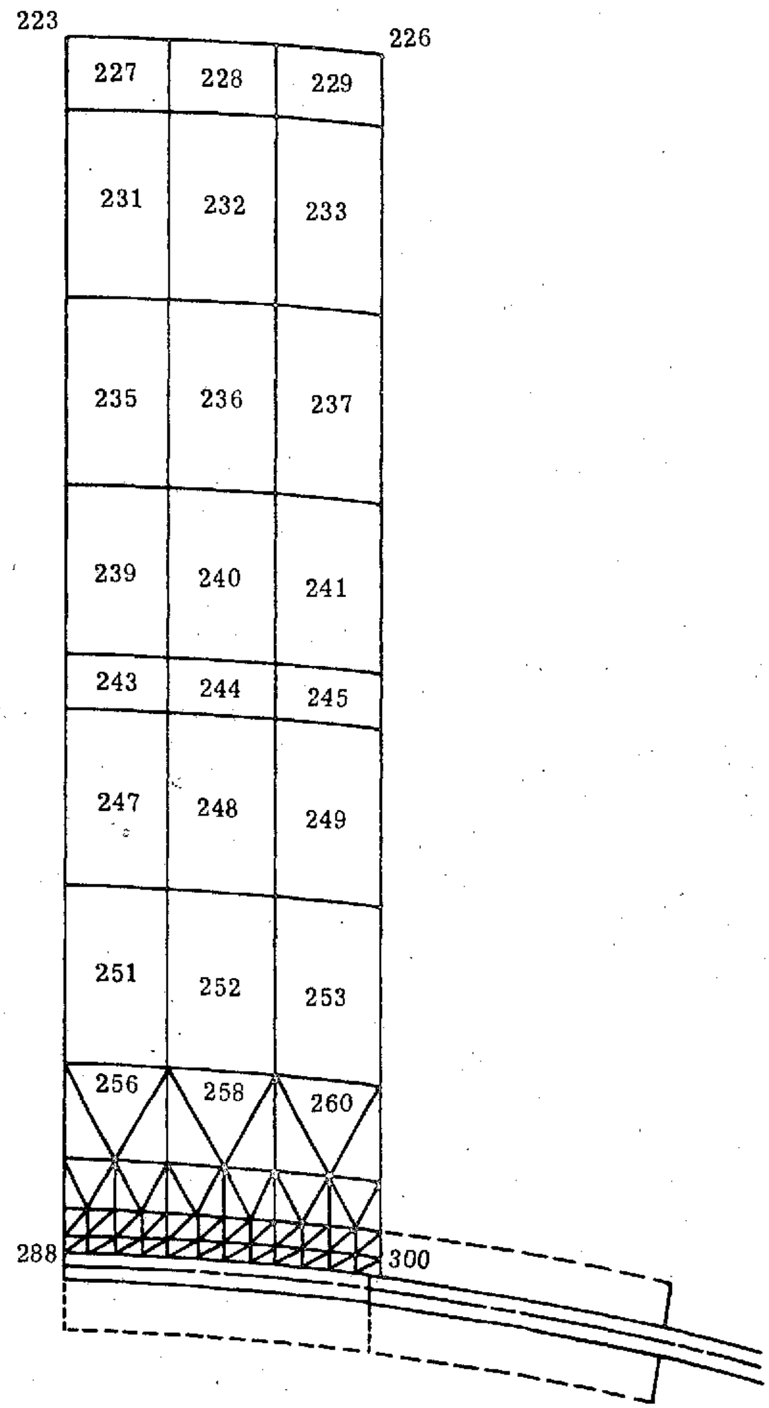

Figure 3.4.3.- Left diagonal arrangement of triangular (LDT) elements for pipe.

SHELL THICKNESS = 1.084			
		INSIDE SCF ON SHELL @ ϕ = 0 & ρ_a	
SHELL RADIAL SECTION DESCRIPTION	PIPE DESCRIPTION	NASTRAN	% DIFFERENCE
LDT (First Row Removed)	LDT	2.189	-12.09
LDT (First Row Removed)	RDT	2.197	-11.77
RQ	RQ	2.227	-10.56
RDT	RDT	2.282	- 8.35
LDT	RQ	2.428	- 2.49
LDT	RDT	2.447	- 1.73
LDT T of First Row = T/2	RDT	2.462	- 1.12
RLDT T of First Row = T/2	RDT	2.524	+ 1.37
		"EXACT" Ref(1)	2.490
	SHELL THICKNESS = 1.25		
RQ	RQ	2.213	-16.80
LDT T of First Row=T/2	RDT	2.563	- 3.65
		"EXACT" REF(1,3)	2.660
	SHELL THICKNESS = 2.167		
RQ	RQ	2.513	-18.14
LDT	RDT	2.793	- 9.02
		"EXACT" REF(1)	3.070

Table 3.4.1 - Peak SCF For Finite Element Models For a Cylindrical Shell With Pipe: ρ_a = 13.0, R = 112.0, ν = 0.3, And t = 1.3.

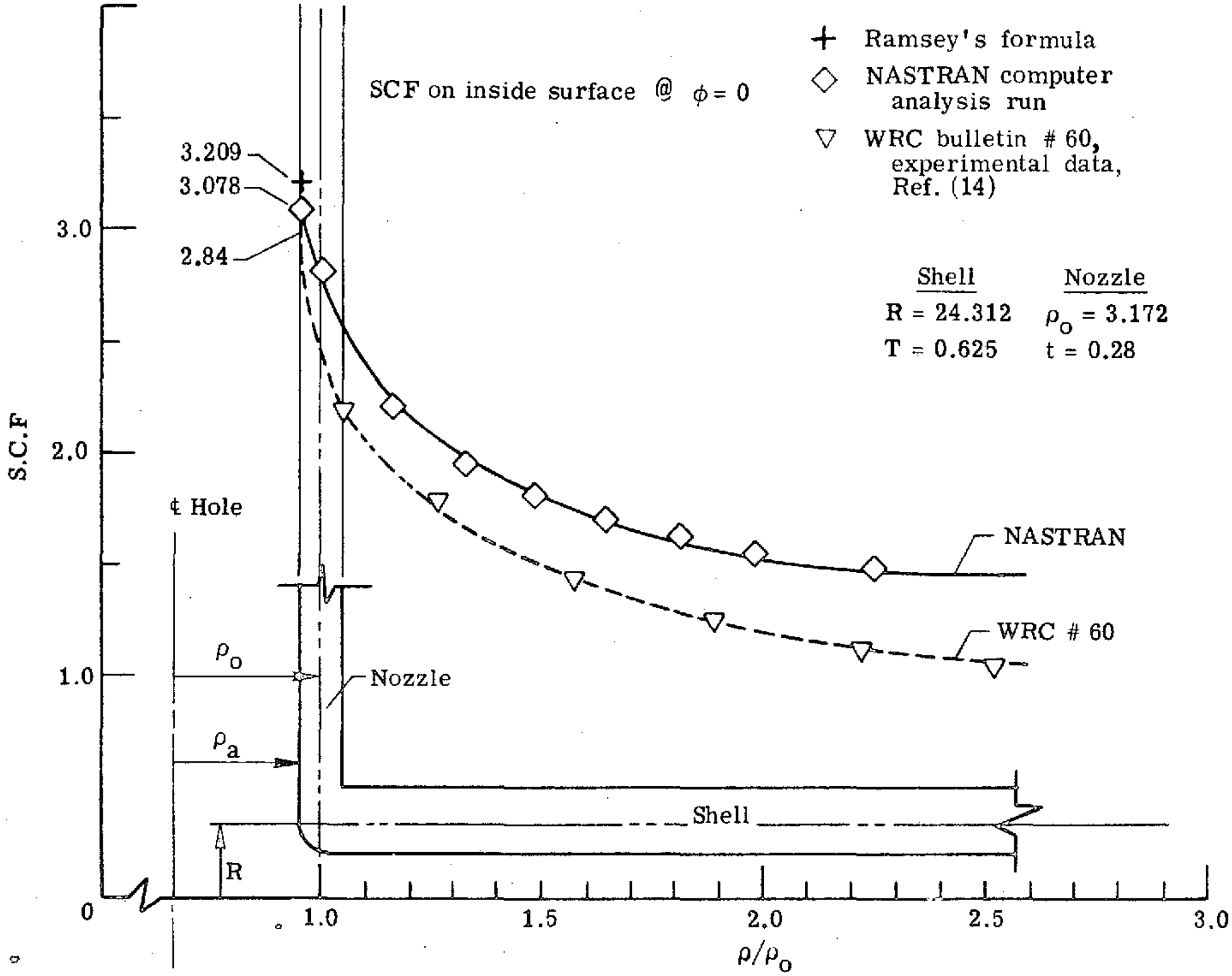

Figure 3.4.4.- Comparison of NASTRAN results with experimental data for shell and pipe.

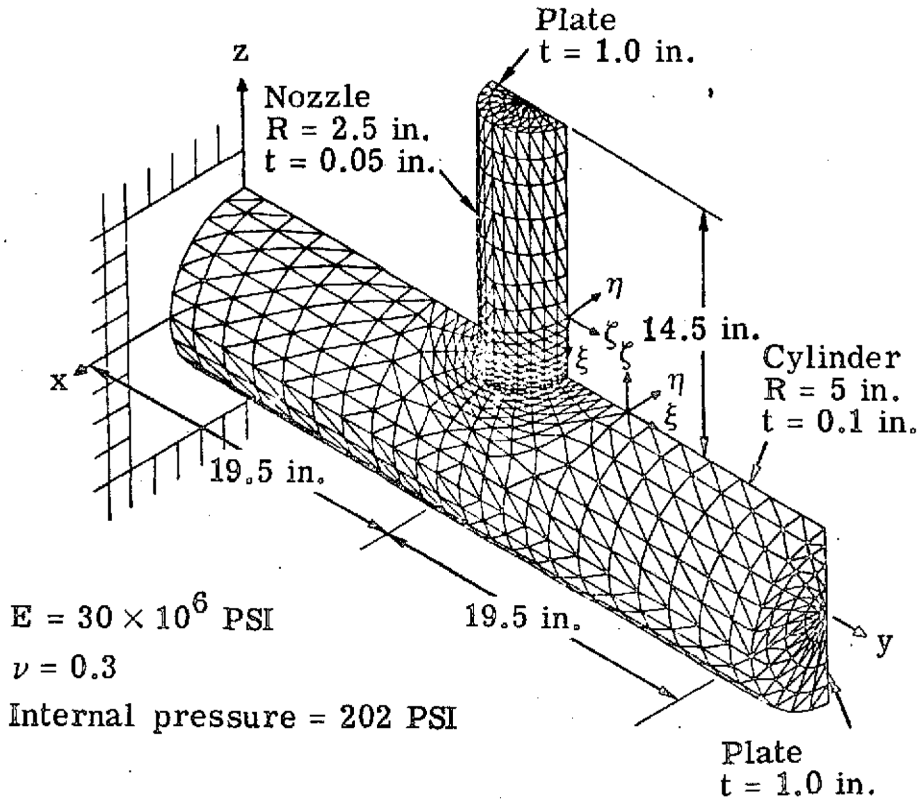

Figure 3.4.5.- Nozzle (pipe)-to-cylinder (shell) intersection model from Prince.[7]

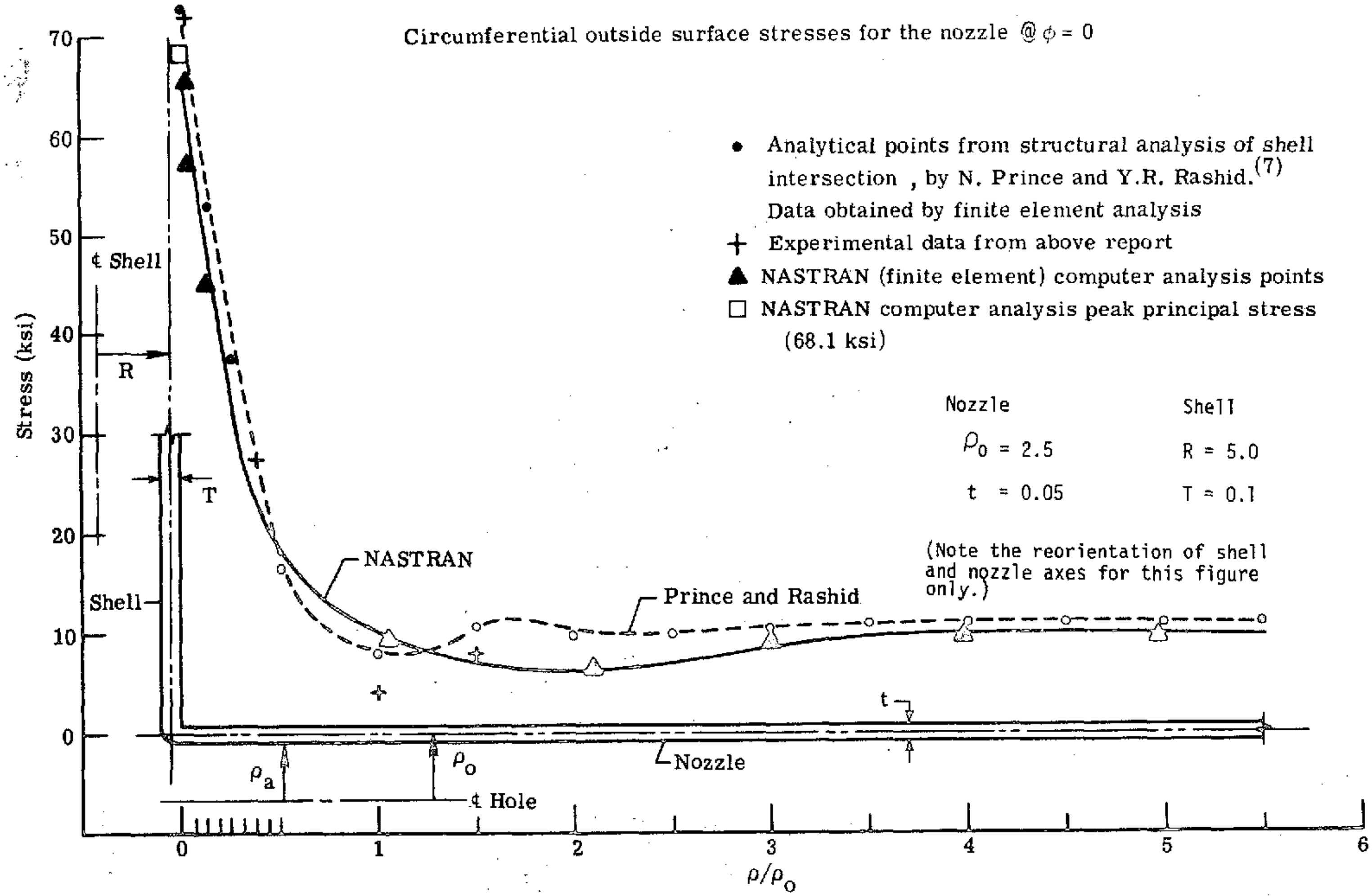

Figure 3.4.6.- Comparison of NASTRAN results with analytical and experimental data for shell and pipe.

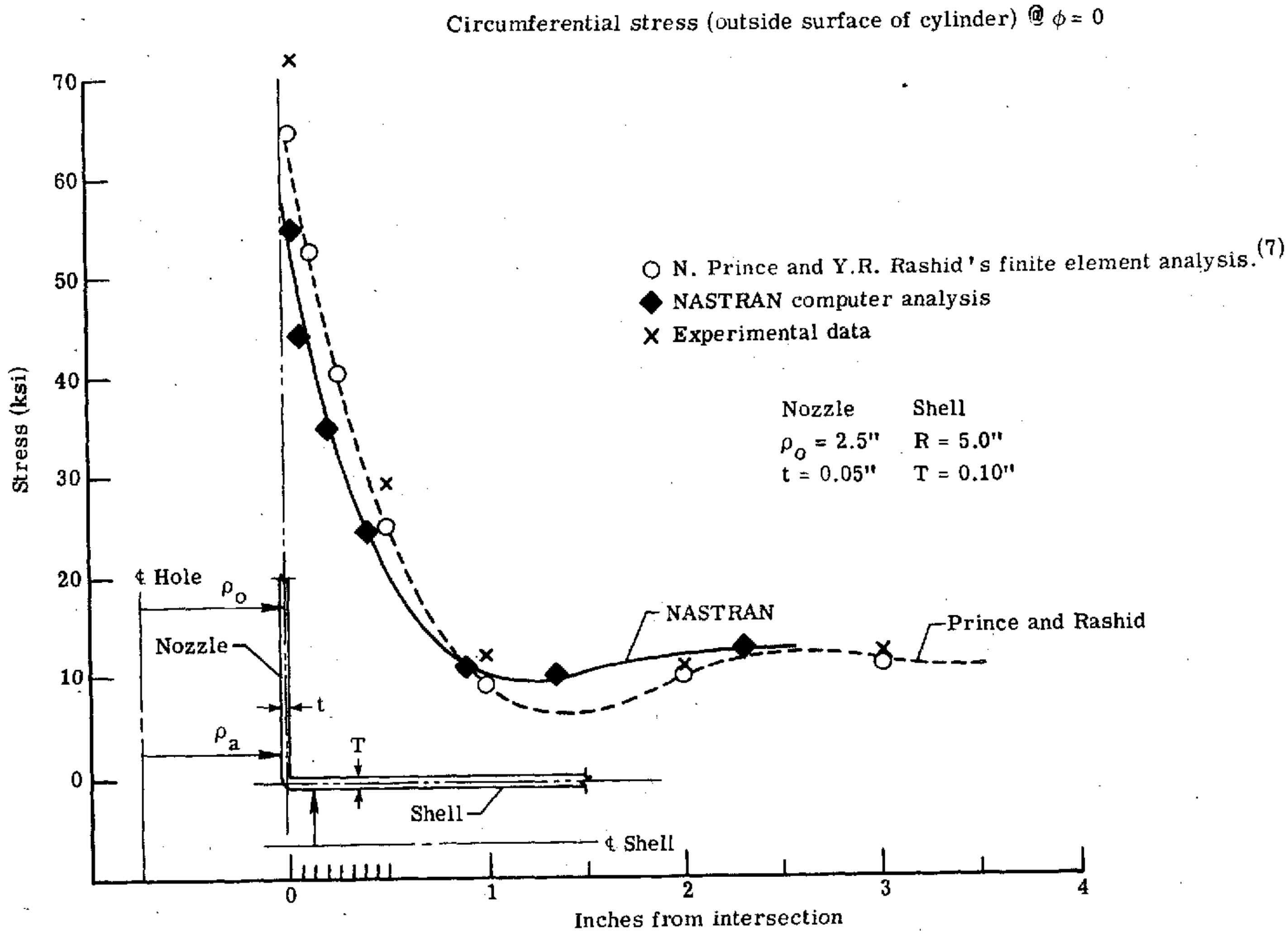

Figure 3.4.7.- Comparison of NASTRAN results with analystical and experimental data for shell and pipe.

3.5 Shell, Pipe, and Pad

The preceding sections provided comparisons of the accuracy of a variety of finite element solutions to theoretical, numerical, and experimental results. Results for this specific case (shell, pipe, and pad) are limited; however, a configuration was chosen to test the MPC cards. This configuration is two intersecting circular cylinders reinforced with a pad. The same shell and pipe models in Sections 3.3 and 3.4 are used; consequently, a quarter of the pad is modeled: outside pad radius, ρ_p; and pad thickness, t_p; and all of the shell and pad parameters previously described. Typical finite element models for a pad are similar to those of the shell "radial" section, see Figures 3.5.1 through 3.5.3. A summary of the peak SCF computer solutions for a shell/pipe/pad configuration is presented in Table 3.5.1.

There have been six shell/pipe/pad configurations experimentally investigated.[14,15,17,22,24] The NASTRAN result as compared to first set of data[14] is shown in Figure 3.5.4. The dashed line is the author's extension of the available experimental curve. The descriptions of the two models to show convergence is presented in Table 3.5.2. The second comparison[15] is shown in Figure 3.5.5 and presented in Table 3.5.3. This trend comparison is outstanding. The accuracies of the two, -3.85% and -4.42%, is remarkable. The convergence of these NASTRAN models for the two experimental cases lends authenticity to the first numerical case for which there is no comparison. Therefore, the LDT shell, RDT pipe, and LDT pad will be used as the finite element model for other numerical NASTRAN results. The other four experimental results will be presented in Chapter V (for comparison to the formula developed in Chapter IV).

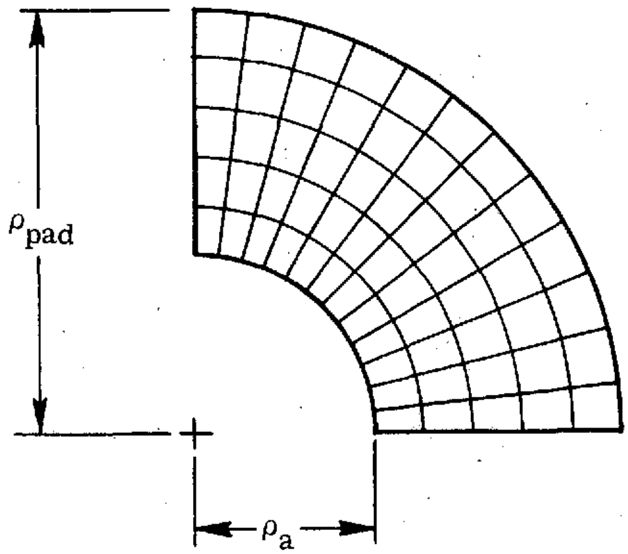

Figure 3.5.1.- RQ elements for pad(s).

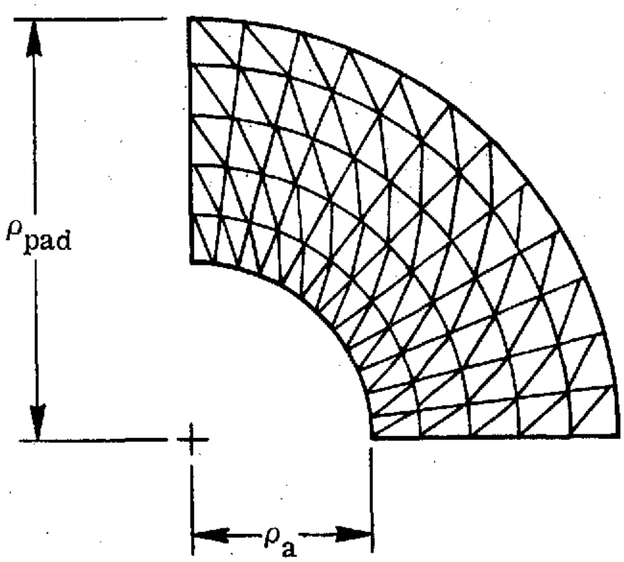

Figure 3.5.2.- RDT elements for pad.

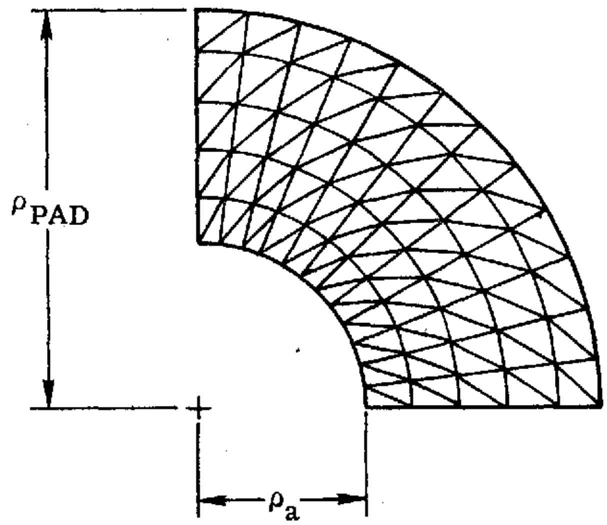

Figure 3.5.3.- LDT elements for pad(s).

SHELL RADIAL SECTION DESCRIPTION	PIPE DESCRIPTION	TOP PAD DESCRIPTION	SHELL SCF (INSIDE) $\phi = 0$ & ρ_a
RQ	RDT	RQ	1.711
RDT	RDT	RQ	1.808
RDT	RDT	RDT	1.831
LDT	RDT	LDT	1.868

Table 3.5.1 - Peak SCF For Finite Element Models for Cylindrical Shells With Pipe and Pad: $\rho_a = 13.0$, $T = 1.25$ $R = 112.0$, $\nu = 0.3$, $t = 1.3$, $t_p = 1.5$, & $\rho_p = 25.0$

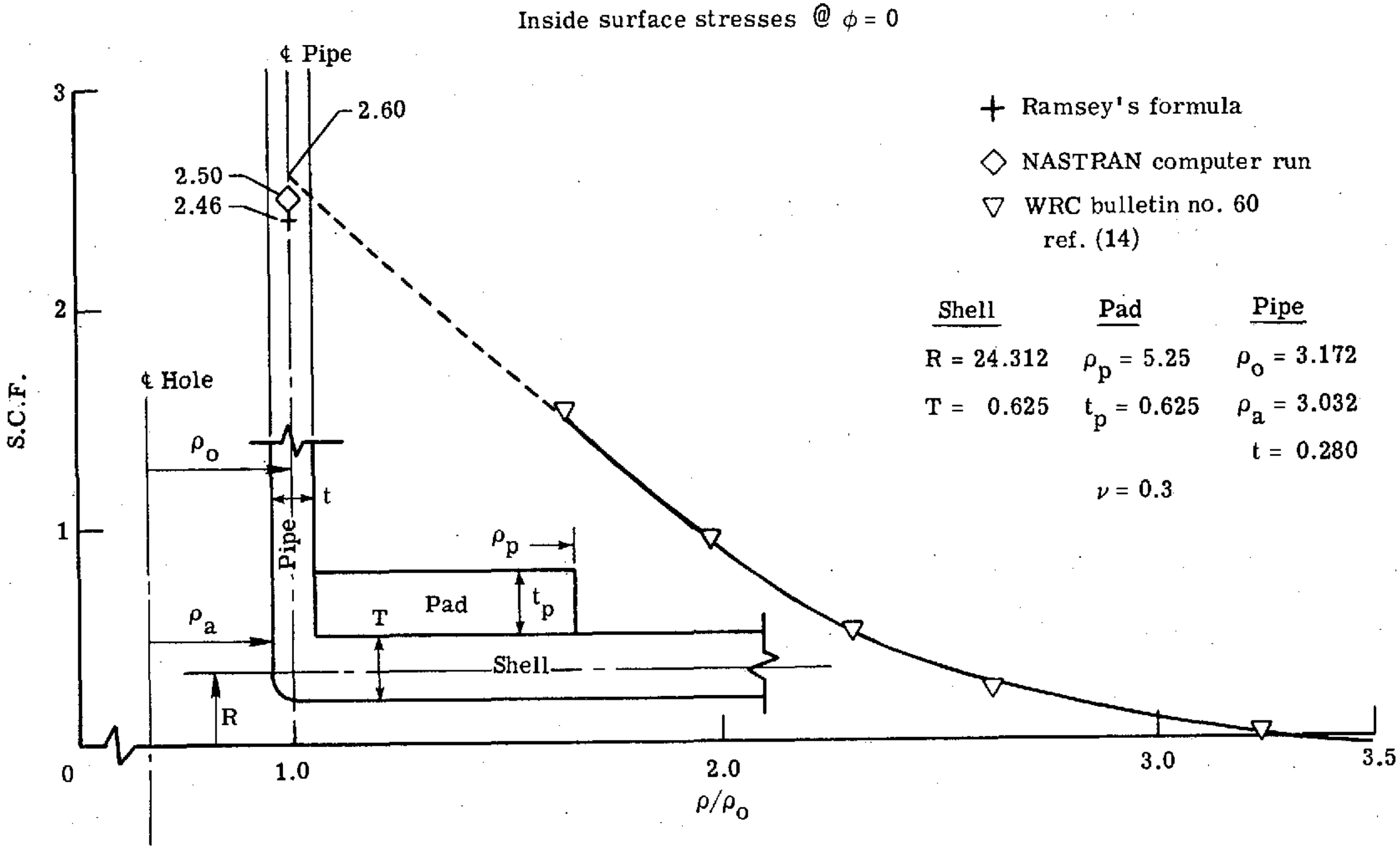

Figure 3.5.4.- Comparison of NASTRAN results with experimental data for shell, pipe and pad.

SHELL RADIAL SECTION DESCRIPTION	PIPE DESCRIPTION	PAD DESCRIPTION	SHELL PEAK SCF (I/S)	
			$\phi = 0$ & ρ_o NASTRAN	% DIFF
RQ	RDT	RQ	2.116	-18.62
LDT	RDT	LDT	2.498	-3.85
		"EXACT" REF (14) →		2.60

TABLE 3.5.2 - PEAK SCF FOR FINITE ELEMENT MODELS FOR A PRESSURIZED CYLINDRICAL SHELL WITH PIPE AND PAD: $\rho_o = 3.172$, $t = 0.280$, $R = 24.312$, $T = 0.625$, $\rho_p = 5.25$, $t_p = 0.625$, AND $\nu = 0.3$.

SHELL RADIAL SECTION DESCRIPTION	PIPE DESCRIPTION	PAD DESCRIPTION	SHELL PEAK SCF (I/S)	
			$\phi = 0$ & ρ_o NASTRAN	% DIFF
RQ	RDT	RQ	2.362	-5.90
LDT	RDT	LDT	2.399	-4.42
		"EXACT" REF (15) →		2.51

TABLE 3.5.3 - PEAK SCF FOR THE FINITE ELEMENT MODELS FOR A CYLINDRICAL SHELL WITH PIPE AND PAD: $\rho_o = 5.0785$, $t = 0.593$, $R = 19.0$, $T = 2.0$, $\rho_p = 9.482$, $t_p = 2.0$,

3.6 Shell, Pipe, and Pads

The shell, pipe, and pads configuration is often used in the design and construction of pressure vessels. One experimental investigation for this configuration was located through a paper by Kitching and Perkins.[23] The experimental results were for two intersecting circular cylinders (pipe and shell) reinforced with two pads (inside and outside of the shell) as shown in Figure 3.6.1. The experimental result was obtained during an investigation by the British Welding Research Association (BWRA).[24] The same shell, pipe, and pad models in previous sections are used; moreover, a quarter of the second pad is modeled identical to Figures 3.5.1 and 3.5.3. A summary of the peak SCF computer solutions, for the simplest and most accurate type (from previous sections) finite element configurations, is shown in Table 3.6.1. This is the only shell/pipe/pads experimental or numerical result available and the LDT type model has a difference of 9% above the exact answer. "However, the actual maximum value (SCF) would be slightly higher than the one measured in the test since it is impossible to measure immediately at a point of discontinuity."[23] The discontinuity point would be at the NASTRAN peak SCF location - inside shell surface at $\phi = 0$ and ρ_a. The difference would be < 9%, which is within engineering requirements. Therefore, the LDT shell, RDT pipe, and LDT pad(s) will be used in modeling all other numerical NASTRAN results.

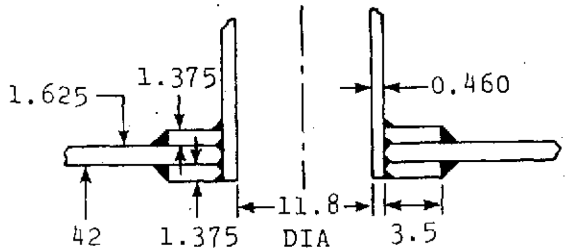

FIGURE 3.6.1 - DETAILS OF NOZZLE (PIPE) IN A SHELL REINFORCED WITH TWO PADS IN BWRA STUDIES.(24)

SHELL "RADIAL" SECTION DESCRIPTION	PIPE DESCRIPTION	TOP PAD DESCRIPTION	BOT. PAD DESCRIPTION	SCF	
				NASTRON	% DIFF
RQ	RDT	RQ	RQ	1.662	-7.67
LDT	RDT	LDT	LDT	1.964	9.11
				"EXACT" REF (24)	$\boxed{1.80}$

TABLE 3.6.1 - PEAK SCF FOR FINITE ELEMENT MODELS FOR A PRESSURIZED CYLINDER WITH PIPE AND PADS: ρ_o = 6.13, t = 0.46, R = 21.8125, T = 1.625, ρ_{OP} = 9.86, t_{OP} = 1.375, ρ_{ip} = 9.86, t_{ip} = 1.375, AND ν = 0.3.

CHAPTER IV

FORMULA

4.1 Introduction

In practical applications one frequently encounters problems in which a circular cylindrical shell is submitted to the action of forces distributed symmetrically with respect to the axis of the cylinder. The stress distribution in wind tunnels, cylindrical containers, and circular pipes under uniform internal pressure are examples of such problems.[34]

For the case of circular cylindrical shells arbitrarily loaded, two first approximation theories are of prime importance - (1) Love's first approximation theory and (2) its simplified version due to Donnell. The simplified version led to three partial differential equations in three displacement components. These three equations contain terms which higher approximation theories have shown to be negligible. It is therefore permissible to simplify the equations by omitting such terms.[9] If these terms are omitted (only pressure is considered) and the thickness of the shell is constant, these Donnell equations lead to a single fourth order equation in w, the radial deflection, for the case of axisymmetrically loaded circular cylindrical shells. This equation obtained by a number of authors[9,34-36] is

$$\frac{d^4w}{dZ^4} + \frac{ETw}{R^2D} = \frac{p}{D} \tag{13}$$

with

$$D = \frac{ET^3}{12(1 - \nu^2)}$$

where
- w is the radial deflection
- E is Young's Modulus of the shell
- R is the shell mid radius
- T is the shell thickness
- p is the internal pressure
- ν is the Poisson's ratio of the shell.

For the case of unsymmetrically loaded circular cylinders, the linear shallow, thin shell equations may be readily combined into two differential equations involving only the membrane stress function F and the normal displacement w. The compatibility and equilibrium equations are

$$\nabla^4 F = \frac{ET}{R} \frac{\partial^2 w}{\partial z^2}$$

(14)

$$\nabla^4 w + \frac{1}{RD} \frac{\partial F}{\partial z^2} = \frac{p}{D}$$

where $\nabla^4 = \frac{\partial}{\partial Z^4} + \frac{2\partial}{\partial Z^2 \partial y^2} + \frac{\partial}{\partial y^4}$.

Elimination of the function F between the two equations above yields an eighth order partial differential equation in w of the form

$$\nabla^8 w + \frac{Et}{DR^2} \frac{\partial^4 w}{\partial Z^4} = \frac{p}{D} \qquad (15a)$$

or

$$\nabla^8 w + 64\beta^4 \frac{\partial^4 w}{\partial Z^4} = \frac{p}{D} \qquad (15b)$$

where

$$\beta^4 \equiv \frac{ET}{16R^2 D} = \frac{3(1 - \nu^2)}{16R^2 T^2} .$$

Equations (15) are known as Donnell's linear theory.[1-3, 9-11]

4.2 Force Around Hole

The result of a perturbation solution to Equation (15b), modified to include a circular hole covered by a membrane (Figure 4.2.1), through terms of order $(\beta\rho_a)^2$ is a stress concentration factor at the hole-shell boundary.[2]

$$SCF = \frac{3}{2} + \cos 2\phi + \pi(\beta\rho_a)^2(1 + \tfrac{5}{4}\cos 2\phi) + \ldots \qquad (16)$$

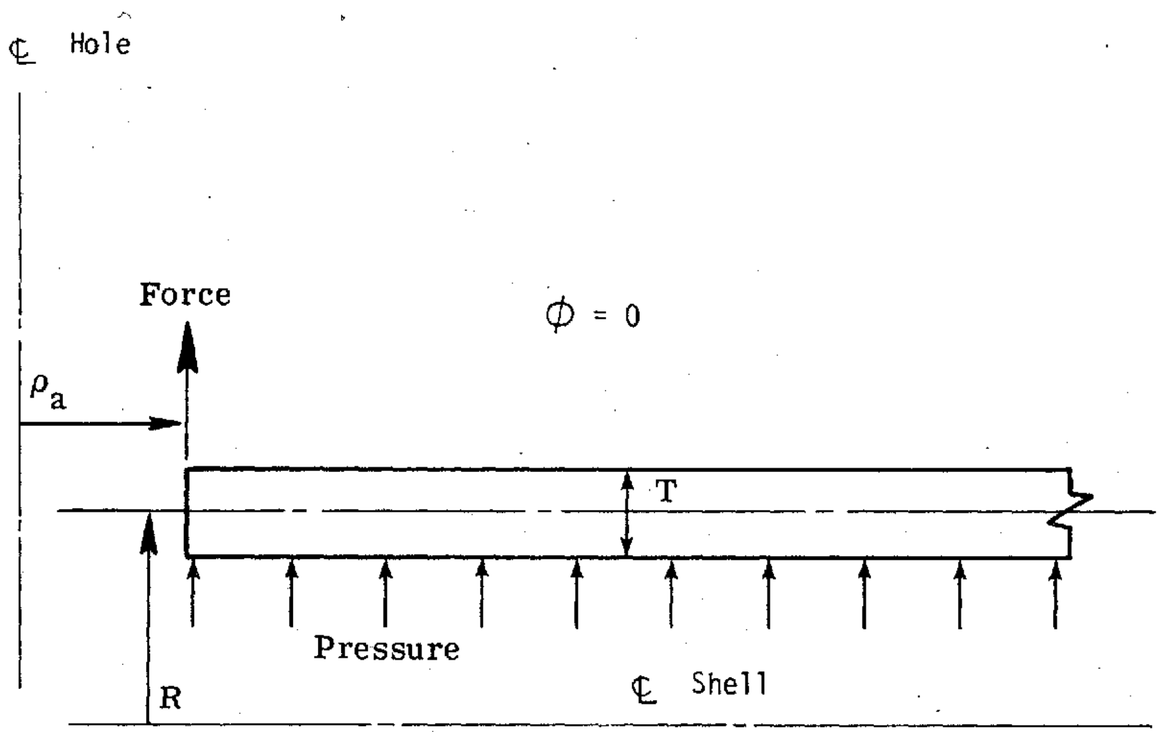

Figure 4.2.1.- Penetration (radius ρ_a) in a pressurized cylindrical shell (mid radius R, thickness T, and Poisson's ratio ν) covered by a membrane.

For the case of $\phi = 0$, Equation (16) becomes

$$SCF = 2.5 + \frac{9}{4}\pi \quad (\beta\rho_a)^2 \tag{17}$$

where ρ_a is the hole radius.

Savin's formula[4] for the same problem is

$$SCF = 2.5 + \frac{2.3}{RT}\rho_a^2 \quad . \tag{18}$$

Lind's equation[26] is

$$SCF = 1 + 4\ \beta\rho_a\ (1 \pm \frac{T}{2R}) \quad . \tag{19}$$

Mershon[27] obtained for the same problem but with a pipe intersecting the shell hole

$$SCF = 2.5 + \frac{\rho_o}{R}\ (\frac{2R}{T})^{1/2} = 2.5 + (\frac{2}{RT})^{1/2}\ \rho_o \tag{20}$$

where ρ_o is the pipe mid radius.

Mershon's Equation (20) is restricted to $t/T \simeq 0$ (force around hole only) or t/T small - where t is pipe thickness.

For $\nu = 0.3$, these Equations (16 through 20) reduce to

$$SCF_{\text{Van Dyke}} = 2.5 + \frac{2.92\ \rho_a{}^2}{RT} \tag{21a}$$

$$SCF_{Savin} = 2.5 + 2.3 \frac{\rho_a^{\,2}}{RT} \quad (21b)$$

$$SCF_{Lind} = 1 + 2.585 \frac{\rho_a}{(RT)^{1/2}} \quad (21c)$$

$$SCF_{Mershon} = \frac{2.5 + 1.414 \rho_o}{(RT)^{1/2}} \quad (21d)$$

The first attempt at a rational analysis of a long pressurized cylindrical shell having a small circular hole and closed at its ends is due to Lur'e.[6] Due to errors introduced in the boundary conditions, his results are incorrect. The terms in Equation (16) of order $(\beta\rho_a)^2$ were one-half the values obtained originally by Lur'e. This error was also confirmed by Eringen[8] and Lekkerkerker[1]. Eringen, Naghdi, and Thiel[3] presented a study using the exact solution of partial differential equations of thin, shallow, cylindrical shell theory. The boundary conditions were satisfied by use of Fourier series and the least square error technique through the aid of extensive numerical calculations of the force only around a circular hole in a cylindrical shell. A comparison of the results from this "exact" approach with Equation (21) is shown in Figure 4.2.2.

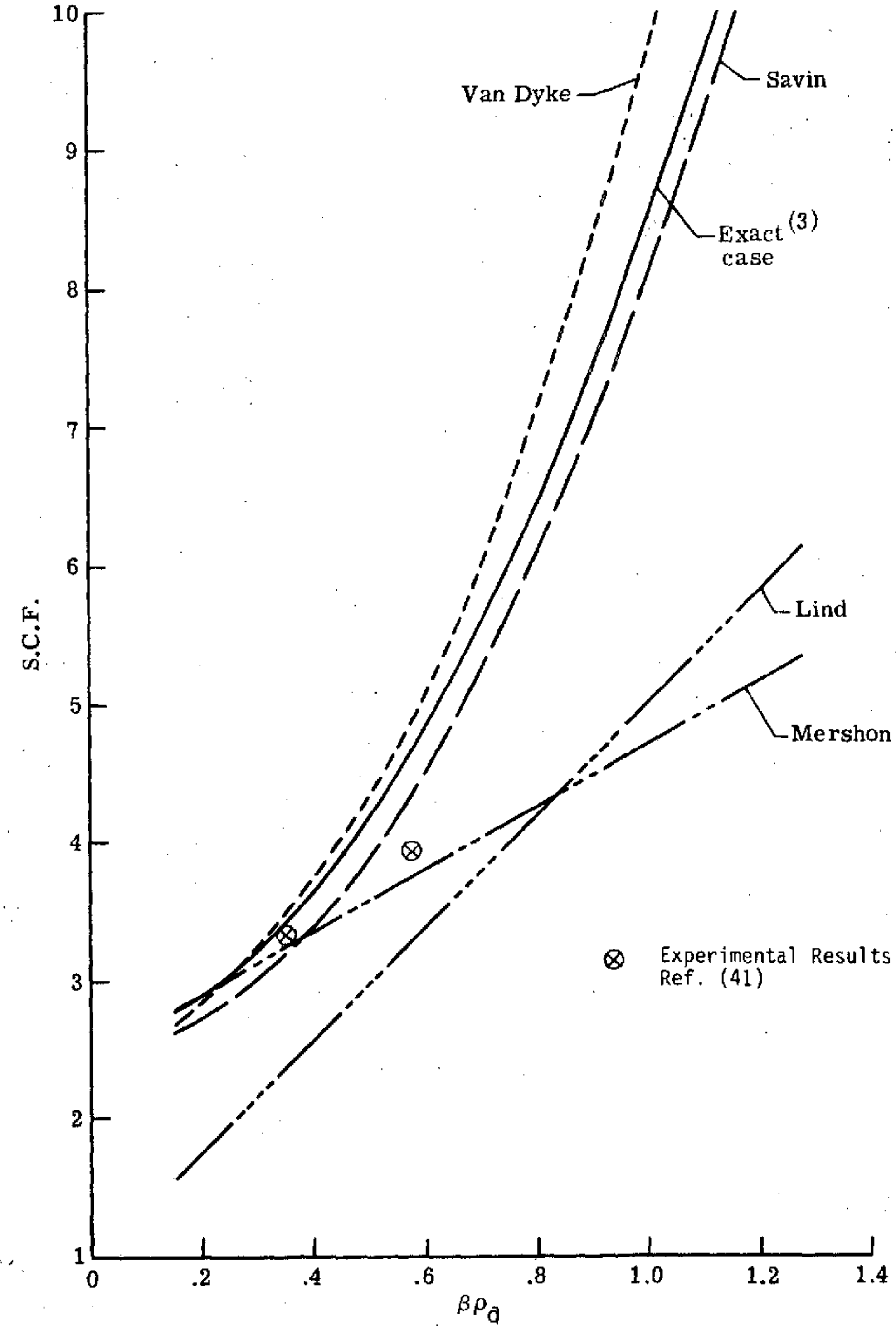

Figure 4.2.2.- Comparison of formulas with exact results.

The two experimental results are those of Houghtan and Rothwell.[41] In both of these experiments, only the membrane stresses were measured. The stress concentration factors correspond to the ratio of the maximum membrane stress at the hole to the membrane stress in the shell far from the hole. Excellent agreement is shown for the first data point ($\beta\rho_a = 0.35$). The experimental membrane covering the hole consisted of a very flexible, thin metal plug. This may have introduced slight restraints on the freedom of the hole edge. By measuring only the membrane stress and, perhaps, introducing the slight restraint, the peak SCF for the second experiment would be higher due to the larger size hole ($\beta\rho_a = 0.58$).

The Van Dyke Equation (21a) is the only conservative equation in comparison with the "exact" results[3] and the first experimental case. Van Dyke's starting series for small $\beta\rho_a$, given by Equation (16), is generally accurate to a $\beta\rho_a$ of about 0.3.[2] The required engineering accuracy is exceeded for $\beta\rho_a > 0.6$; therefore, this equation is the one chosen to improve on in the following format for the force around the hole

$$SCF_{Force} = 2.5 + \lambda \frac{\rho_a^2}{RT} \tag{22}$$

where 2.5 is the stress concentration factor for a flat plate weakened by a circular hole with the plate stretched per unit length in one direction and with one-half of this stretch per unit length in the other direction,

and

$\frac{\rho_a^{\,2}}{RT}$ is a function to increase the stress due to shell curvature and thickness, and hole size,

with λ for values of $\frac{\rho_a}{(RT)^{1/2}}$ shown in Figure 4.2.3.

The values of λ to go in Equation (22) can be taken from this curve (Figure 4.2.3) or the maximum value of $\lambda = 2.7$ could be used. This value is used in Equation (22) in this report. For $\nu = 0.3$ the result is

$$SCF_{\text{Force}} = 2.5 + 2.7 \frac{\rho_a^{\,2}}{RT} \qquad (23a)$$

or for any ν

$$SCF_{\text{Force}} = 2.5 + 6.537 \, (\beta\rho_a)^2 \qquad (23b)$$

where $\beta\rho_a = \frac{(3(1-\nu^2))^{1/4}}{2} \; \frac{\rho_a}{(RT)^{1/2}}$.

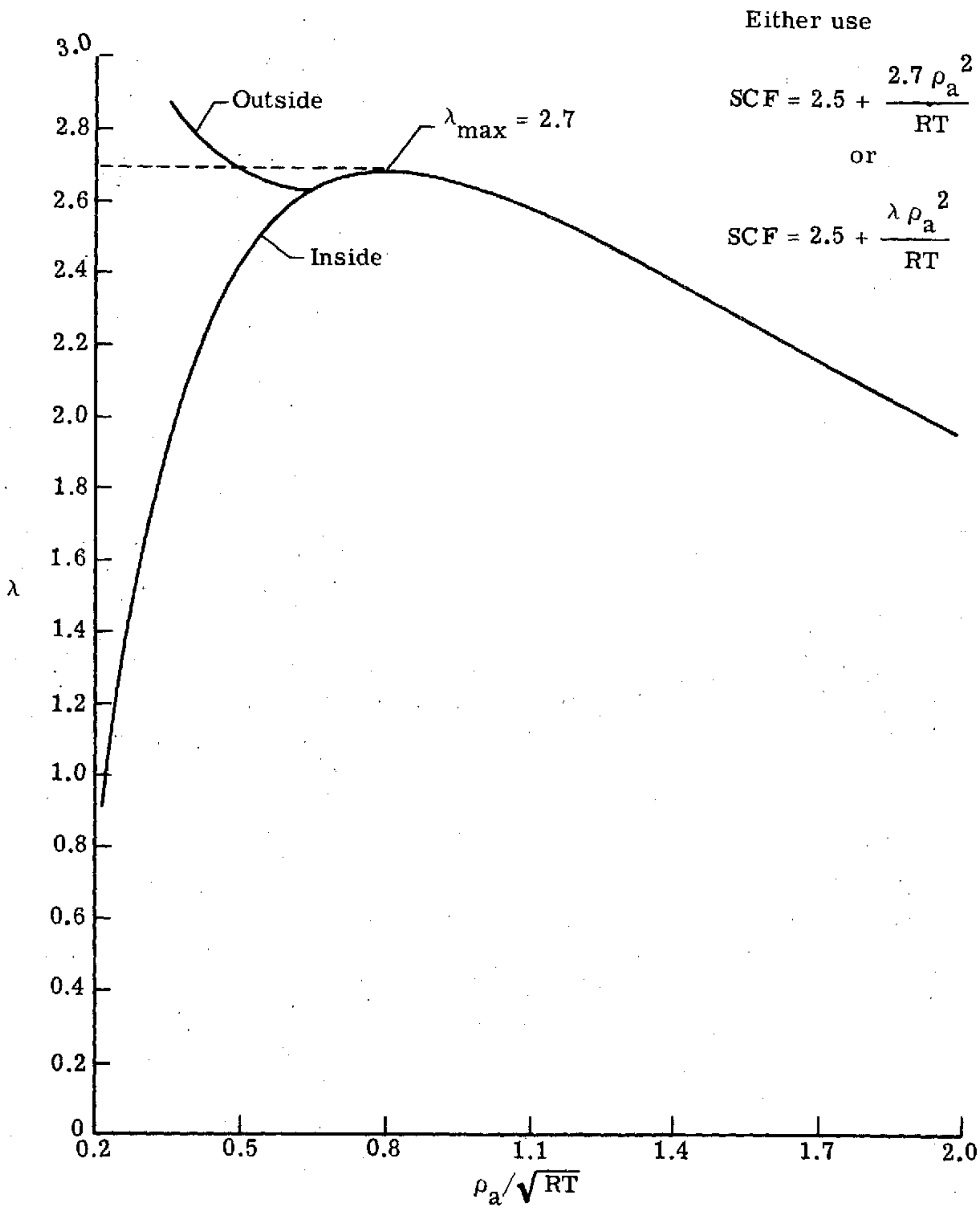

Figure 4.2.3.- Values of λ in shell with force equation.

4.3 Pipe Around Hole

The installation (physically or analytically) of a pipe into a cylindrical shell (Figure 4.3.1) reduces the peak stress concentration factor at the shell-pipe juncture. A function or reduction factor is needed to decrease this stress due to a small amount of reinforcement from the pipe. The reduction is dependent on the amount of pipe reinforcement (opening and pipe thickness) not needed to withstand the pressure. Thus, the following form is assumed

$$SCF_{Pipe} = SCF_{Force} \text{ (reduction factor)}. \qquad (24)$$

The usual pressurization of cylindrical vessels (wind tunnels) is analogous to a suddenly applied load.[37] The dynamic response of a structure due to this type load is a dynamic load factor of "one minus some term." Therefore, the above reduction factor takes the form

$$1 - (\beta\rho_o)^2 \text{ (pipe to shell thickness ratio)} \qquad (25)$$

where ρ_o is mid surface radius of the pipe and β is modified to include Poisson's ratio of the pipe. The pipe to shell thickness ratio (to be of the same order as β) will be taken as $(t/T)^{1/4}$. Equation (24) becomes

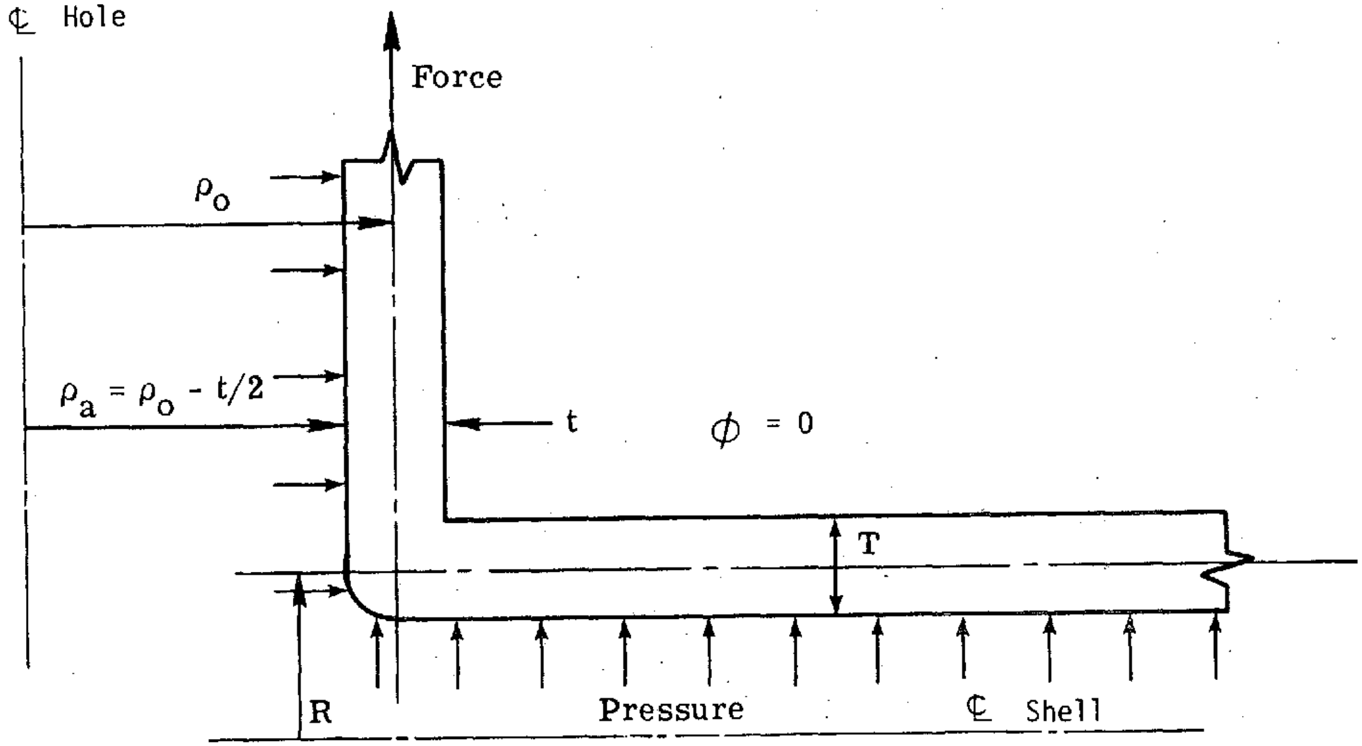

Figure 4.3.1.- Pipe (mid radius ρ_o, thickness t, and Poission's ratio ν_p) in a pressurized cylindrical shell (mid radius R, thickness T and Poission's ratio ν).

$$SCF_{pipe} = SCF_{force} \left| 1 - (\beta_1 \rho_o)^2 \left(\frac{t}{T}\right)^{1/4} \right| . \quad (26)$$

The total equation (23 and 26) developed thus far is

$$SCF_{pipe} = (2.5 + 6.537\ (\beta\rho_a)^2) \left| 1 - (\beta_1 \rho_o)^2 \left(\frac{t}{T}\right)^{1/4} \right| . \quad (27)$$

4.4 Pipe and Reinforcing Pad Around Hole

The addition of an inner or outer reinforcing pad to a pipe in a cylindrical shell is shown in Figure 4.4.1. The two new parameters introduced with this configuration are the outside radius (ρ_p) and the thickness (t_p) of the inner or outer pad. The major parameters from Equation (27) that contribute to this configuration's influence on the SCF are the mid radius (R), the thickness (T) of the shell and the inside radius (ρ_a), the thickness (t) of the pipe. Thus, a function to decrease the stress due to a reinforcing pad around the pipe or hole should contain ρ_p, R, ρ_a, t_p, and t or T. This function should be similar to $\beta\rho$ and multiplied times a pad to shell or pipe thickness ratio to some power. Note that

$$\beta\rho = \frac{(3(1 - \nu^2))^{1/4}}{2} \frac{\rho}{(RT)^{1/2}} \propto \frac{\rho_p}{(R\ \rho_a)^{1/2}} . \quad (28)$$

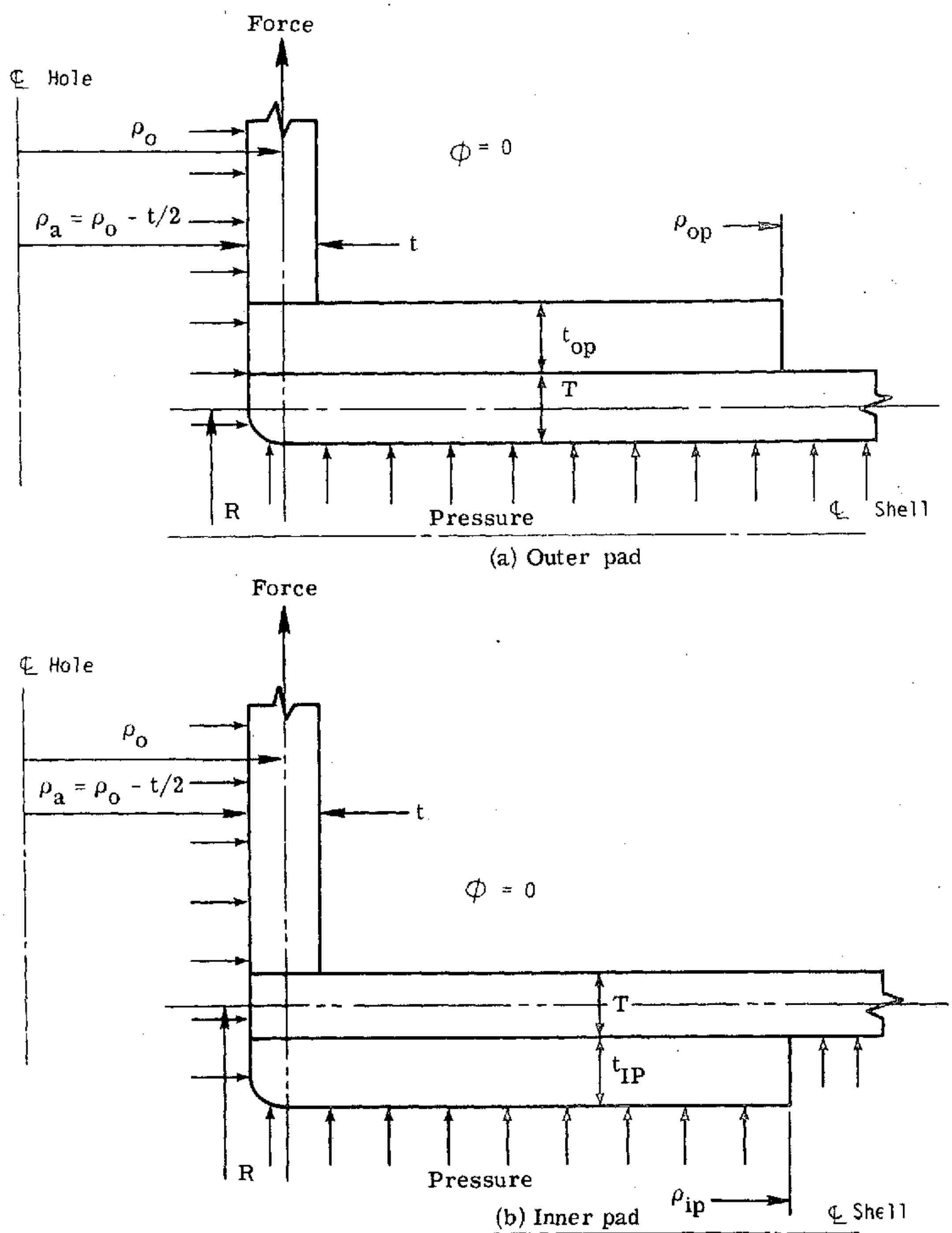

Figure 4.4.1.- Pipe (mid radius ρ_o, thickness t, and Poisson's ratio ν_p) in a pressurized cylindrical shell (mid radius R, thickness T and Poisson's ratio ν) reinforced with an inner or outer pad (outside radius ρ_p and thickness t_p).

The pad to shell or pipe thickness ratio (to be of the same order as β) will be taken as $(t_p/TH)^{1/4}$.

Therefore, the reduction in peak stress concentration factor due to an inner or outer reinforcing pad to a pipe in a cylindrical shell is

$$\frac{\rho_p}{(R\ \rho_a)^{1/2}} \left(\frac{t_p}{TH}\right)^{1/4} \tag{29}$$

where $TH = \begin{cases} t & \text{for case of a thin, thin shell where pipe thickness is more important than the shell} \\ T & \text{for approaching case of a thick shell where shell thickness is more important than the pipe.} \end{cases}$

The limits as to when each thickness should be used ($TH=t$ for $\frac{R}{T} > 33$ and $TH=T$ for $\frac{R}{T} \leq 33$) are discussed in Chapters V and VI under the presentation and discussion of results. The SCF equation becomes

$$SCF_{pad} = SCF_{pipe} - \frac{\rho_p}{(R\ \rho a)^{1/2}} \left(\frac{t_p}{TH}\right)^{1/4} \tag{30}$$

The total equation (27 and 30) developed thus far is

$$SCF_{pad} = (2.5 + 6.537(\beta\rho_a)^2)\left|1 - (\beta_1\rho_o)^2\left(\frac{t}{T}\right)^{1/4}\right| - \frac{\rho_p}{(R\ \rho_a)^{1/2}} \left(\frac{t_p}{TH}\right)^{1/4} \tag{31}$$

where ρ_p is outer or inner outside pad radius and t_p is outer or inner pad thickness.

4.5 Pipe and Reinforcing Pads Around Hole

The addition of inner and outer reinforcing pads to a pipe in a cylindrical shell is shown in Figure 4.5.1. The only new parameters introduced with this configuration are the outside radius and thickness of the second reinforcing pad. Therefore, the same type of term as Equation (29) will apply as a reduction to Equation (31) to obtain the peak stress concentration factor for two pads. The general SCF equation becomes

$$SCF = (2.5 + 6.537(\beta\rho_a)^2)\left|1 - (\beta_1\rho_o)^2\left(\frac{t}{T}\right)^{1/4}\right| - \frac{\rho_{op}}{(R\ \rho_a)}^{1/2}\left(\frac{t_{op}}{TH}\right)^{1/4} - \frac{\rho_{ip}}{(R\ \rho_a)}^{1/2}\left(\frac{t_{ip}}{TH}\right)^{1/4} \tag{32}$$

where subscripts o and i are for the outer and inner pads, respectively.

One can obtain the peak SCF for any of the previously developed five cases (force, pipe, outer pad, inner pad, and outer and inner pads) by merely substituting the appropriate parameters in Equation (32). For example, the pipe problem would be solved with $\rho_{op} = \rho_{ip} = t_{op} = t_{ip} = 0$, which would result in Equation (27). The practical approach

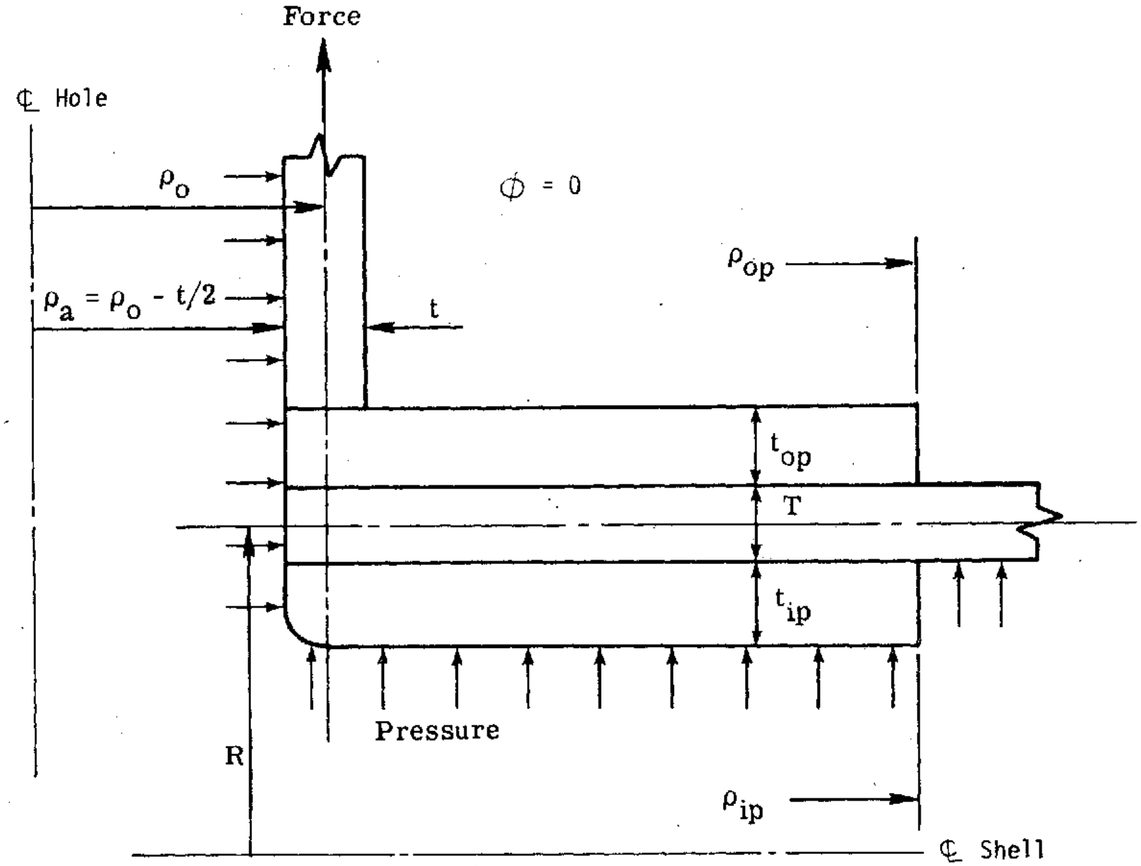

Figure 4.5.1.- Pipe and shell reinforced with inner and outer pads.

in the construction of cylindrical shells is to generally reinforce around pipes; therefore, these five configurations are the major thrust of this research. Another combination of cases can be addressed, i.e. force ($t = 0$) and pad(s). The physical significance of force, no pipe, and pad(s) could be (1) a cap welded to a reinforcing pad to close off an opening and (2) glass ports for observing the inside of cylindrical pressure vessels (test sections).

The accuracy of the formula is determined by comparing to available and applicable published numerical, theoretical, and experimental data and to the analytical (NASTRAN) results. Many different cases and examples of this formula were pursued in order to uncover the restrictions in the formula. The accuracy, results, and applications are presented and discussed in Chapters V and VI.

Since the formula is compared to theoretical (Shell theory) and to the author's computer (NASTRAN) results, the reliability of the answers from shell theory and NASTRAN in this study is needed. An analogy to the cylindrical shell problem is the example of pure bending of an infinite plate with a circular hole. Reissner[42] addresses this problem by including the effect of transverse shear deformations. It is assumed in Shell theory and NASTRAN that the stresses vary linearly across the thickness. Reissner obtained a factor 6/5 (in lieu of 1.0) in front of the transverse shear deformation terms in the stress-strain equations for two-dimensional plate theory. The significance of this difference is presented by comparing to an exact (three-dimensional elasticity theory) analysis of the plate with a circular hole subject to pure bending. The effect of transverse shear on the peak stress concentration factor is negligible provided ρ_a/T is greater than about 3.0. Therefore, even though Reissner's paper is concerned with a flat plate, the effect of transverse shear on this study will be negligible as long as $\rho_a/T > 3.0$ and $R/T > 25.0$.

It is permitted in NASTRAN to use any shear factor in front of the transverse shear deformation terms.[43,44] The factor used in this study is 1.0. Therefore, a slightly different SCF than the exact answer will be obtained. All of the theoretical and NASTRAN results presented in this study have a ρ_a/T ratio greater than 4.0, except the NASTRAN configurations where the shell thickness equals 8.96 ($\rho_a/T = 1.2$ and $R/T = 13$). It will be shown in Chapter V that for experimental results for $\rho_a/T < 0.6$ and $R/T \leq 15$, the transverse shear effects are not negligible.

CHAPTER V

PRESENTATION OF NUMERICAL RESULTS

5.1 Introduction

The finite element technique described in Section 2.1 has been used to complete numerical analyses for the configurations previously described (Section 2.2, Chapters III and IV): shell with force around hole, shell and pipe, and shell/pipe/pad(s). The units used throughout this study are in the English or American System (inches and pounds). Except where noted in these results, Poisson's ratio is taken as 0.3 and Young's modulus as 29 x 10^6 psi. The membrane stress of a cylindrical shell is well known.

$$\sigma_m = P \frac{R}{T} \tag{33}$$

The ratio of the largest principal stress at a point in question to that which would occur at that point if the shell were not penetrated will be called a stress concentration factor (SCF). This is defined by

$$\mathrm{SCF} = \frac{\text{Max. stress}}{\sigma_m} \tag{34}$$

where σ_m is defined by Equation (33).

The numerical (NASTRAN) results were calculated using Langley Research Center's CDC-6000 series computers. All of the NASTRAN models are composed of triangular and quadrilateral elements with both inplane and bending stiffness. The pressurized cylindrical shell with a circular penetration is modeled as follows:

1. General shell, Figure 3.3.1
2. Radial shell section, Figure 3.3.4
3. Pipe, Figure 3.4.2
4. Pad(s), Figure 3.5.3.

For all of the tabulated results, the peak SCF at the shell/hole or pipe/pad(s) juncture is given. Appendix A contains a representative NASTRAN run. The detail computer printouts of the numerous cases fill a volume of 7 cubic feet; therefore, for brevity, Appendix B contains typical one page summaries of the NASTRAN runs presented in this section and Chapter III. These summaries for shell thicknesses 0.896 and 2.215 are organized in the following configurations: force, pipe, pipe and pad, pipe and pads, force and pad, and force and pads.

The one page summary defines parameters used to model thatconfiguration: shell mid radius (R) and thickness (T); hole radius (ρ_a); pipe mid radius (ρ_o) and thickness (t); outer pad outside radius (ρ_{op}) and thickness (t_{op}); inner pad outside radius (ρ_{ip}) and thickness (t_{ip}); and Poisson's radio of shell (ν), pipe (ν_p), and pad(s) (ν_{PAD}). The location of each SCF is determined by (1) the angle (ϕ, see Figures 2.2.1 and 2.2.2); (2) inside surface (I/s) or outside surface (O/s) of shell, pipe, and pad(s); and (3) ratio of the grid point location (ρ, see Figures 2.2.1 and 2.2.2) divided by the pipe mid radius (ρ_o). The peak SCF used as the design criterion is the largest of all SCF values computed for a configuration.

The accuracy of the NASTRAN results is determined by comparing to theoretical and experimental data. Since limited data are available for reinforced penetrations, many different configurations were modeled to supplement the published "exact" data to provide the accuracy and restrictions to the formula.

5.2 Formula Restrictions and Conditions

The accuracy of the formula presented in Chapter IV was improved by imposing certain restrictions and conditions based on the results in this chapter. These results were from experimental, theoretical, published numerical, and the NASTRAN analytical results. The general restrictions inherent in any shell theory or finite element solution are as follows:

1. $\frac{\rho_o}{R} \leq \frac{1}{2}$ (Equation (9))

$$\left.\begin{array}{ll} 2. & \dfrac{\rho_o}{t} > 10 \\[2ex] 3. & \dfrac{R}{T} > 10 \end{array}\right\} \text{(thin shell theory)}$$

4. $\rho_a/T \geq 1.2$ (Transverse shear effect).

There are other conditions that the author has used to improve the accuracy of the formula. These conditions are

1. $\frac{t}{T} < 0.4$; use $SCF_{pipe} = SCF_{force}$,

   but retain the calculated SCF_{pipe} for $SCF_{pad(s)}$.

2. $TH = \begin{Bmatrix} t & \text{for } \frac{R}{T} > 33 \\ T & \text{for } \frac{R}{T} \leq 33 \end{Bmatrix}$ in Equation (32).

3. If ASME "coded" top or bottom pad[39] (approximately $A_{hole} \leq A_{reinf.}$), see Figure 5.2.1, and $\frac{\rho_o}{t} > 10$, then treat as a two pad problem with $\frac{1}{2}\,t_p$ on top and $\frac{1}{2}\,t_p$ on bottom.

4. $(\beta_1\,\rho_o)^2\,(\frac{t}{T})^{1/4} \leq 1.9$ or pipe is "ill-conditioned."

5. If $(\beta_1\,\rho_o)^2\,(\frac{t}{T})^{1/4} > 1.0$, treat as "coded" pad - condition 3.

6. If $0.9 < (\beta_1\,\rho_o)^2\,(\frac{t}{T})^{1/4} < 1.3$, use

   $e^{-(\beta_1\,\rho_o)^2\,(\frac{t}{T})^{1/4}}$ in Equation (32) in place of Equation (25).

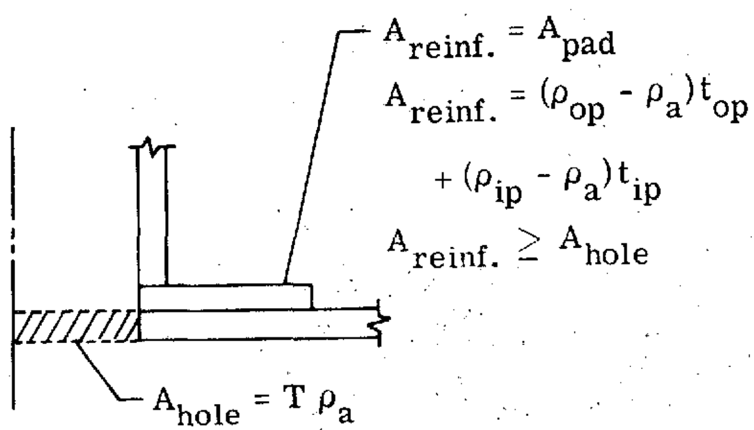

Figure 5.2.1.- Illustration of "reinforcement" required for ASME coded top or bottom pad. (38)

7. If $t = 0$ and configuration is pad(s) reinforced, then $\rho_p \equiv 2\ \rho_p$, TH = T, and treat as "coded" pad.
8. SCF from Equations (31) and (32) is always ≥ 1.0.

All the formula stress concentration factors are obtained from a computer program which is based on Equation (32) and these restrictions and conditions.

5.3 Force, Pipe, and Pipe/Pad(s)

Several calculations were obtained for the configuration of Figure 4.2.1, force around the hole. These results were computed to compare with theoretical ("exact") results[1,2,3] as well as to provide check points for the formula presented in Chapter IV, Equation (32). Throughout this chapter, the formula answers will be referred to as SCF Ramsey. The comparisons between NASTRAN/"exact" (N-E), Ramsey/NASTRAN (R-N), and Ramsey/"exact" (R-E) for different shell and force configurations are presented in Table 5.3.1. The second result in this table for $\frac{R}{T} = 156.5$ will arbitrarily be defined as the only membrane result. All other results in this table are in the thin shell theory realm, $\frac{R}{T} > 10$. The overall differences of the comparisons of the results are as follows: N-E, 17.4% and -8.9%; R-N, 8.6% and -12.8%; and R-E, approximately ±5%. The minus sign in this study always indicates less than and the plus sign greater than

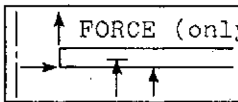

PEAK SCF @ $\phi = 0$ & ρ_a ON INSIDE SURFACE $\nu_S = 0.3$ $\frac{R}{T} > 10$

ρ_a	R	T	SCF NASTRAN	SCF "EXACT"	SCF RAMSEY	% DIFF N-E/R-N	% DIFF R-E
2.42	25	0.2	6.497	5.534	5.663	17.40 / -12.84	2.33
7.09	50	0.32	9.603	10.4	10.983	- 7.66 / 14.37	5.61
4.84	50	0.40	6.199	5.534	5.663	+12.02 / - 8.65	2.33
8.712	90	0.72	5.746	5.534	5.663	3.83 / - 1.44	2.33
10.842	112	0.896	5.406	5.534	5.663	- 2.31 / 4.75	2.33
13.0	112	1.084	5.907	6.027	6.259	- 1.99 / 5.95	3.85
14.52	150	1.2	5.404	5.534	5.663	- 2.35 / 4.79	2.33
13.309	112	1.25	5.643	5.746	5.916	- 1.79 / 4.84	2.96
13.0	112	1.25	5.555	5.614	5.760	- 1.05 / 3.69	2.60
12.285	112	1.25	5.374	5.319	5.411	1.03 / 0.69	1.73
12.25	50	2.0	6.033	6.257	6.552	- 3.58 / 8.60	4.71
13.309	112	2.1667	4.478	4.457	4.471	0.47 / - 0.16	0.31
10.7667	112	2.1667	3.884	3.774	3.790	2.92 / - 2.42	0.42
13.0	112	2.1667	4.464	4.371	4.380	2.13 / - 1.88	0.21
12.285	112	2.1667	4.331	4.170	4.179	+ 3.86 / - 3.51	0.22
13.2	72	2.215	5.233	5.353	5.450	- 2.24 / 4.15	1.81
12.01	112	2.9867	3.836	3.639	3.664	5.41 / - 4.48	.69
10.752	112	8.96	2.694	2.958	2.811	- 8.93 / 4.34	-4.97

Table 5.3.1 - NASTRAN, EXACT(1, 2, 3), and Formula Comparisons for Different Shell and Force Configurations.

the "exact" value. In Figure 5.3.1 all three curves (NASTRAN, "exact" and formula) are approaching the flat plate ($\beta = 0$) value at 2.5. For $\beta\rho_a < 0.6$ the three curves concide. For $\beta\rho_a > 0.6$ the NASTRAN curve is below (as expected) the "exact", and the formula curve is above (as desired).

The shell and pipe configurations (Figure 4.3.1) are presented in Tables 5.3.2 through 5.3.6 for different types of comparisons for various categories. The types of comparisons are as follows: NASTRAN/exact/Ramsey, Table 5.3.2; analytical/Ramsey, Table 5.3.4; and experimental/Ramsey, Tables 5.3.3, 5.3.5 and 5.3.6. The categories are defined as the following: thin shell, $\frac{R}{T} \geq 10$; and thick shell, $\frac{R}{T} < 10$; thin pipe, $\frac{\rho_o}{t} \geq 10$; and thick pipe, $\frac{\rho_o}{t} < 10$. Several NASTRAN thin shell and thin pipe configurations were modeled to compare to theoretical[1,11], numerical[7], and experimental[7,14,17,20,24] results (see Table 5.3.2(a) and 5.3.3(a). The overall differences of the thin shell and pipe NASTRAN results from the "exact" are -14.0% to 8.9%. The formula differences between NASTRAN and "exact"[1,7,11,14,17,20,24] are approximately $\pm$14%. Note the configuration where $\nu_p = 0.3$ and 0.5. The accuracy of the formula as compared to both NASTRAN solutions is approximately 3%.

The thin shell and thick pipe results are shown in Tables 5.3.2(b) and 5.3.3(b). Those in Table 5.3.2(b) are

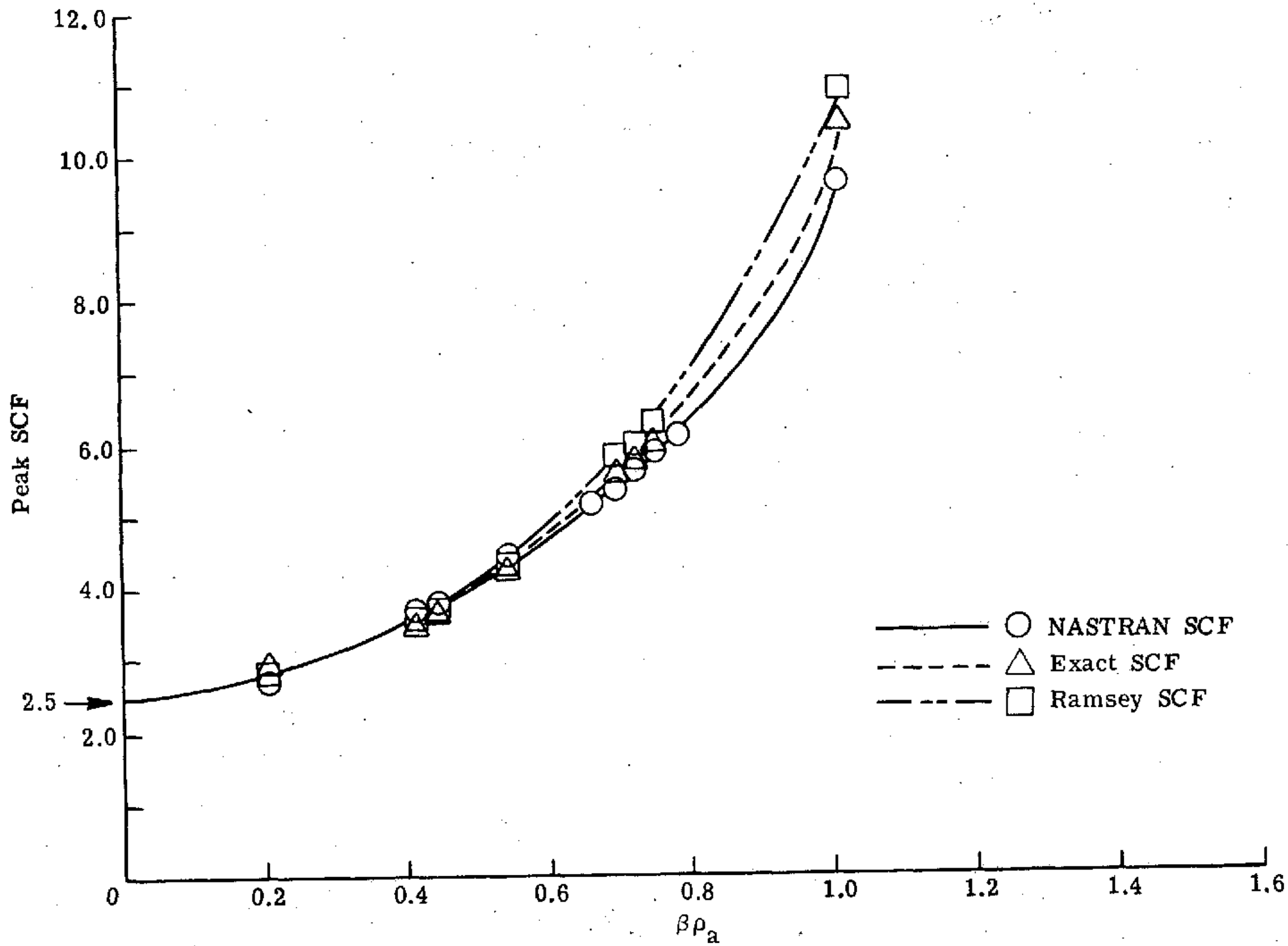

Figure 5.3.1.- Effect of shell thickness and curvature, and hole size ($\beta\rho_a$) on peak SCF for shell and force (t = 0) configurations.

Table 5.3.2 - NASTRAN, EXACT, and Formula Comparisons for Different Thin Shell and Thick/Thin Pipe Configurations: $\nu = 0.3$, $\nu_p = 0.3$; except as noted.

ρ_a	R	T	t	SCF NASTRAN	SCF "EXACT" Ref.(1, 11)	SCF RAMSEY	% DIFF N-E/R-N	% DIFF R-E
2.42	25	0.2	0.16	2.812	2.856	2.898	$\frac{-1.54}{3.06}$	1.47
7.09	50	0.32	0.32	3.139	-	3.921	24.91	
4.84	50	0.40	0.34	2.776	2.856	2.844	$\frac{-2.80}{2.44}$	- 0.42
8.712	90	0.72	0.576	2.760	2.856	2.898	$\frac{-3.36}{5.00}$	1.47
10.842	112	0.896	0.717	2.812	-	2.897	3.02	
10.842	112	0.896	0.717(ν_p = 0.5)	3.061	-	3.152	2.97	
13.0	112	1.084	1.3	2.462	2.490	2.107	$\frac{-1.12}{-14.42}$	-15.38
14.52	150	1.2	0.96	2.721	2.856	2.898	$\frac{-4.73}{6.51}$	1.47
13.309	112	1.25	0.6825	3.544	3.420	3.120	$\frac{3.63}{-11.96}$	- 8.77
13.0	112	1.25	1.3	2.563	2.660	2.562	$\frac{-3.65}{-0.04}$	- 3.68
12.25	50	2.00	0.5	4.728	4.94	-	- 4.29	
13.309	112	2.1667	0.682	4.211	4.459	4.471	$\frac{-5.56}{6.17}$	0.27
10.7667	112	2.1667	0.86668	2.992	3.157	3.146	$\frac{-5.23}{5.15}$	-0.35
13.0	112	2.1667	1.3	2.793	3.07	3.158	$\frac{-9.02}{13.07}$	2.87
13.2	72	2.215	1.1	2.809	3.268	3.210	$\frac{-14.04}{14.28}$	1.77
10.752	112	8.96	0.896	2.770	2.790	2.811	$\frac{-0.72}{1.48}$	0.75

(a) Thin Pipe $\frac{\rho_o}{t} \geq 10$

TABLE 5.3.2 - (concluded)

ρ_a	R	T	t	SCF NASTRAN	SCF "EXACT" Ref. ( )	SCF RAMSEY	% DIFF. N-E/R-N	% DIFF. R-E
3.032	24.312	0.625	0.28	3.078	2.84 (14)	3.209	8.38/4.26	12.99
6.0	21.8125	1.625	1.625	-	2.60 (24)	2,407		-7.42
2.475	5.0	0.1	.05	6.743	7.129 (7)	-	-5.42	-1.47
6.0	21.8125	1.625	1.000	-	3.000 (24)	2.956		

(a) Thin Pipe $\frac{\rho o}{t} \geq 10$

ρ_a	R	T	t	Ref.	SCF NASTRAN	SCF "EXACT"	SCF RAMSEY	% DIFF. N-E/R-N	% DIFF. R-E
12.285	112	2.1667	2.73	(1,11)	2.347	(2.580)	2.775	- 4.03/18.24	7.56
12.285	112	1.25	2.73	(1,11)	1.867	-	1.795	- 3.9	-
12.01	112	2.9867	4.48	(1,11)	2.332	2.345	2.647	- 0.55/13.51	12.88
4.125	22.6725	4.845	0.938	(24)	-	3.3	2.918		-11.576
4.125	22.6725	4.845	0.938	(24)	-	2.7	2.918		8.074
5.9375	22.6725	4.845	1.438	(24)	-	3.3	3.367		2.03

(b) Thick Pipe ($\rho_o/t < 10$)

Table 5.3.3 - Experimental and Formula Comparisons for Thin Shell (R/T $\geq$ 10) and Thin/Thick Pipe Configurations.

ρ_a	R	T	t	Reference	SCF "EXACT"	SCF RAMSEY	% DIFF
3.06	11.860	0.281	0.25	(17)	3.050	2.975	- 2.46
0.98	7.659	0.153	0.021	(20)	4.750	4.713	- 0.78
6.00	21.813	1.625	0.380	(17)	5.000	5.242	4.84

(a) THIN PIPE ($\rho_o/t \geq 10$)

0.97	24.844	1.688	0.730	(17)	3.120	2.524	-19.10
0.97	24.844	1.688	0.218	↓	3.060	2.561	-16.31
1.91	24.844	1.688	1.095	↓	2.980	2.589	-13.12
1.91	24.844	1.688	0.729	↓	2.980	2.622	-12.01
6.00	21.813	1.625	1.625	↓	2.700	2.407	-10.85
3.72	24.844	1.688	1.593	↓	2.910	2.719	- 6.56
6.00	21.813	1.625	1.000	↓	3.100	2.956	- 4.65

(b) THICK PIPE ($\frac{\rho_o}{t} < 10$)

slightly more accurate than the thin pipe results for both the formula ($\pm12\%$) and NASTRAN (-4%) as compared to the "exact"[1,11;24] results. For the same category, it is shown in Table 5.3.3(b) that the formula comparisons are below the experimental[17] by 19%. The first four configurations in Table 5.3.3(b) and the last three in Table 5.3.2(b) have $\rho_a/T \leq 1.1$. At the end of Chapter IV, it was stated that transverse shear effects would be negligible provided $\rho_a/T > 3.0$ and $R/T \geq 25.0$. Both of these requirements are violated. Therefore, the low SCF from the formula is to be expected since the hole is too small and/or the shell too thick. Therefore, the overall accuracy of the formula for a thin shell and thick pipe is approximately $\pm12\%$ by not including the configurations where $\rho_a/T < 1.1$ and $\frac{R}{T} < 14.7$.

The theoretical comparison of Eringen's[11] analytical results to the formula for the shell and pipe configurations is presented in Table 5.3.4. The accuracy between the two of $\pm8\%$ is remarkable. The cases are tabulated by per cent difference from lowest to highest. These are the only valid cases from this report. The others violated all four of <u>his</u> theoretical requirements:

$R/T > 10$, $\rho_o/t > 10$, $\beta\rho_o < 0.5$, and $\rho_o/R \leq 1/3$.

Tables 5.3.5 and 5.3.6 present numerous experimental[8,11,16,17,19,21,22,135] configurations for thick

Table 5.3.4 - Formula and Analytical[11] Comparison for Shell and Pipe Configurations.

CASE NO.	2R/T	ρo/R	$\beta\rho_o$	t/T	SCF-LIT (Ref.(11)	SCF RAMSEY	% DIFF
131	250.00	.050	.35900	.1000	3.63	3.330	-8.26
104	100.00	.100	.45400	.1000	4.11	3.823	-6.98
102	100.00	.100	.45400	.4000	3.31	3.130	-5.43
125	250.00	.025	.18000	.0250	2.86	2.709	-5.27
132	250.00	.050	.35900	.0500	3.52	3.337	-5.20
124	250.00	.025	.18000	.0500	2.85	2.708	-5.00
126	250.00	.025	.18000	.0125	2.85	2.710	-4.91
127	250.00	.025	.18000	.0062	2.85	2.711	-4.89
64	50.00	.050	.16100	.0125	2.80	2.667	-4.75
130	250.00	.050	.35900	.2000	3.48	3.317	-4.68
20	10.00	.250	.35900	.1250	3.42	3.261	-4.63
63	50.00	.050	.16100	.0250	2.79	2.665	-4.47
16	10.00	.100	.14400	.0250	2.75	2.628	-4.42
97	100.00	.050	.22700	.0500	2.96	2.831	-4.37
98	100.00	.050	.22700	.0250	2.96	2.834	-4.25
99	100.00	.050	.22700	.0125	2.96	2.836	-4.20
21	10.00	.250	.35900	.0625	3.44	3.302	-4.01
32	25.00	.050	.11400	.0125	2.69	2.583	-3.99
91	100.00	.025	.11400	.0125	2.69	2.584	-3.96
92	100.00	.025	.11400	.0062	2.69	2.584	-3.94
18	10.00	.250	.35900	.5000	2.82	2.711	-3.88
38	25.00	.100	.22700	.0250	2.94	2.831	-3.71
103	100.00	.100	.45400	.2000	3.94	3.797	-3.64
39	25.00	.250	.56800	2.0000	2.22	2.142	-3.51
123	250.00	.025	.18000	.1000	2.80	2.704	-3.42
31	25.00	.050	.11400	.0250	2.67	2.581	-3.33
90	100.00	.025	.11400	.0250	2.67	2.583	-3.27
62	50.00	.050	.16100	.0500	2.75	2.662	-3.20
129	250.00	.050	.35900	.4000	3.05	2.953	-3.17
37	25.00	.100	.22700	.0500	2.91	2.824	-2.95
96	100.00	.050	.22700	.1000	2.91	2.824	-2.95
15	10.00	.100	.14400	.0500	2.70	2.662	-2.89
19	10.00	.250	.35900	.2500	3.27	3.183	-2.65
56	50.00	.025	.08000	.0125	2.61	2.541	-2.63
57	50.00	.025	.0800	.0062	2.61	2.542	-2.61
119	250.00	.010	.07200	.0050	2.60	2.534	-2.55
120	250.00	.010	.07200	.0025	2.60	2.534	-2.55
105	100.00	.100	.45400	.0500	3.93	3.837	-2.38
11	10.00	.050	.07200	.0125	2.59	2.582	-2.24
118	250.00	.010	.07200	.0100	2.59	2.533	-2.18
55	50.00	.025	.08000	.0250	2.59	2.541	-1.91
89	100.00	.025	.11400	.0500	2.63	2.581	-1.86
117	250.00	.010	.07200	.0200	2.58	2.533	-1.81
30	25.00	.050	.11400	.0500	2.62	2.578	-1.61
10	10.00	.050	.07200	.0250	2.57	2.530	-1.54

Table 5.3.4 (Continued)

CASE NO.	2R/T	ρo/R	$\beta\rho_o$	t/T	SCF-LIT Ref.(11)	SCF RAMSEY	% DIFF
134	250.00	.050	.35900	.0125	3.38	3.342	-1.12
116	250.00	.010	.07200	.0400	2.55	2.533	-0.68
71	50.00	.100	.32100	.0250	3.19	3.168	-0.68
69	50.00	.100	.32100	.1000	3.16	3.148	-0.37
133	250.00	.050	.35900	.0250	3.35	3.340	-0.29
70	50.00	.100	.32100	.0500	3.17	3.162	-0.27
54	50.00	.025	.08000	.0500	2.54	2.539	-0.04
9	10.00	.050	.07200	.0500	2.52	2.527	0.29
36	25.00	.100	.22700	.1000	2.79	2.811	0.75
61	50.00	.050	.16100	.1000	2.63	2.656	0.97
6	13.13	.129	.21300	.1335	2.72	2.750	1.11
114	250.00	.010	.07200	.1600	2.49	2.530	1.59
14	10.00	.100	.14400	.1000	2.56	2.609	1.93
106	100.00	.100	.45400	.0250	3.77	3.843	1.94
115	250.00	.010	.07200	.0800	2.48	2.532	2.08
43	25.00	.250	.56800	.1250	4.42	4.526	2.39
35	25.00	.100	.22700	.2000	2.72	2.786	2.41
87	100.00	.025	.11400	.2000	2.51	2.571	2.45
34	25.00	.100	.22700	.4000	2.56	2.626	2.58
88	100.00	.025	.11400	.1000	2.51	2.578	2.70
60	50.00	.050	.16100	.2000	2.56	2.643	3.24
29	25.00	.050	.11400	.1000	2.49	2.571	3.27
41	25.00	.250	.56800	.5000	3.02	3.123	3.40
53	50.00	.025	.08000	.1000	2.45	2.536	3.50
122	250.00	.025	.18000	.2000	2.60	2.698	3.76
86	100.00	.025	.11400	.4000	2.43	2.533	4.24
59	50.00	.050	.16100	.4000	2.46	2.565	4.27
95	100.00	.050	.22700	.2000	2.69	2.811	4.50
68	50.00	.100	.32100	.2000	2.97	3.122	5.12
8	10.00	.050	.07200	.1000	2.39	2.522	5.51
52	50.00	.025	.08000	.2000	2.39	2.530	5.85
28	25.00	.050	.11400	.2000	2.41	2.560	6.20
137	250.00	.100	.71800	.4000	3.20	3.403	6.35
44	25.00	.250	.56800	.0625	4.28	4.567	6.71
67	50.00	.100	.32100	.4000	2.64	2.820	6.80
121	250.00	.025	.18000	.4000	2.44	2.616	7.20
94	100.00	.050	.22700	.4000	2.49	2.672	7.29
13	10.00	.100	.14400	.2000	2.41	2.586	7.32
128	250.00	.050	.35900	.8000	2.65	2.844	7.34
101	100.00	.100	.45400	.8000	2.72	2.933	7.82

Table 5.3.5 - Experimental and Formula Comparisons for Different Thick Shell and Pipe (R/T and $\rho_o/t < 10$) Configurations.

ρ_a	R	T	t	Reference	SCF "EXACT"	SCF RAMSEY	% DIFF. R-E
1.41	3.67	0.590	0.445	(21)	3.070	2.620	-14.66
0.91	3.652	0.553	0.281		3.360	2.920	-13.10
0.91	3.653	0.555	0.285		3.320	2.915	-12.20
0.56	3.286	1.011	0.093		3.090	2.755	-10.84
0.91	3.656	0.563	0.279		3.280	2.921	-10.95
1.00	19.000	2.000	0.188		2.780	2.571	- 7.52
1.41	3.670	0.590	0.400		2.840	2.745	- 3.35
0.44	3.694	0.568	0.073	(8,11,21)	2.800	2.749	- 1.82
1.09	3.578	0.377	0.434	(21)	2.280	2.235	- 1.97
1.41	3.315	1.009	0.236		4.110	4.105	- 0.12
0.68	3.658	0.565	0.112		3.040	3.104	2.11
0.91	3.653	0.565	0.227		2.900	2.985	2.93
0.17	3.516	0.565	0.027		2.450	2.539	3.63
0.51	3.670	0.490	0.218	(16)	2.520	2.683	6.47

Table 5.3.6 - Formula and Experimental Comparison for Thick Shell and Thick Pipe Configurations.

ρ_a	R	T	t	Reference	SCF "EXACT"	SCF RAMSEY	% DIFF.
4.78	19.00	2.0	2.405	(17)	3.140	2.444	-22.17
2.88	9.50	1.0	0.432	(22)	3.779	3.216	-14.90
0.91	3.652	0.553	0.281	(21)	3.360	2.920	-13.10
0.92	3.648	0.546	0.280		3.360	2.928	-12.86
0.91	3.653	0.550	0.285	(17)	3.320	2.915	-12.20
4.13	22.673	4.845	0.94		3.300	2.919	-11.55
0.95	3.653	0.555	0.285	(21)	3.320	2.940	-11.45
0.56	3.286	1.011	0.092	(17)	3.090	2.755	-10.84
0.91	3.656	0.563	0.279	(17, 21)	3.280	2.921	-10.95
3.72	24.844	4.188	0.593	(17)	3.100	2.859	- 7.77
1.45	19.0	2.0	1.144	(17)	2.750	2.547	- 7.38
1.0	19.0	2.0	0.188	(17, 135)	2.760	2.571	- 6.85
0.92	3.650	0.565	0.277	(19)	2.900	2.931	1.07
5.94	22.673	4.845	1.440	(17)	3.300	3.367	2.03
0.91	3.658	0.565	0.227	(17, 21)	2.900	2.985	2.93
0.68	3.658	0.565	0.112	(17, 21)	3.000	3.104	3.47
0.17	3.658	0.565	0.027		2.450	2.538	3.59
0.51	3.620	0.490	0.369		2.220	2.593	16.80

shells and pipes. The comparison between the formula and these experiments are presented to illustrate the need to impose the restrictions presented in Section 5.2. The differences between the formula and thick shell and pipe experimental results are -22% to +17%.

The shell/pipe/pad (top and bottom) configurations (Figure 4.4.1) are listed in Tables 5.3.7 through 5.3.9. The same categories as shell and pipe are maintained for the shell/pipe/pad comparisons. The comparisons are for NASTRAN, formula, and six experimental results. The thin shell and pipe ($\frac{R}{T}$ and $\frac{\rho_o}{t} \geq 10$) cylinders with a top pad are presented in Table 5.3.7. The differences of the formula as compared to NASTRAN for the top pad are -15.9% to 11.4%. The thin shell and pipe with a bottom pad are listed in Table 5.3.8. The formula differences for the bottom pad as compared to NASTRAN and the one experimental result[24] are -16.1% to +3.2%. The thick pipe ($\frac{\rho_o}{t} < 10$), thin/thick shell, and pad results are shown in Table 5.3.9.

The last three configurations in Table 5.3.7 and first three in Table 5.3.9 have only one difference - Poisson's ratio. There are 0.8% (Table 5.3.7) and 1.0% (Table 5.3.9) differences between the NASTRAN SCF for all ν's = 0.3 and for $\nu = 0.3$, $\nu_p = \nu_{pad} = 0.5$. Based on these six examples, the formula only provides a different Poisson's ratio for

Table 5.3.7 - NASTRAN, EXPERIMENTAL, and Formula Comparison for Thin Shell, Thin Pipe, and Top Pad Configurations.

ρ_a/ρ_o	R	T	t	ρ_{op}	t_{op}	SCF NASTRAN	SCF RAMSEY	% Diff.
2.42 2.50	25	0.2	0.16	4.25	0.125	2.403	2.384	- 0.79
7.09 7.25	50	0.32	0.32	11.25	0.25	2.889	2.976	3.01
4.84 5.01	50	0.4	0.34	8.5	0.25	2.369	2.338	- 1.31
8.712 9.00	90	0.72	0.576	14.75	0.50	2.303	2.389	3.73
10.842 11.2	112	0.896	0.7168	19.85935	0.50	2.403	2.377	- 1.08
10.842 11.2	112	0.896	0.7168	20.0	1.00	1.945	1.848	- 4.99
14.52 15.00	150	1.200	0.96	23.0	1.00	2.154	2.400	11.42
13.309 13.65	112	1.25	0.6825	24.999	1.50	2.134	1.795	-15.89
13.0 13.65	112	1.25	1.3	24.999	1.50	1.868	1.883	0.80
12.031 12.50	125	1.25	0.938	21.5	1.50	1.924	2.030	5.51
12.25 12.50	50	2.00	0.50	21.0	1.50	2.908	2.772	- 4.68
13.309 13.65	112	2.1667	0.6825	24.999	1.50	2.421	2.620	8.22
10.7667 11.2	112	2.1667	0.86668	18.5625	1.50	2.396	2.533	5.72
13.0 13.65	112	2.1667	1.3	24.999	1.50	2.259	2.479	9.74

TABLE 5.3.7 - (Concluded)

ρ_a/ρ_o	R	T	t	ρ_{op}	t_{op}	SCF NASTRAN	SCF RAMSEY	% Diff.	SCF "Exact" or Notes
13.2 13.75	72	2.215	1.10	23.0	1.50	2.783	2.533	- 8.98	
10.752 11.2	112	8.96	0.896	20.64	5.00	2.316	2.215	- 4.36	
3.032 3.172	24.312	0.625	0.28	5.25	0.625	2.498	2.461	- 3.85 - 1.48 - 5.35	Ref. (14) 2.60 $\nu=0.3$
3.032 3.172	24.312	0.625	0.28	5.25	0.625	2.484	2.546	2.50	$\nu=0.3$ $\nu_p=0.5$ $\nu_{pad}=0.3$
3.032 3.172	24.312	0.625	0.28	5.25	0.625	2.476	2.546	2.83	$\nu=0.3$ $\nu_p=0.5$ $\nu_{pad}=0.5$

Table 5.3.8 - NASTRAN and Formula Comparison for Thin Shell, Thin Pipe, and Bottom Pad Configurations.

ρ_a/ρ_o	R	T	t	ρ_{ip}	t_{ip}	SCF NASTRAN	SCF RAMSEY	% DIFF.	SCF "Exact" Ref. (24)
10.842 11.2	112	0.896	0.7168	20.25	1.00	1.779	1.835	3.15	—
13.0 13.65	112	1.25	1.30	25.0	1.50	1.824	1.883	3.23	—
13.2 13.75	72	2.215	1.10	23.0	1.50	3.019	2.533	-16.10	—
5.9 6.135	21.813	1.625	0.469	9.869	2.75		1.827	-3.84	1.900

Table 5.3.9 - NASTRAN, Experimental, and Formula Comparison for Thick/Thin Shell, Thick Pipe, and Top Pad Configurations.

ρ_a/ρ_o	R	T	t	ρ_{op}	t_{op}	NOTES	SCF NASTRAN	SCF "EXACT"	SCF RAMSEY	% DIFF N-E/R-N	% DIFF R-E
4.782 5.0785	19	2.0	0.593	9.482	2.0		2.399	(15) 2.51	2.277	-4.42 -5.09	-9.28
4.782 5.0785	19	2.0	0.593	9.482	2.0	$\nu_p=0.5$	2.349		2.355	0.26	
4.782 5.0785	19	2.0	0.593	9.482	2.0	$\nu_p=\nu_{PA}=0.5$	2.372		2.355	-0.72	
2.88 3.095	9.5	1.0	0.43	4.858	2.0			(17) 2.07	2.105		+1.7
2.88 3.095	9.5	1.0	0.43	5.437	1.125			(17) 2.22	2.149		-3.2
2.8815 3.0975	9.5	1.0	0.432	5.4375	1.125			(22) 2.295	2.145		-6.5

(a) Thick Shell.

Table 5.3.9 (Continued)

ρ_a/ρ_o	R	T	t	ρ_{op}	t_{op}	SCF NASTRAN	SCF RAMSEY	% DIFF.
12.285 13.65	112	2.1667	2.73	24.999	1.50	1.914	2.195	14.68
12.01 14.25	112	2.9867	4.48	18.0	2.00	2.212	2.246	1.54
12.285 13.65	112	1.25	2.73	24.999	1.50	1.379	1.215	-11.89

(b) Thin Shell

the shell and pipe. The overall differences between NASTRAN and the formula for the shell/pipe/and pad (top and bottom) are -16.1% to 11.4%. The comparisons between experiments and the formula are -9.3% to 1.7% differences.

The NASTRAN/formula comparisons for shell, pipe, and pads configurations (see Figure 4.5.1) are presented in Table 5.3.10. All of these results are for thin shell and pipe except the three thick pipe configurations denoted by an asterisk (*) in the "exact" column. The "two pad" experimental investigation presented in Chapter III is also included. The configuration that is presented in Appendix A as a representative NASTRAN program is indicated by "Appendix A" in the "exact" column. Most of the SCF values obtained are for configurations that represent current pressure vessel analysis, design, and construction - i.e. identical inner and outer pad thicknesses and outside radii. The fifth through the seventh configurations in Table 5.3.10 have different geometries for the two pads. The accuracy of the formula for these examples is approximately $\pm 6\%$. The overall accuracy is -8.91% to +14.65% difference.

Figures 5.3.2 and 5.3.3 are representative of the manner in which peak stress concentration factors (SCF) for a pressurized cylindrical shell are affected by (1) thickness and curvature of shell and hole size ($\beta\rho_a$), and (2) reinforcement configurations (pipe and pipe/pad(s)).

Table 5.3.10 - NASTRAN, Experimental and Formula Comparison for Thin Shell, Thin Pipe, and Pads Configuration.

ρ_a & ρ_o	R	T	t	ρ_{oP}	t_{oP}	ρ_{iP}	t_{iP}	SCF NASTRAN	SCF "EXACT"	SCF RAMSEY	% DIFF.
2.42 2.50	25	0.2	0.16	4.25	0.125	4.25	0.125	1.871	-	1.870	0.05
7.09 7.25	50	0.32	0.32	11.25	0.25	11.25	0.25	1.940	**	2.032	4.74
4.84 5.01	50	0.4	0.34	8.5	0.25	8.5	0.25	1.846		1.832	- 0.76
8.712 9.000	90	0.72	0.576	14.75	0.50	14.75	0.50	1.735		1.881	8.42
10.842 11.2	112	0.896	0.7168	19.85935	0.50	19.85935	0.50	1.967		1.856	- 5.64
10.842 11.2	112	0.896	0.7168	19.85935	0.50	17.43	0.75	1.855		1.871	0.86
10.842 11.2	112	0.896	0.7168	19.85935	0.50	19.85935	1.00	1.656		1.757	6.10
14.52 15.00	150	1.200	0.960	23.0	1.00	23.0	1.00	1.659		1.902	14.65
13.309 13.65	112	1.25	0.6825	24.999	1.50	24.999	1.50	1.383		1.544	11.64
13.0 13.65	112	1.25	1.3	24.999	1.50	24.999	1.50	1.295		1.204	- 7.03
12.285 13.65	112	1.25	2.73	24.999	1.50	24.999	1.50	1.032	*	1.000	- 3.10
12.25 12.50	50	2.00	0.50	21.0	1.50	21.0	1.50	2.177		1.983	- 8.91
13.309 13.65	112	2.1667	0.6825	24.999	1.50	24.999	1.50	1.904		1.832	- 3.78
10.7667 11.2	112	2.1667	0.86668	18.5625	1.50	18.5625	1.50	1.876		1.920	2.35

TABLE 5.3.10 - (Concluded)

ρ_a & ρ_o	R	T	t	ρ_{oP}	t_{oP}	ρ_{iP}	t_{iP}	SCF NASTRAN	SCF "EXACT"	SCF RAMSEY	% DIFF.
13.0 13.65	112	2.1667	1.3	24.999	1.50	24.999	1.50	1.820		1.800	-1.10
12.285 13.65	112	2.1667	2.73	24.999	1.50	24.999	1.50	1.626	*	1.615	-0.68
13.2 13.75	72	2.215	1.10	23.0	1.50	23.0	1.50	1.957	APPENDIX A	1.856	-5.16
12.01 14.25	112	2.9867	4.48	18.0	2.00	18.0	2.00	1.935	*	1.845	-4.65
10.752 11.2	112	8.96	0.896	20.64	5.00	20.64	5.00	1.527		1.701	11.40
5.90 6.13	21.813	1.625	0.460	9.86	1.38	9.86	1.38	1.964	Ref.(23&24) 1.80	1.838	9.11 -6.42 2.11

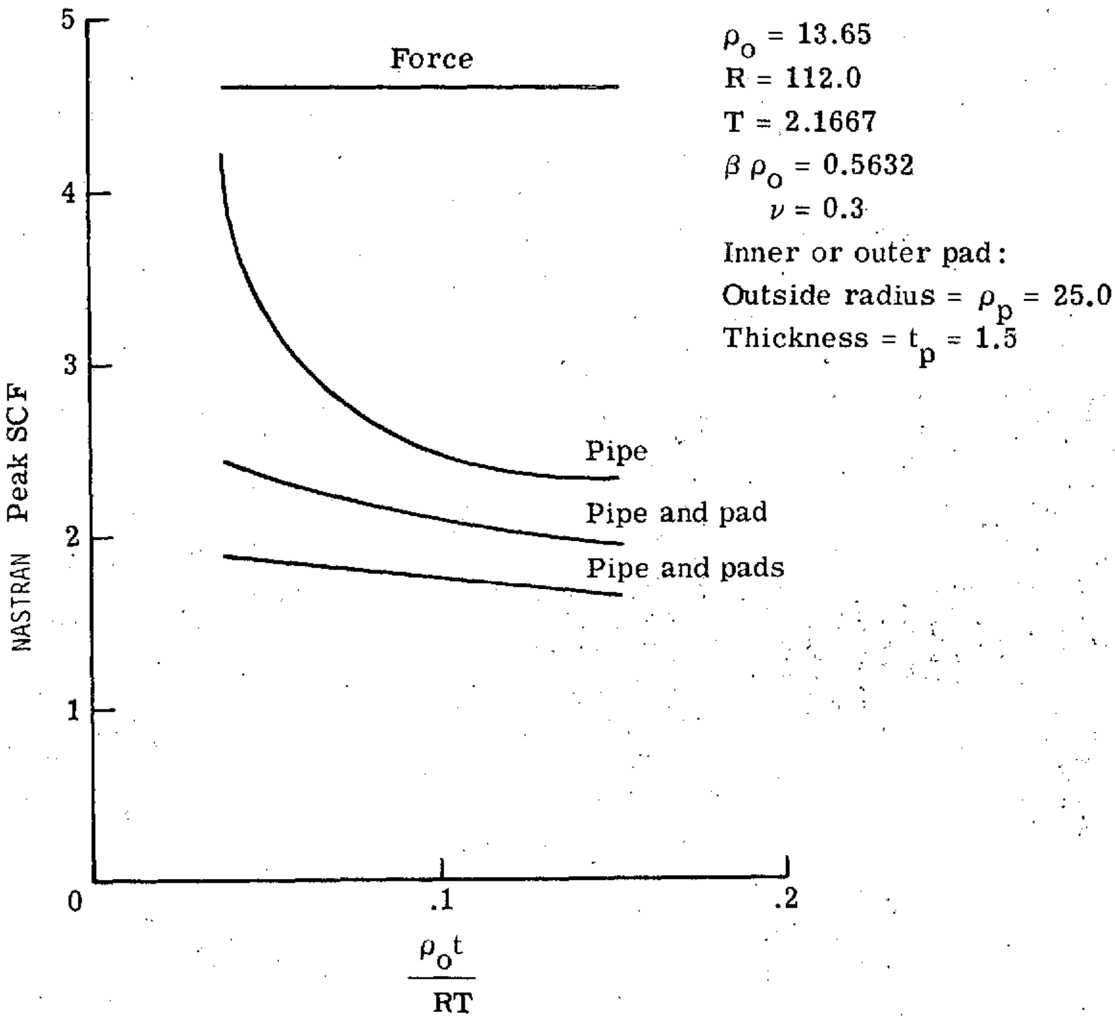

Figure 5.3.2.- Effect of reinforcement (pipe and pipe/pad(s) configurations) on peak SCF for a pressurized cylindrical shell ($\beta \rho_o$ = 0.5632).

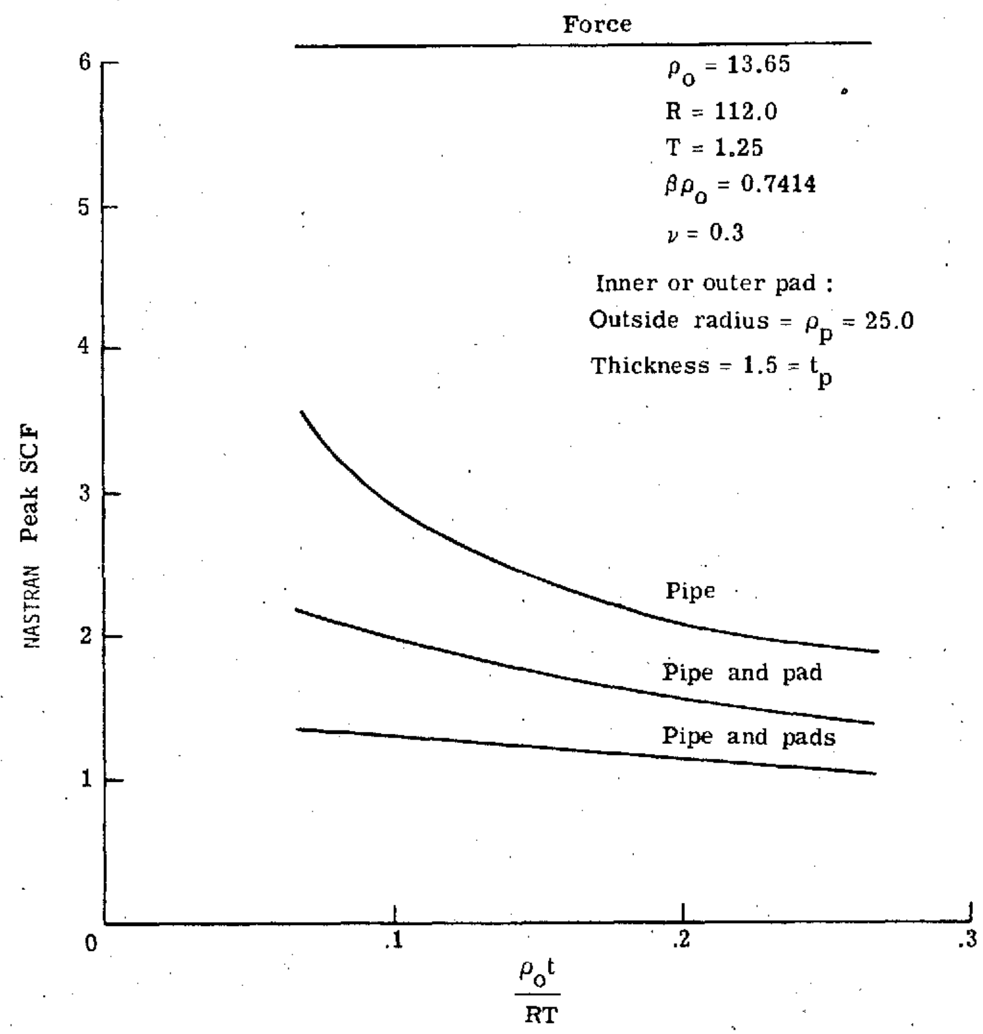

Figure 5.3.3.- Effect of reinforcement (pipe and pipe/pad(s) configurations) on peak SCF for a pressurized cylindrical shell ($\beta\rho_o$ = .7414).

The force value in each figure was obtained from Figure 5.3.1. For both $\beta\rho_o = 0.5632$ and $\beta\rho_o = 0.7414$, the largest reduction in SCF is due to the reinforcement either offered from a "thick" pipe or from a "thin" pipe and one pad. This was typical of all results obtained. The SCF reduction due to a second pad was always minor in comparison to that obtained from a thick pipe or pipe/pad configuration. Although more pronounced for the smaller $\beta\rho_o$ (analogons to smaller hole), the peak stress concentration factors for the shell and pipe rapidly increase as $\frac{\rho_o t}{RT}$ decreases. This is indicative of the transverse shear effects (small ρ_o/T). Extension of the pipe and pad(s) curves to the peak SCF ordinate at $t = 0$ yields the answer for the shell/force/pad(s) configurations.

5.4 Force and Pad(s)

It was stressed in Chapter IV that the primary thrust of the analysis would be for the cases previously presented. Another type of configuration can be solved by the formula. This is for $t = 0$ and the hole reinforced by one or two pads. Table 5.4.1 contains comparisons of formula to NASTRAN results for thin, pressurized, cylindrical shells with pad(s) reinforcing a hole covered with a membrane (force only). This type of configuration is identical to Figure 4.2.1 plus one or two reinforcing pads. The formula results for

Table 5.4.1 - Comparison of Formula to NASTRAN Results for Thin Shell with Pad(s) Reinforcing a Hole.

ρ_a	R	T	ρ_p	t_p	TOP or BOT.	SCF NASTRAN	SCF RAMSEY	% DIFF
4.84	50	0.4	8.5	0.25	TOP	5.158	4.691	- 9.05
4.84	50	0.4	8.5	0.25	BOT.	3.589	4.029	12.26
10.842	112	0.896	19.86	0.50	TOP	5.174	4.678	- 9.59
10.842	112	0.896	19.86	0.50	BOT.	3.810	4.006	5.14
12.031	125	1.25	21.50	1.50	BOT.	3.656	3.840	5.03
13.2	72	2.215	23.0	1.50	TOP	3.912	4.097	4.73
11.0	72	1.44	20.0	1.875	TOP	3.766	4.133	9.75
11.0	72	1.44	20.0	1.875	BOT.	3.654	4.133	13.11

(a) Force and Pad

ρ_a	R	T	ρ_{op}	t_{op}	ρ_{ip}	t_{ip}	SCF NASTRAN	SCF RAMSEY	% DIFF
4.84	50	0.4	8.5	0.25	8.5	0.25	3.197	3.057	- 4.38
8.172	90	0.72	14.75	0.50	14.75	0.50	2.655	2.620	- 1.32
10.842	112	0.896	19.86	0.50	19.86	0.50	3.364	3.021	-10.20
11.0	72	1.44	20.0	1.875	20.0	1.875	1.668	1.580	- 5.28

(b) Force and Pads

the top pad configuration have an accuracy of approximately ±9.7%, whereas all of bottom pad stress concentration factors were 5% to 13% above the NASTRAN results. All of the force and pads formula results were below the NASTRAN answers. The difference range is -10.2% to -1.3%.

CHAPTER VI

DISCUSSION OF RESULTS

This study provides numerical predictions of peak stress concentration factors around nonreinforced and reinforced penetrations. Numerical results have been correlated with published formulas, as well as theoretical and experimental results. Most of the configurations have been for thin shells, and all are based on linear elastic structures. Some thick shell NASTRAN and published results were obtained. An accuracy study was made of the finite element program for each of the configurations considered important in pressure vessel technology. A formula was developed to predict the peak stress concentration factor for analysis and/or design in conjunction with the ASME Pressure Vessel Code. The accuracy of the empirical formula is determined by comparing to numerical, theoretical, and experimental data.

The peak stress concentration factors (SCF) presented in Chapter V have confirmed that the 3.3 limit imposed by the ASME Code is indeed conservative for the vast majority of cases. The peak SCF results due to reinforcement (pipe or pad(s)) around a circular penetration in cylindrical, pressurized shells suggest a different number. If fact, 78.5% (124 out of 158) of the shell and pipe configurations were less than 3.3. Using the procedure for a well designed penetration presented in Ref. (25) and shown approximately in Figure 5.2.1, the one pad problems (32) were checked for ASME Code reinforcement requirements. The six "coded" pad configurations are as follows: Table 5.3.7, first two t = 1.25 configurations (SCF = 2.134 and 1.868); Table 5.3.8, second and fourth configurations (SCF = 1.824 and 1.827); and Table 5.3.9, first T = 1.0 and T = 1.25 configurations (SCF = 2.07 and 1.379). All of the other 26 one pad configurations were not "coded" and yet had peak SCF results equal to or below 3.0. The two pad problems were mostly "coded" (by choice). The seven configurations in Table 5.3.10 which are not "coded" are the first five examples and those with T = 1.2 and T = 4.48. For the two pad configuration only one of the twenty problems had a peak SCF outside of the range of 1.0 to 2.0. This was a "coded" pads configuration (T = 2.0 and R/T = 25) with a peak SCF = 2.177. Based on these results, a "thick" pipe (Figure 5.3.3), "coded" pad, or two pad configuration would have a peak SCF of about 2.2 (2/3 of the 3.3 limit), whereas the shell and pipe configuration could achieve the "well designed penetration" (SCF = 3.3) definition.

All of the peak SCF results are summarized in Table 6.1 according to thick, thin, or membrane shell definitions. The NASTRAN results compared to published values, +17.4% to

TABLE 6.1

SCF % DIFFERENCE SUMMARY

CASES	THIN SHELL & PIPE			THIN SHELL & THICK PIPE			MEM. SHELL & THIN PIPE			THICK SHELL & PIPE		
	NASTRAN TO EXACT	RAMSEY TO NASTRAN	RAMSEY TO EXACT	NASTRAN TO EXACT	RAMSEY TO NASTRAN	RAMSEY TO EXACT	NASTRAN TO EXACT	RAMSEY TO NASTRAN	RAMSEY TO EXACT	NASTRAN TO EXACT	RAMSEY TO NASTRAN	RAMSEY TO EXACT
FORCE	- 8.93 TO 17.40	-12.84 TO 8.60	- 4.97 TO 4.71	-	-	-	-7.66	14.37	5.61	-	-	-
PIPE	-14.04 TO + 8.88	-14.42 TO 14.28	-15.38 TO 12.99	-4.03 TO -0.55	- 3.90 TO 18.24	-10.85 TO 12.88	-	24.91	-	-	-	-22.17 TO 16.80
PIPE & PAD	- 3.85	-16.10 TO 11.42	-5.35 TO -3.84	-	-11.89 TO 14.68	-	-	3.01	-	-4.42	-5.09 TO -0.72	-9.28 TO +1.70
PIPE & PADS	9.11	- 8.91 TO 14.65	2.11	-	- 4.65 TO - 0.68	-	-	4.74	-	-	-	-
FORCE & TOP PAD	-	- 9.59 TO 9.75	-	-	-	-	-	-	-	-	-	-
FORCE & BOT PAD	-	+ 5.03 +13.11	-	-	-	-	-	-	-	-	-	-
FORCE & PADS	-	-10.20 TO - 1.32	-	-	-	-	-	-	-	-	-	-

-8.9%, are high, as expected, when the membrane category is approached and low for an almost thick shell. This same general trend is true for the shell and pipe examples. The thin shell and pipe NASTRAN accuracy is +8.8% to -14.0%. There is not enough data to determine any trend for the pipe and pad(s) NASTRAN results.

The formula results compare favorably with NASTRAN and the published "experimental, theoretical, and numerical" data. The results for individual comparisons to NASTRAN and "exact" are shown in Table 6.1 by categories. The thin shell approximate percent difference results are as follows: force, ±4.8%; pipe, ±14.4%; pipe and pad, ±13.7%; pipe and pads, ±11.7%; force and top pad, ±9,7%; force and bottom pad, 13%; and force and pads, -10%.

One application of this formula is to an ASME Code "hillside" (elliptical hole) penetration. The amplification factor by the code for this penetration is $1 + 2\sin^2$ (the angle the axis of the pipe makes with the normal to the shell wall). Two experimental results were obtained.[15,38] This amplification factor was multiplied times the (circular) peak SCF from the formula to obtain the following comparisons:

1. "Exact" SCF = 1.840[15] vs formula SCF = 1.826 (-0.8% difference) for $\rho_a = 4.782$, $R = 19.0$, $T = 1.0$, $t = 0.593$, $\rho_{op} = 7.438$, $t_{op} = 11.625$ $\nu = 0.3$, and the angle = 20°.

2. "Exact SCF = 2.897[38] vs formula SCF = 2.897 (-9.9% difference) for ρ_a = 11.94, R = 69.185, T = 1.995, ν = 0.3, and the angle = 45°.

CHAPTER VII

SUMMARY

The effect on stresses in a cylindrical shell with a circular penetration subject to internal pressure has been investigated. A general purpose finite element (NASTRAN) computer program was utilized to supplement the limited data for reinforced penetrations. A mesh generation computer program was developed to "automatically" punch input cards in the format acceptable to NASTRAN. This program is readily adaptable to solving a general finite element shell problem. The NASTRAN compatibility equations for a shell/pipe or a shell/pipe/pad(s) configuration were successfully implemented. This provides a quick access to a detail SCF for a reinforced nozzle in a pressure vessel. The accuracy of the finite element model has been investigated. Moreover, for an immediate, approximate solution to this complex problem, the formula may be utilized.

The formula is (1) more accurate than the published nonreinforced penetration formulas and, (2) believed to be the only formula applicable for reinforced penetrations in pressurized cylindrical shells. The accuracy of the formula was determined by comparing to the numerical, theoretical, and experimental data. It has been shown that the shell and pipe configuration can easily achieve the "well designed penetration" (SCF = 3.3) definition. A reinforced penetration (thick pipe, coded pad, or two pads) would have a peak SCF of about 2.2 (2/3 of the 3.3 limit).

This formula can be used to obtain the peak stress concentration factor for reinforced or nonreinforced penetrations in pressurized cylindrical shells. Thus, in the analysis and design of a new pressure vessel, the formula could save (1) the time to perform a detail analysis; (2) the time to construct the reinforcing pad(s) which are not always required; and (3) the extra cost of materials, fabrication, and weld examination. Also, fatigue analyses can be performed to obtain the remaining life in the penetration welds of cylindrical shells. If the remaining life is small or exhausted, then a nondestructive examination (NDE, i.e. magnetic particle, ultrasonic, or radiographic) and/or repair of these penetrations would be performed.

This type of verification (analyses and partial field work) of structural integrity of welds is invaluable since it is not practical to examine and/or repair every weld in all pressure vessels. The economics and feasibility of a validation program (6000 pressure components at Langley Research Center within the next five years) would be impractical without this formula. There have been six tunnels (pressure vessels) for which this procedure (formula and NDE) has been followed. For example, the world's first known "cryogenic" tunnel utilizing nitrogen as the working medium[40] incorporated this formula in obtaining the expected life of this facility.

REFERENCES

LIST OF REFERENCES

1. Lekkerkerker, J. G.: On the Stress Distribution in Cylindrical Shells Weakened by a Circular Hole. Ph.D. Dissertation, February 1965.

2. Van Dyke, P.: Stresses About a Circular Hole in a Cylindrical Shell. Journal, AIAA, Vol. 3, No. 9, September 1965, pp. 1733-1742.

3. Eringen, A. C.; Naghdi, A. K.; and Thiel, C. C.: State of Stress in a Circular Cylindrical Shell with a Circular Hole. Welding Research Council Bulletin, No. 102, January 1965.

4. Savin, G. N.: Stress Concentration Around Holes. Pergamon Press, New York, 1961, pp. 114-116.

5. Durelli, A. J.; del Rio, C. J.; Parks, V. J.; Feng, H.: Stresses in a Pressurized Cylinder with a Hole. Proceedings, ASCE, Vol. 93, No. ST5, October 1967, pp. 383-399.

6. Lur'e, A. I.: Statics of Thin-Walled Elastic Shells. Moscow, 1947, TRANSL. AEC - TR - 3798, 1959, pp. 147-200.

7. Prince, N.; and Rashid, Y. R.: Structural Analysis of Shell Intersections. First International Conference on Pressure Vessel Technology, ASME, Design and Analysis, September 29 - October 2, 1969, pp. 245-254.

8. Eringen, A. C.; Naghdi, A. K.; Mahmood, S. S.; Thiel, C. C.; and Ariman, T.: Analysis of Stress and Deformation in Two Normally Intersecting Cylindrical Shells Subject to Internal Pressure. General Technology Corp., Tech. Report, No. 3-8, December 1965.

9. Baker, E. H.; Capperi, A. P.; Kovalevsky, L.; Rish, F. L.; and Verette, R. M.: Shell Analysis Manual. NASA CR-912, April 1968, pp. 77-79.

10. Savin, G. N.: Stress Distribution Around Holes. NASA TT F-607, November 1970.

11. Eringen, A. C.; Naghdi, A. K.; Mahmood, S. S.; Theil, C. C.; and Ariman, T.: Stress Concentrations in Two Normally Intersecting Cylindrical Shells Subject to Internal Pressure. Welding Research Council Bulletin, No. 139, April 1969.

12. Hansberry, J. W.; and Jones, N.: A Theoretical Study of the Elastic Behavior of Two Normally Intersecting Cylindrical Shells. Journal of Engineering for Industry, Transactions, ASME, August 1969, pp. 563-572.

13. Leckie, F. A.; and Penny, R. K.: Stress Concentration Factors for the Stresses at Nozzle Intersections in Pressure Vessels, Welding Research Council Bulletin, No. 90, September 1963, pp. 19-26.

14. Cranch, E. T.: An Experimental Investigation of Stresses in the Neighborhood of Attachments to a Cylindrical Shell. Welding Research Council Bulletin, No. 60, May 1960.

15. Pickett, A. G.; and Grigory, S. C.: Cylic Pressure Tests of Full-Size Pressure Vessels. Welding Research Council Bulletin, No. 135, November 1968.

16. Leven, M. M.: Photoelastic Determination of the Stresses in Reinforced Openings in Pressure Vessels. Welding Research Council Bulletin, No. 113, April 1966, pp. 25-52.

17. Mershon, J. L.: PVRC Research on Reinforcement of Openings in Pressure Vessels. Welding Research Council Bulletin, No. 77, May 1962.

18. Riley, W. F.: Experimental Determination of Stress Distributions in Thin-Walled Cylindrical and Spherical Pressure Vessels with Circular Nozzles. Welding Research Council Bulletin, No. 108, September 1965, pp. 1-10.

19. Mershon, J. L.: Preliminary Evaluation of PVRC Photoelastic Test Data on Reinforced Openings in Pressure Vessels. Welding Research Council Bulletin, No. 113, April 1966, pp. 53-70.

20. Leven, M. M.: Photoelastic Determination of Stresses at an Opening in a Thin Walled Cylindrical Pressure Vessel. Pressure Vessel Research Committee, Report 67-9D7-PHOTO-R1, August 1967.

21. Taylor, C. E.; and Lind, N. C.: Photoelastic Study of the Stresses Near Openings in Pressure Vessels. Welding Research Council Bulletin, No. 113, April 1966, pp. 1-24.

22. Hardenbergh, D. E.; Zamrik, S. Y.; and Edmondson, A. J.: Experimental Investigation of Stresses in Nozzles in Cylindrical Pressure Vessels. Welding Research Council Bulletin, No. 89, July 1963.

23. Kitching, R.; and Perkins, J.: Stress Analysis of Rim and Ring Reinforced Openings in Pressure Vessels. Journal of Nuclear Engineering, June 1963, pp. 192-194.

24. Wells, A. A,; et al: Stress Analysis of Nozzles in Cylindrical Pressure Vessels. Institution of Mechanical Engineers, Proceedings of Pressure Vessel Research Towards Better Design, January 1961.

25. ASME Boiler and Pressure Vessel Code. Section VII, Divisions 1 and 2, 1974 Edition.

26. Lind, N. C.: Stress Concentration of Holes in Pressurized Cylindrical Shells. AIAA Journal, Vol. 6, No. 7, 1969, pp. 1397-1938.

27. Mershon, J. L.: Reinforcement of Openings Under Internal Pressure. Welding Research Council Bulletin, No. 95, April 1964.

28. McCormick, C. W.: The NASTRAN's User's Manual. NASA SP-222(01), June 1972.

29. Ramsey, J. W., Jr.: Finite Element Analysis for Buckling of Semirigid Space Frames, Master's Thesis, University of Virginia, June 1968, pp. 3-18.

30. MacNeal, R. H.: The Theoretical Manual. NASA SP-221, September 1970.

31. Clough R. W.; and Johnson, C. P.: Finite Element Analysis of Arbitrary Thin Shells. American Concrete Institute, SP-28, 1971, pp. 333-364.

32. Clough, R. W. and Tocher, J. L.: Finite Element Stiffness Matrices for Analysis of Plate Bending. Proc. of Conference on Matrix Methods in Structural Mechanics, Air Force Flight Dynamics Laboratory Report AFFDL-TR-66-80. December 1965.

33. Melosh, R. J.: The Optimum Approach to Analysis of Elastic Continua. Proceedings, Computer Oriented Analysis of Shell Structures, AFFDL-TR-71-79, June 1971, pp. 862-898.

34. Timoshenko, S.; and Wolnowsky - Krieger, S.: Theory of Plates and Shells. McGraw-Hill Book Company, Inc., New York, 1959, pp. 466-532.

35. Billington, D. P.: Thin Shell Concrete Structures. McGraw-Hill Book Company, Inc., New York, 1965, pp. 1-35.

36. Langhaar, H. L.: Energy Methods in Applied Mechanics. John Wiley and Sons, Inc., New York, 1962, pp. 177-200.

37. Norris, C. H.; et al: Structural Design for Dynamic Loads. McGraw-Hill Book Company, Inc., New York, 1959, pp. 61-72.

38. Taylor, J. T.; Lewis, P. E.; and Ramsey, J. W., Jr.: A Procedure for Verifying the Structural Integrity of an Existing Pressurized Wind Tunnel. ASME National Pressure Vessel Conference, June 1974; and ASME JEMT, October 1974, pp. 283-291.

39. Wilson, J. F.; and Taylor, J. T.: An Automated Program for Reinforcement Requirements for Openings in Cylindrical Pressure Vessels. NASA TMX 72648, January 1975.

40. Wilson, J. F.; Ware, G. D.; and Ramsey, J. W., Jr.: Pilot Cryo Tunnel: Attachments, Seals, and Insulation. ASCE National Structural Conference, No. 2239, April 1974.

41. Houghton, D. S.; Rothwell, A.: The Effect of Curvature on the Stress Concentrations Around Holes in Shells. The College of Aeronautics, Cranfield, England, No. 156, May 1962.

42. Reissner, E.: On Transverse Bending of Plates, Including the Effect of Transverse Shear Deformation. Int. J. Soilds Structures, Vol. 11, 1975, pp. 569-573.

43. Narayanaswami, R.; and Adelman, H. M.: Inclusion of Transverse Shear Deformation in Finite Element Displacement Formulations. AIAA Journal, Vol. 12, No. 11, November 1974, pp. 1613-1614.

44. Narayanaswami, R.: New Triangular Plate-Bending Finite Element with Transverse Shear Flexibility. AIAA Journal, Vol. 12, No. 12, December 1974, pp. 1761-1763.

APPENDICES

N A S T R A N   E X E C U T I V E   C O N T R O L   D E C K   E C H O

```
ID RAMSEY,CUTOUT1
APP DISPLACEMENT
SOL 1,0
TIME   333
CEND
```

APPENDIX A

SAMPLE NASTRAN COMPUTER PROGRAM

SHELL, PIPE, AND PADS

$\rho_a = 13.2$; $R = 72$, $T = 2.215$; $t = 1.10$; $\rho_{op} = 23.0$; $t_{op} = 1.50$;
$\rho_{ip} = 23.0$; $t_{ip} = 1.50$.

```
A=13.200 RR=  72.0 TS=2.215 TP=1.100 TPAD=1.500 PO=13.750

LTPT

                              C A S E   C O N T R O L   D E C K   E C H O
         CARD
         COUNT
           1        LABEL= LTPT
           2        TITLE=   PIPE AND BOTH PADS REINFORCED HOLE IN CYLINDRICAL SHELL
           3        SUBTITLE=A=13.200 RR=  72.0 TS=2.215 TP=1.100 TPAD=1.500 PO=13.750
           4        LOAD=6
           5        MPC=36
           6        SPC=5
           7        STRESS=ALL
           8        LINE=35
           9        BEGIN BULK


*** USER INFORMATION MESSAGE 207, BULK DATA NOT SORTED,XSORT WILL RE-ORDER DECK.
```

A=13.200 RR= 72.0 TS=2.215 TP=1.100 TPAD=1.500 P0=13.750

LTPT

S O R T E D B U L K D A T A E C H O

CARD COUNT	. 1 ..	2 ..	3 ..	4 ..	5 ..	6 ..	7 ..	8 ..	9 ..	10 .
1-	CORD2C	40		0.0	0.0	0.0	0.0	0.0	+100.0	+Z
2-	+Z	+100.0	0.0	+100.0						
3-	CQUAD2	227	51	227	228	224	223			
4-	CQUAD2	228	51	228	229	225	224			
5-	CQUAD2	229	51	229	230	226	225			
6-	CQUAD2	231	51	231	232	228	227			
7-	CQUAD2	232	51	232	233	229	228			
8-	CQUAD2	233	51	233	234	230	229			
9-	CQUAD2	235	51	235	236	232	231			
10-	CQUAD2	236	51	236	237	233	232			
11-	CQUAD2	237	51	237	238	234	233			
12-	CQUAD2	239	51	239	240	236	235			
13-	CQUAD2	240	51	240	241	237	236			
14-	CQUAD2	241	51	241	242	238	237			
15-	CQUAD2	243	51	243	244	240	239			
16-	CQUAD2	244	51	244	245	241	240			
17-	CQUAD2	245	51	245	246	242	241			
18-	CQUAD2	247	51	247	248	244	243			
19-	CQUAD2	248	51	248	249	245	244			
20-	CQUAD2	249	51	249	250	246	245			
21-	CQUAD2	251	51	251	252	248	247			
22-	CQUAD2	252	51	252	253	249	248			
23-	CQUAD2	253	51	253	254	250	249			
24-	CQUAD2	628	41	628	632	633	631			
25-	CQUAD2	629	41	629	631	642	643			
26-	CQUAD2	630	41	630	637	638	632			
27-	CQUAD2	631	41	631	633	641	642			
28-	CQUAD2	632	41	632	638	639	633			
29-	CQUAD2	633	41	633	639	640	641			
30-	CQUAD2	634	41	634	650	651	635			
31-	CQUAD2	635	41	635	651	652	636			
32-	CQUAD2	636	41	636	652	653	637			
33-	CQUAD2	637	41	637	653	654	638			
34-	CQUAD2	638	41	638	654	655	639			
35-	CQUAD2	639	41	639	655	656	640			

A=13.200 RR= 72.0 TS=2.215 TP=1.100 TPAD=1.500 PO=13.750

LTPT

S O R T E D B U L K D A T A E C H O

CARD COUNT	1	2	3	4	5	6	7	8	9	10
36-	CQUAD2	640	41	640	656	657	658			
37-	CQUAD2	641	41	641	640	658	659			
38-	CQUAD2	642	41	642	641	659	660			
39-	CQUAD2	643	41	643	642	660	661			
40-	CQUAD2	644	41	644	643	661	662			
41-	CQUAD2	645	41	645	644	662	663			
42-	CQUAD2	646	41	646	645	663	664			
43-	CQUAD2	657	41	673	674	675	657			
44-	CQUAD2	674	41	684	685	686	674			
45-	CQUAD2	685	41	692	693	694	685			
46-	CQUAD2	702	41	702	704	705	703			
47-	CQUAD2	704	41	704	706	707	705			
48-	CQUAD2	706	41	706	710	711	707			
49-	CQUAD2	708	41	708	712	713	709			
50-	CQUAD2	709	41	709	713	714	710			
51-	CQUAD2	710	41	710	714	715	711			
52-	CQUAD2	712	41	712	716	717	713			
53-	CQUAD2	713	41	713	717	718	714			
54-	CQUAD2	714	41	714	718	719	715			
55-	CQUAD2	716	41	716	720	721	717			
56-	CQUAD2	717	41	717	721	722	718			
57-	CQUAD2	718	41	718	722	723	719			
58-	CQUAD2	720	41	720	724	725	721			
59-	CQUAD2	721	41	721	725	726	722			
60-	CQUAD2	722	41	722	726	727	723			
61-	CQUAD2	724	41	724	728	729	725			
62-	CQUAD2	725	41	725	729	730	726			
63-	CQUAD2	726	41	726	730	731	727			
64-	CTRIA2	255	51	255	256	251				
65-	CTRIA2	256	51	256	257	252				
66-	CTRIA2	257	51	257	258	252				
67-	CTRIA2	258	51	258	259	253				
68-	CTRIA2	259	51	259	260	253				
69-	CTRIA2	260	51	260	261	254				
70-	CTRIA2	262	51	262	263	255				

A=13.200 RR= 72.0 TS=2.215 TP=1.100 TPAD=1.500 PO=13.750

LIPT

S O R T E D   B U L K   D A T A   E C H O

CARD COUNT	1	2	3	4	5	6	7	8	9	10
71-	CTRIA2	263	51	263	264	256				
72-	CTRIA2	264	51	264	265	256				
73-	CTRIA2	265	51	265	266	257				
74-	CTRIA2	266	51	266	267	257				
75-	CTRIA2	267	51	267	268	258				
76-	CTRIA2	268	51	268	269	258				
77-	CTRIA2	269	51	269	270	259				
78-	CTRIA2	270	51	270	271	259				
79-	CTRIA2	271	51	271	272	260				
80-	CTRIA2	272	51	272	273	260				
81-	CTRIA2	273	51	273	274	261				
82-	CTRIA2	311	75	311	312	325				
83-	CTRIA2	312	75	312	313	326				
84-	CTRIA2	313	75	313	314	327				
85-	CTRIA2	314	75	314	315	328				
86-	CTRIA2	315	75	315	316	329				
87-	CTRIA2	316	75	316	317	330				
88-	CTRIA2	317	75	317	318	331				
89-	CTRIA2	318	75	318	319	332				
90-	CTRIA2	319	75	319	320	333				
91-	CTRIA2	320	75	320	321	334				
92-	CTRIA2	321	75	321	322	335				
93-	CTRIA2	322	75	322	323	336				
94-	CTRIA2	324	44	324	325	338				
95-	CTRIA2	325	44	325	326	339				
96-	CTRIA2	326	44	326	327	340				
97-	CTRIA2	327	44	327	328	341				
98-	CTRIA2	328	44	328	329	342				
99-	CTRIA2	329	44	329	330	343				
100-	CTRIA2	330	44	330	331	344				
101-	CTRIA2	331	44	331	332	345				
102-	CTRIA2	332	44	332	333	346				
103-	CTRIA2	333	44	333	334	347				
104-	CTRIA2	334	44	334	335	348				
105-	CTRIA2	335	44	335	336	349				

A=13.200 RR= 72.0 TS=2.215 TP=1.100 TPAD=1.500 PO=13.750

LTPT

S O R T E D   B U L K   D A T A   E C H O

CARD COUNT	. 1 ..	2 ..	3 ..	4 ..	5 ..	6 ..	7 ..	8 ..	9 ..	10 .
141-	CTRIA2	374	44	374	375	388				
142-	CTRIA2	411	43	411	412	425				
143-	CTRIA2	412	43	412	413	426				
144-	CTRIA2	413	43	413	414	427				
145-	CTRIA2	414	43	414	415	428				
146-	CTRIA2	415	43	415	416	429				
147-	CTRIA2	416	43	416	417	430				
148-	CTRIA2	417	43	417	418	431				
149-	CTRIA2	418	43	418	419	432				
150-	CTRIA2	419	43	419	420	433				
151-	CTRIA2	420	43	420	421	434				
152-	CTRIA2	421	43	421	422	435				
153-	CTRIA2	422	43	422	423	436				
154-	CTRIA2	424	43	424	425	438				
155-	CTRIA2	425	43	425	426	439				
156-	CTRIA2	426	43	426	427	440				
157-	CTRIA2	427	43	427	428	441				
158-	CTRIA2	428	43	428	429	442				
159-	CTRIA2	429	43	429	430	443				
160-	CTRIA2	430	43	430	431	444				
161-	CTRIA2	431	43	431	432	445				
162-	CTRIA2	432	43	432	433	446				
163-	CTRIA2	433	43	433	434	447				
164-	CTRIA2	434	43	434	435	448				
165-	CTRIA2	435	43	435	436	449				
166-	CTRIA2	437	43	437	438	451				
167-	CTRIA2	438	43	438	439	452				
168-	CTRIA2	439	43	439	440	453				
169-	CTRIA2	440	43	440	441	454				
170-	CTRIA2	441	43	441	442	455				
171-	CTRIA2	442	43	442	443	456				
172-	CTRIA2	443	43	443	444	457				
173-	CTRIA2	444	43	444	445	458				
174-	CTRIA2	445	43	445	446	459				
175-	CTRIA2	446	43	446	447	460				

A=13.200 RR= 72.0 TS=2.215 TP=1.100 TPAD=1.500 PO=13.750

1TPT

S O R T E D   B U L K   D A T A   E C H O

CARD COUNT	. 1 ..	2 ..	3 ..	4 ..	5 ..	6 ..	7 ..	8 ..	9 ..	10
106-	CTRIA2	337	44	337	338	351				
107-	CTRIA2	338	44	338	339	352				
108-	CTRIA2	339	44	339	340	353				
109-	CTRIA2	340	44	340	341	354				
110-	CTRIA2	341	44	341	342	355				
111-	CTRIA2	342	44	342	343	356				
112-	CTRIA2	343	44	343	344	357				
113-	CTRIA2	344	44	344	345	358				
114-	CTRIA2	345	44	345	346	359				
115-	CTRIA2	346	44	346	347	360				
116-	CTRIA2	347	44	347	348	361				
117-	CTRIA2	348	44	348	349	362				
118-	CTRIA2	350	44	350	351	364				
119-	CTRIA2	351	44	351	352	365				
120-	CTRIA2	352	44	352	353	366				
121-	CTRIA2	353	44	353	354	367				
122-	CTRIA2	354	44	354	355	368				
123-	CTRIA2	355	44	355	356	369				
124-	CTRIA2	356	44	356	357	370				
125-	CTRIA2	357	44	357	358	371				
126-	CTRIA2	358	44	358	359	372				
127-	CTRIA2	359	44	359	360	373				
128-	CTRIA2	360	44	360	361	374				
129-	CTRIA2	361	44	361	362	375				
130-	CTRIA2	363	44	363	364	377				
131-	CTRIA2	364	44	364	365	378				
132-	CTRIA2	365	44	365	366	379				
133-	CTRIA2	366	44	366	367	380				
134-	CTRIA2	367	44	367	368	381				
135-	CTRIA2	368	44	368	369	382				
136-	CTRIA2	369	44	369	370	383				
137-	CTRIA2	370	44	370	371	384				
138-	CTRIA2	371	44	371	372	385				
139-	CTRIA2	372	44	372	373	386				
140-	CTRIA2	373	44	373	374	387				

A=13.200 RR= 72.0 TS=2.215 TP=1.100 TPAD=1.500 PO=13.750

LTPT

S O R T E D B U L K D A T A E C H O

CARD COUNT	. 1 ..	2 ..	3 ..	4 ..	5 ..	6 ..	7 ..	8 ..	9 ..	10 .
176-	CTRIA2	447	43	447	448	461				
177-	CTRIA2	448	43	448	449	462				
178-	CTRIA2	450	43	450	451	464				
179-	CTRIA2	451	43	451	452	465				
180-	CTRIA2	452	43	452	453	466				
181-	CTRIA2	453	43	453	454	467				
182-	CTRIA2	454	43	454	455	468				
183-	CTRIA2	455	43	455	456	469				
184-	CTRIA2	456	43	456	457	470				
185-	CTRIA2	457	43	457	458	471				
186-	CTRIA2	458	43	458	459	472				
187-	CTRIA2	459	43	459	460	473				
188-	CTRIA2	460	43	460	461	474				
189-	CTRIA2	461	43	461	462	475				
190-	CTRIA2	463	43	463	464	477				
191-	CTRIA2	464	43	464	465	478				
192-	CTRIA2	465	43	465	466	479				
193-	CTRIA2	466	43	466	467	480				
194-	CTRIA2	467	43	467	468	481				
195-	CTRIA2	468	43	468	469	482				
196-	CTRIA2	469	43	469	470	483				
197-	CTRIA2	470	43	470	471	484				
198-	CTRIA2	471	43	471	472	485				
199-	CTRIA2	472	43	472	473	486				
200-	CTRIA2	473	43	473	474	487				
201-	CTRIA2	474	43	474	475	488				
202-	CTRIA2	511	41	511	512	525				
203-	CTRIA2	512	41	512	513	526				
204-	CTRIA2	513	41	513	514	527				
205-	CTRIA2	514	41	514	515	528				
206-	CTRIA2	515	41	515	516	529				
207-	CTRIA2	516	41	516	517	530				
208-	CTRIA2	517	41	517	518	531				
209-	CTRIA2	518	41	518	519	532				
210-	CTRIA2	519	41	519	520	533				

A=13.200 RR= 72.0 TS=2.215 TP=1.100 TPAD=1.500 P0=13.750

LTPT

S O R T E D B U L K D A T A E C H O

CARD COUNT	. 1 ..	2 ..	3 ..	4 ..	5 ..	6 ..	7 ..	8 ..	9 ..	10 .
211-	CTRIA2	520	41	520	521	534				
212-	CTRIA2	521	41	521	522	535				
213-	CTRIA2	522	41	522	523	536				
214-	CTRIA2	524	41	524	525	538				
215-	CTRIA2	525	41	525	526	539				
216-	CTRIA2	526	41	526	527	540				
217-	CTRIA2	527	41	527	528	541				
218-	CTRIA2	528	41	528	529	542				
219-	CTRIA2	529	41	529	530	543				
220-	CTRIA2	530	41	530	531	544				
221-	CTRIA2	531	41	531	532	545				
222-	CTRIA2	532	41	532	533	546				
223-	CTRIA2	533	41	533	534	547				
224-	CTRIA2	534	41	534	535	548				
225-	CTRIA2	535	41	535	536	549				
226-	CTRIA2	537	41	537	538	551				
227-	CTRIA2	538	41	538	539	552				
228-	CTRIA2	539	41	539	540	553				
229-	CTRIA2	540	41	540	541	554				
230-	CTRIA2	541	41	541	542	555				
231-	CTRIA2	542	41	542	543	556				
232-	CTRIA2	543	41	543	544	557				
233-	CTRIA2	544	41	544	545	558				
234-	CTRIA2	545	41	545	546	559				
235-	CTRIA2	546	41	546	547	560				
236-	CTRIA2	547	41	547	548	561				
237-	CTRIA2	548	41	548	549	562				
238-	CTRIA2	550	41	550	551	564				
239-	CTRIA2	551	41	551	552	565				
240-	CTRIA2	552	41	552	553	566				
241-	CTRIA2	553	41	553	554	567				
242-	CTRIA2	554	41	554	555	568				
243-	CTRIA2	555	41	555	556	569				
244-	CTRIA2	556	41	556	557	570				
245-	CTRIA2	557	41	557	558	571				

PIPE AND BOTH PADS REINFORCED HOLE IN CYLINDRICAL SHELL JUNE 28, 1974 NASTRAN 2/

A=13.200 RR= 72.0 TS=2.215 TP=1.100 TPAD=1.500 PO=13.750

LTPT

S O R T E D B U L K D A T A E C H O

CARD COUNT	1	2	3	4	5	6	7	8	9	10
246-	CTRIA2	558	41	558	559	572				
247-	CTRIA2	559	41	559	560	573				
248-	CTRIA2	560	41	560	561	574				
249-	CTRIA2	561	41	561	562	575				
250-	CTRIA2	563	41	563	564	577				
251-	CTRIA2	564	41	564	565	578				
252-	CTRIA2	565	41	565	566	579				
253-	CTRIA2	566	41	566	567	580				
254-	CTRIA2	567	41	567	568	581				
255-	CTRIA2	568	41	568	569	582				
256-	CTRIA2	569	41	569	570	583				
257-	CTRIA2	570	41	570	571	584				
258-	CTRIA2	571	41	571	572	585				
259-	CTRIA2	572	41	572	573	586				
260-	CTRIA2	573	41	573	574	587				
261-	CTRIA2	574	41	574	575	588				
262-	CTRIA2	576	41	576	577	590				
263-	CTRIA2	577	41	577	578	591				
264-	CTRIA2	578	41	578	579	592				
265-	CTRIA2	579	41	579	580	593				
266-	CTRIA2	580	41	580	581	594				
267-	CTRIA2	581	41	581	582	595				
268-	CTRIA2	582	41	582	583	596				
269-	CTRIA2	583	41	583	584	597				
270-	CTRIA2	584	41	584	585	598				
271-	CTRIA2	585	41	585	586	599				
272-	CTRIA2	586	41	586	587	600				
273-	CTRIA2	587	41	587	588	601				
274-	CTRIA2	589	41	589	590	603				
275-	CTRIA2	590	41	590	591	604				
276-	CTRIA2	591	41	591	592	605				
277-	CTRIA2	592	41	592	593	606				
278-	CTRIA2	593	41	593	594	607				
279-	CTRIA2	594	41	594	595	608				
280-	CTRIA2	595	41	595	596	609				

A=13.200 RR= 72.0 TS=2.215 TP=1.100 TPAD=1.500 P0=13.750

LTPT

S O R T E D   B U L K   D A T A   E C H O

CARD COUNT	. 1 ..	2 ..	3 ..	4 ..	5 ..	6 ..	7 ..	8 ..	9 ..	10
281-	CTRIA2	596	41	596	597	610				
282-	CTRIA2	597	41	597	598	611				
283-	CTRIA2	598	41	598	599	612				
284-	CTRIA2	599	41	599	600	613				
285-	CTRIA2	600	41	600	601	614				
286-	CTRIA2	602	41	602	603	616				
287-	CTRIA2	603	41	603	604	617				
288-	CTRIA2	604	41	604	605	618				
289-	CTRIA2	605	41	605	606	619				
290-	CTRIA2	606	41	606	607	620				
291-	CTRIA2	607	41	607	608	621				
292-	CTRIA2	608	41	608	609	622				
293-	CTRIA2	609	41	609	610	623				
294-	CTRIA2	610	41	610	611	624				
295-	CTRIA2	611	41	611	612	625				
296-	CTRIA2	612	41	612	613	626				
297-	CTRIA2	613	41	613	614	627				
298-	CTRIA2	615	41	616	666	615				
299-	CTRIA2	616	41	617	665	616				
300-	CTRIA2	617	41	618	646	617				
301-	CTRIA2	618	41	619	645	618				
302-	CTRIA2	619	41	620	629	619				
303-	CTRIA2	620	41	621	628	620				
304-	CTRIA2	621	41	622	628	621				
305-	CTRIA2	622	41	623	630	622				
306-	CTRIA2	623	41	624	635	623				
307-	CTRIA2	624	41	625	634	624				
308-	CTRIA2	625	41	626	649	625				
309-	CTRIA2	626	41	627	648	626				
310-	CTRIA2	627	41	627	647	648				
311-	CTRIA2	647	41	668	648	647				
312-	CTRIA2	648	41	668	669	648				
313-	CTRIA2	649	41	669	650	649				
314-	CTRIA2	650	41	669	670	650				
315-	CTRIA2	651	41	670	652	651				

A=13.200 RR= 72.0 TS=2.215 TP=1.100 TPAD=1.500 PO=13.750

LTPT

S O R T E D B U L K D A T A E C H O

CARD COUNT	. 1 ..	2 ..	3 ..	4 ..	5 ..	6 ..	7 ..	8 ..	9 ..	10 .
316-	CTRIA2	652	41	670	671	652				
317-	CTRIA2	653	41	671	654	653				
318-	CTRIA2	654	41	671	672	654				
319-	CTRIA2	655	41	672	656	655				
320-	CTRIA2	656	41	672	673	656				
321-	CTRIA2	658	41	675	676	658				
322-	CTRIA2	659	41	676	660	659				
323-	CTRIA2	660	41	676	677	660				
324-	CTRIA2	661	41	677	662	661				
325-	CTRIA2	662	41	677	678	662				
326-	CTRIA2	663	41	678	664	663				
327-	CTRIA2	664	41	678	679	664				
328-	CTRIA2	665	41	679	666	665				
329-	CTRIA2	666	41	679	680	666				
330-	CTRIA2	668	41	681	669	668				
331-	CTRIA2	669	41	681	682	669				
332-	CTRIA2	670	41	682	671	670				
333-	CTRIA2	671	41	682	683	671				
334-	CTRIA2	672	41	683	673	672				
335-	CTRIA2	673	41	683	684	673				
336-	CTRIA2	675	41	686	687	675				
337-	CTRIA2	676	41	687	677	676				
338-	CTRIA2	677	41	687	688	677				
339-	CTRIA2	678	41	688	679	678				
340-	CTRIA2	679	41	688	689	679				
341-	CTRIA2	681	41	690	682	681				
342-	CTRIA2	682	41	690	691	682				
343-	CTRIA2	683	41	691	684	683				
344-	CTRIA2	684	41	691	692	684				
345-	CTRIA2	686	41	694	695	686				
346-	CTRIA2	687	41	686	695	687				
347-	CTRIA2	688	41	695	696	688				
348-	CTRIA2	689	41	688	696	689				
349-	CTRIA2	690	41	690	697	691				
350-	CTRIA2	691	41	691	697	698				

A=13.200 RR= 72.0 TS=2.215 TP=1.100 TPAD=1.500 PO=13.750

LIPT

SORTED BULK DATA ECHO

CARD COUNT	. 1 ..	2 ..	3 ..	4 ..	5 ..	6 ..	7 ..	8 ..	9 ..	10
351-	CTRIA2	692	41	692	698	693				
352-	CTRIA2	693	41	693	698	699				
353-	CTRIA2	694	41	694	693	700				
354-	CTRIA2	695	41	695	694	700				
355-	CTRIA2	696	41	696	695	701				
356-	CTRIA2	697	41	697	708	698				
357-	CTRIA2	698	41	698	708	709				
358-	CTRIA2	699	41	699	709	710				
359-	CTRIA2	700	41	700	699	706				
360-	CTRIA2	701	41	701	700	702				
361-	CTRIA2	1256	51	256	252	251				
362-	CTRIA2	1258	51	258	253	252				
363-	CTRIA2	1260	51	260	254	253				
364-	CTRIA2	1263	51	263	256	255				
365-	CTRIA2	1265	51	265	257	256				
366-	CTRIA2	1267	51	267	258	257				
367-	CTRIA2	1269	51	269	259	258				
368-	CTRIA2	1271	51	271	260	259				
369-	CTRIA2	1273	51	273	261	260				
370-	CTRIA2	1615	41	615	666	667				
371-	CTRIA2	1616	41	616	665	666				
372-	CTRIA2	1618	41	618	645	646				
373-	CTRIA2	1619	41	619	644	645				
374-	CTRIA2	1620	41	620	628	629				
375-	CTRIA2	1622	41	622	630	628				
376-	CTRIA2	1623	41	623	635	636				
377-	CTRIA2	1624	41	624	634	635				
378-	CTRIA2	1625	41	625	649	634				
379-	CTRIA2	1626	41	626	648	649				
380-	CTRIA2	1627	41	617	646	665				
381-	CTRIA2	1629	41	629	643	644				
382-	CTRIA2	1630	41	636	637	630				
383-	CTRIA2	1648	41	648	669	649				
384-	CTRIA2	1650	41	650	670	651				
385-	CTRIA2	1652	41	652	671	653				

A=13.200 RR= 72.0 TS=2.215 TP=1.100 TPAD=1.500 PO=13.750

LTPT

S O R T E D   B U L K   D A T A   E C H O

CARD COUNT	. 1 ..	2 ..	3 ..	4 ..	5 ..	6 ..	7 ..	8 ..	9 ..	10 .
386-	CTRIA2	1654	41	654	672	655				
387-	CTRIA2	1656	41	656	673	657				
388-	CTRIA2	1657	41	675	658	657				
389-	CTRIA2	1658	41	658	676	659				
390-	CTRIA2	1660	41	660	677	661				
391-	CTRIA2	1662	41	662	678	663				
392-	CTRIA2	1664	41	664	679	665				
393-	CTRIA2	1666	41	666	680	667				
394-	CTRIA2	1669	41	669	682	670				
395-	CTRIA2	1671	41	671	683	672				
396-	CTRIA2	1673	41	673	684	674				
397-	CTRIA2	1674	41	686	675	674				
398-	CTRIA2	1675	41	675	687	676				
399-	CTRIA2	1677	41	677	688	678				
400-	CTRIA2	1679	41	679	689	680				
401-	CTRIA2	1682	41	682	691	683				
402-	CTRIA2	1684	41	684	692	685				
403-	CTRIA2	1685	41	694	686	685				
404-	CTRIA2	1687	41	695	688	687				
405-	CTRIA2	1691	41	691	698	692				
406-	CTRIA2	1693	41	693	699	700				
407-	CTRIA2	1695	41	695	700	701				
408-	CTRIA2	1698	41	698	709	699				
409-	CTRIA2	1699	41	699	710	706				
410-	CTRIA2	1700	41	700	704	702				
411-	CTRIA2	2619	41	619	629	644				
412-	CTRIA2	2623	41	623	636	630				
413-	CTRIA2	2625	41	649	650	634				
414-	CTRIA2	2627	41	646	664	665				
415-	CTRIA2	2629	41	628	631	629				
416-	CTRIA2	2630	41	630	632	628				
417-	CTRIA2	2700	41	700	706	704				
418-	CTRIA2	3311	75	311	325	324				
419-	CTRIA2	3312	75	312	326	325				
420-	CTRIA2	3313	75	313	327	326				

ORIGINAL PAGE IS OF POOR QUALITY

A=13.200 RR= 72.0 TS=2.215 TP=1.100 TPAD=1.500 PO=13.750

LTPT

S O R T E D   B U L K   D A T A   E C H O

CARD COUNT	. 1 ..	2 ..	3 ..	4 ..	5 ..	6 ..	7 ..	8 ..	9 ..	10 .
421-	CTRIA2	3314	75	314	328	327				
422-	CTRIA2	3315	75	315	329	328				
423-	CTRIA2	3316	75	316	330	329				
424-	CTRIA2	3317	75	317	331	330				
425-	CTRIA2	3318	75	318	332	331				
426-	CTRIA2	3319	75	319	333	332				
427-	CTRIA2	3320	75	320	334	333				
428-	CTRIA2	3321	75	321	335	334				
429-	CTRIA2	3322	75	322	336	335				
430-	CTRIA2	3324	44	324	338	337				
431-	CTRIA2	3325	44	325	339	338				
432-	CTRIA2	3326	44	326	340	339				
433-	CTRIA2	3327	44	327	341	340				
434-	CTRIA2	3328	44	328	342	341				
435-	CTRIA2	3329	44	329	343	342				
436-	CTRIA2	3330	44	330	344	343				
437-	CTRIA2	3331	44	331	345	344				
438-	CTRIA2	3332	44	332	346	345				
439-	CTRIA2	3333	44	333	347	346				
440-	CTRIA2	3334	44	334	348	347				
441-	CTRIA2	3335	44	335	349	348				
442-	CTRIA2	3337	44	337	351	350				
443-	CTRIA2	3338	44	338	352	351				
444-	CTRIA2	3339	44	339	353	352				
445-	CTRIA2	3340	44	340	354	353				
446-	CTRIA2	3341	44	341	355	354				
447-	CTRIA2	3342	44	342	356	355				
448-	CTRIA2	3343	44	343	357	356				
449-	CTRIA2	3344	44	344	358	357				
450-	CTRIA2	3345	44	345	359	358				
451-	CTRIA2	3346	44	346	360	359				
452-	CTRIA2	3347	44	347	361	360				
453-	CTRIA2	3348	44	348	362	361				
454-	CTRIA2	3350	44	350	364	363				
455-	CTRIA2	3351	44	351	365	364				

A=13.200 RR= 72.0 TS=2.215 TP=1.100 TPAD=1.500 PD=13.750

1TPT

S O R T E D   B U L K   D A T A   E C H O

CARD COUNT	. 1 ..	2 ..	3 ..	4 ..	5 ..	6 ..	7 ..	8 ..	9 ..	10
456-	CTRIA2	3352	44	352	366	365				
457-	CTRIA2	3353	44	353	367	366				
458-	CTRIA2	3354	44	354	368	367				
459-	CTRIA2	3355	44	355	369	368				
460-	CTRIA2	3356	44	356	370	369				
461-	CTRIA2	3357	44	357	371	370				
462-	CTRIA2	3358	44	358	372	371				
463-	CTRIA2	3359	44	359	373	372				
464-	CTRIA2	3360	44	360	374	373				
465-	CTRIA2	3361	44	361	375	374				
466-	CTRIA2	3363	44	363	377	376				
467-	CTRIA2	3364	44	364	378	377				
468-	CTRIA2	3365	44	365	379	378				
469-	CTRIA2	3366	44	366	380	379				
470-	CTRIA2	3367	44	367	381	380				
471-	CTRIA2	3368	44	368	382	381				
472-	CTRIA2	3369	44	369	383	382				
473-	CTRIA2	3370	44	370	384	383				
474-	CTRIA2	3371	44	371	385	384				
475-	CTRIA2	3372	44	372	386	385				
476-	CTRIA2	3373	44	373	387	386				
477-	CTRIA2	3374	44	374	388	387				
478-	CTRIA2	3411	43	411	425	424				
479-	CTRIA2	3412	43	412	426	425				
480-	CTRIA2	3413	43	413	427	426				
481-	CTRIA2	3414	43	414	428	427				
482-	CTRIA2	3415	43	415	429	428				
483-	CTRIA2	3416	43	416	430	429				
484-	CTRIA2	3417	43	417	431	430				
485-	CTRIA2	3418	43	418	432	431				
486-	CTRIA2	3419	43	419	433	432				
487-	CTRIA2	3420	43	420	434	433				
488-	CTRIA2	3421	43	421	435	434				
489-	CTRIA2	3422	43	422	436	435				
490-	CTRIA2	3424	43	424	438	437				

A=13.200 RR= 72.0 TS=2.215 TP=1.100 TPAD=1.500 RO=13.750

LTPT

S O R T E D B U L K D A T A E C H O

CARD COUNT	. 1 ..	2 ..	3 ..	4 ..	5 ..	6 ..	7 ..	8 ..	9 ..	10 .
491-	CTRIA2	3425	43	425	439	438				
492-	CTRIA2	3426	43	426	440	439				
493-	CTRIA2	3427	43	427	441	440				
494-	CTRIA2	3428	43	428	442	441				
495-	CTRIA2	3429	43	429	443	442				
496-	CTRIA2	3430	43	430	444	443				
497-	CTRIA2	3431	43	431	445	444				
498-	CTRIA2	3432	43	432	446	445				
499-	CTRIA2	3433	43	433	447	446				
500-	CTRIA2	3434	43	434	448	447				
501-	CTRIA2	3435	43	435	449	448				
502-	CTRIA2	3437	43	437	451	450				
503-	CTRIA2	3438	43	438	452	451				
504-	CTRIA2	3439	43	439	453	452				
505-	CTRIA2	3440	43	440	454	453				
506-	CTRIA2	3441	43	441	455	454				
507-	CTRIA2	3442	43	442	456	455				
508-	CTRIA2	3443	43	443	457	456				
509-	CTRIA2	3444	43	444	458	457				
510-	CTRIA2	3445	43	445	459	458				
511-	CTRIA2	3446	43	446	460	459				
512-	CTRIA2	3447	43	447	461	460				
513-	CTRIA2	3448	43	448	462	461				
514-	CTRIA2	3450	43	450	464	463				
515-	CTRIA2	3451	43	451	465	464				
516-	CTRIA2	3452	43	452	466	465				
517-	CTRIA2	3453	43	453	467	466				
518-	CTRIA2	3454	43	454	468	467				
519-	CTRIA2	3455	43	455	469	468				
520-	CTRIA2	3456	43	456	470	469				
521-	CTRIA2	3457	43	457	471	470				
522-	CTRIA2	3458	43	458	472	471				
523-	CTRIA2	3459	43	459	473	472				
524-	CTRIA2	3460	43	460	474	473				
525-	CTRIA2	3461	43	461	475	474				

A=13.200 BR= 72.0 TS=2.215 TP=1.100 TPAD=1.500 PO=13.750

1TPT

S O R T E D   B U L K   D A T A   E C H O

CARD COUNT	. 1 ..	2 ..	3 ..	4 ..	5 ..	6 ..	7 ..	8 ..	9 ..	10
526-	CTRIA2	3463	43	463	477	476				
527-	CTRIA2	3464	43	464	478	477				
528-	CTRIA2	3465	43	465	479	478				
529-	CTRIA2	3466	43	466	480	479				
530-	CTRIA2	3467	43	467	481	480				
531-	CTRIA2	3468	43	468	482	481				
532-	CTRIA2	3469	43	469	483	482				
533-	CTRIA2	3470	43	470	484	483				
534-	CTRIA2	3471	43	471	485	484				
535-	CTRIA2	3472	43	472	486	485				
536-	CTRIA2	3473	43	473	487	486				
537-	CTRIA2	3474	43	474	488	487				
538-	CTRIA2	3511	41	511	525	524				
539-	CTRIA2	3512	41	512	526	525				
540-	CTRIA2	3513	41	513	527	526				
541-	CTRIA2	3514	41	514	528	527				
542-	CTRIA2	3515	41	515	529	528				
543-	CTRIA2	3516	41	516	530	529				
544-	CTRIA2	3517	41	517	531	530				
545-	CTRIA2	3518	41	518	532	531				
546-	CTRIA2	3519	41	519	533	532				
547-	CTRIA2	3520	41	520	534	533				
548-	CTRIA2	3521	41	521	535	534				
549-	CTRIA2	3522	41	522	536	535				
550-	CTRIA2	3524	41	524	538	537				
551-	CTRIA2	3525	41	525	539	538				
552-	CTRIA2	3526	41	526	540	539				
553-	CTRIA2	3527	41	527	541	540				
554-	CTRIA2	3528	41	528	542	541				
555-	CTRIA2	3529	41	529	543	542				
556-	CTRIA2	3530	41	530	544	543				
557-	CTRIA2	3531	41	531	545	544				
558-	CTRIA2	3532	41	532	546	545				
559-	CTRIA2	3533	41	533	547	546				
560-	CTRIA2	3534	41	534	548	547				

A=13.200 RR= 72.0 TS=2.215 TP=1.100 TPAD=1.500 PO=13.750

LTPT

S O R T E D   B U L K   D A T A   E C H O

CARD COUNT	. 1 ..	2 ..	3 ..	4 ..	5 ..	6 ..	7 ..	8 ..	9 ..	10 .
561-	CTRIA2	3535	41	535	549	548				
562-	CTRIA2	3537	41	537	551	550				
563-	CTRIA2	3538	41	538	552	551				
564-	CTRIA2	3539	41	539	553	552				
565-	CTRIA2	3540	41	540	554	553				
566-	CTRIA2	3541	41	541	555	554				
567-	CTRIA2	3542	41	542	556	555				
568-	CTRIA2	3543	41	543	557	556				
569-	CTRIA2	3544	41	544	558	557				
570-	CTRIA2	3545	41	545	559	558				
571-	CTRIA2	3546	41	546	560	559				
572-	CTRIA2	3547	41	547	561	560				
573-	CTRIA2	3548	41	548	562	561				
574-	CTRIA2	3550	41	550	564	563				
575-	CTRIA2	3551	41	551	565	564				
576-	CTRIA2	3552	41	552	566	565				
577-	CTRIA2	3553	41	553	567	566				
578-	CTRIA2	3554	41	554	568	567				
579-	CTRIA2	3555	41	555	569	568				
580-	CTRIA2	3556	41	556	570	569				
581-	CTRIA2	3557	41	557	571	570				
582-	CTRIA2	3558	41	558	572	571				
583-	CTRIA2	3559	41	559	573	572				
584-	CTRIA2	3560	41	560	574	573				
585-	CTRIA2	3561	41	561	575	574				
586-	CTRIA2	3563	41	563	577	576				
587-	CTRIA2	3564	41	564	578	577				
588-	CTRIA2	3565	41	565	579	578				
589-	CTRIA2	3566	41	566	580	579				
590-	CTRIA2	3567	41	567	581	580				
591-	CTRIA2	3568	41	568	582	581				
592-	CTRIA2	3569	41	569	583	582				
593-	CTRIA2	3570	41	570	584	583				
594-	CTRIA2	3571	41	571	585	584				
595-	CTRIA2	3572	41	572	586	585				

A=13.200 RR= 72.0 TS=2.215 TP=1.100 TPAD=1.500 PO=13.750

LIPT

S O R T E D B U L K D A T A E C H O

CARD COUNT	. 1 ..	2 ..	3 ..	4 ..	5 ..	6 ..	7 ..	8 ..	9 ..	10 .
596-	CTRIA2	3573	41	573	587	586				
597-	CTRIA2	3574	41	574	588	587				
598-	CTRIA2	3576	41	576	590	589				
599-	CTRIA2	3577	41	577	591	590				
600-	CTRIA2	3578	41	578	592	591				
601-	CTRIA2	3579	41	579	593	592				
602-	CTRIA2	3580	41	580	594	593				
603-	CTRIA2	3581	41	581	595	594				
604-	CTRIA2	3582	41	582	596	595				
605-	CTRIA2	3583	41	583	597	596				
606-	CTRIA2	3584	41	584	598	597				
607-	CTRIA2	3585	41	585	599	598				
608-	CTRIA2	3586	41	586	600	599				
609-	CTRIA2	3587	41	587	601	600				
610-	CTRIA2	3589	41	589	603	602				
611-	CTRIA2	3590	41	590	604	603				
612-	CTRIA2	3591	41	591	605	604				
613-	CTRIA2	3592	41	592	606	605				
614-	CTRIA2	3593	41	593	607	606				
615-	CTRIA2	3594	41	594	608	607				
616-	CTRIA2	3595	41	595	609	608				
617-	CTRIA2	3596	41	596	610	609				
618-	CTRIA2	3597	41	597	611	610				
619-	CTRIA2	3598	41	598	612	611				
620-	CTRIA2	3599	41	599	613	612				
621-	CTRIA2	3600	41	600	614	613				
622-	CTRIA2	3602	41	602	616	615				
623-	CTRIA2	3603	41	603	617	616				
624-	CTRIA2	3604	41	604	618	617				
625-	CTRIA2	3605	41	605	619	618				
626-	CTRIA2	3606	41	606	620	619				
627-	CTRIA2	3607	41	607	621	620				
628-	CTRIA2	3608	41	608	622	621				
629-	CTRIA2	3609	41	609	623	622				
630-	CTRIA2	3610	41	610	624	623				

A=13.200 RR= 72.0 TS=2.215 TP=1.100 TPAD=1.500 PO=13.750

LTPT

S O R T E D B U L K D A T A E C H O

CARD COUNT	1	2	3	4	5	6	7	8	9	10
631-	CTRIA2	3611	41	611	625	624				
632-	CTRIA2	3612	41	612	626	625				
633-	CTRIA2	3613	41	613	627	626				
634-	FORCE	6	703	40	38571.4	.0	.0	1.0		
635-	FORCE	6	705	40	77142.8	.0	.0	1.0		
636-	FORCE	6	707	40	77142.8	.0	.0	1.0		
637-	FORCE	6	711	40	55928.5	.0	.0	1.0		
638-	FORCE	6	715	40	34714.3	.0	.0	1.0		
639-	FORCE	6	719	40	34714.3	.0	.0	1.0		
640-	FORCE	6	723	40	34714.3	.0	.0	1.0		
641-	FORCE	6	727	40	35789.5	.0	.0	1.0		
642-	FORCE	6	731	40	18432.4	.0	.0	1.0		
643-	FORCE1	6	223	2280.80	227	223				
644-	FORCE1	6	224	4561.59	228	224				
645-	FORCE1	6	225	4561.59	229	225				
646-	FORCE1	6	226	2280.80	230	226				
647-	GRDSET		40				40	4		
648-	GRID	223		124.800	.00000	13.7500				
649-	GRID	224		124.800	3.15792	11.9078				
650-	GRID	225		124.800	5.47523	6.8750				
651-	GRID	226		124.800	6.32548	.0000				
652-	GRID	227		118.200	.00000	13.7500				
653-	GRID	228		118.200	3.33444	11.9078				
654-	GRID	229		118.200	5.78197	6.8750				
655-	GRID	230		118.200	6.68024	.0000				
656-	GRID	231		111.600	.00000	13.7500				
657-	GRID	232		111.600	3.53188	11.9078				
658-	GRID	233		111.600	6.12519	6.8750				
659-	GRID	234		111.600	7.07728	.0000				
660-	GRID	235		105.000	.00000	13.7500				
661-	GRID	236		105.000	3.75420	11.9078				
662-	GRID	237		105.000	6.51181	6.8750				
663-	GRID	238		105.000	7.52463	.0000				
664-	GRID	239		98.400	.00000	13.7500				
665-	GRID	240		98.400	4.00640	11.9078				

A=13.200 RP= 72.0 TS=2.215 TP=1.100 TPAD=1.500 PO=13.750

1TPT

S O R T E D B U L K D A T A E C H O

CARD COUNT	. 1 ..	2 ..	3 ..	4 ..	5 ..	6 ..	7 ..	8 ..	9 ..	10 .
666-	GRID	241		98.400	6.95067	6.8750				
667-	GRID	242		98.400	8.03256	.0000				
668-	GRID	243		93.642	.00000	13.7500				
669-	GRID	244		93.642	4.21035	11.9078				
670-	GRID	245		93.642	7.30575	6.8750				
671-	GRID	246		93.642	8.44364	.0000				
672-	GRID	247		88.883	.00000	13.7500				
673-	GRID	248		88.883	4.43619	11.9078				
674-	GRID	249		88.883	7.69918	6.8750				
675-	GRID	250		88.883	8.89926	.0000				
676-	GRID	251		84.125	.00000	13.7500				
677-	GRID	252		84.125	4.68767	11.9078				
678-	GRID	253		84.125	8.13756	6.8750				
679-	GRID	254		84.125	9.40709	.0000				
680-	GRID	255		79.366	.00000	13.7500				
681-	GRID	256		79.366	2.56999	13.2815				
682-	GRID	257		79.366	4.96941	11.9078				
683-	GRID	258		79.366	7.03667	9.7227				
684-	GRID	259		79.366	8.62906	6.8750				
685-	GRID	260		79.366	9.63345	3.5588				
686-	GRID	261		79.366	9.97670	.0000				
687-	GRID	262		74.608	.00000	13.7500				
668-	GRID	263		74.608	1.37842	13.6324				
689-	GRID	264		74.608	2.73403	13.2815				
690-	GRID	265		74.608	4.04429	12.7033				
691-	GRID	266		74.608	5.28723	11.9078				
692-	GRID	267		74.608	6.44175	10.9086				
693-	GRID	268		74.608	7.48796	9.7227				
694-	GRID	269		74.608	8.40752	8.3705				
695-	GRID	270		74.608	9.18404	6.8750				
696-	GRID	271		74.608	9.80343	5.2619				
697-	GRID	272		74.608	10.25431	3.5588				
698-	GRID	273		74.608	10.52827	1.7947				
699-	GRID	274		74.608	10.62017	.0000				
700-	GRID	311		70.142	.00000	13.2000				

A=13.200 RR= 72.0 TS=2.215 TP=1.100 TPAD=1.500 PO=13.750

LIPT

S O R T E D   B U L K   D A T A   E C H O

CARD COUNT	. 1 ..	2 ..	3 ..	4 ..	5 ..	6 ..	7 ..	8 ..	9 ..	10
701-	GRID	312		70.142	1.40753	13.0871				
702-	GRID	313		70.142	2.79181	12.7502				
703-	GRID	314		70.142	4.12984	12.1952				
704-	GRID	315		70.142	5.39921	11.4315				
705-	GRID	316		70.142	6.57838	10.4723				
706-	GRID	317		70.142	7.64702	9.3338				
707-	GRID	318		70.142	8.58639	8.0356				
708-	GRID	319		70.142	9.37971	6.6000				
709-	GRID	320		70.142	10.012565.0514					
710-	GRID	321		70.142	10.473263.4164					
711-	GRID	322		70.142	10.753201.7229					
712-	GRID	323		70.142	10.84711.0000					
713-	GRID	324		70.142	.00000	13.7500				
714-	GRID	325		70.142	1.46619	13.6324				
715-	GRID	326		70.142	2.90823	13.2815				
716-	GRID	327		70.142	4.30223	12.7033				
717-	GRID	328		70.142	5.62489	11.9078				
718-	GRID	329		70.142	6.85377	10.9086				
719-	GRID	330		70.142	7.96768	9.7227				
720-	GRID	331		70.142	8.94703	8.3704				
721-	GRID	332		70.142	9.77429	6.8750				
722-	GRID	333		70.142	10.434325.2619					
723-	GRID	334		70.142	10.914893.5587					
724-	GRID	335		70.142	11.206931.7947					
725-	GRID	336		70.142	11.30490.0000					
726-	GRID	337		70.142	.00000	14.8500				
727-	GRID	338		70.142	1.58352	14.7230				
728-	GRID	339		70.142	3.14111	14.3440				
729-	GRID	340		70.142	4.64714	13.7196				
730-	GRID	341		70.142	6.07651	12.8605				
731-	GRID	342		70.142	7.40503	11.7813				
732-	GRID	343		70.142	8.60975	10.5005				
733-	GRID	344		70.142	9.66941	9.0401				
734-	GRID	345		70.142	10.564877.4250					
735-	GRID	346		70.142	11.279605.6828					

ORIGINAL PAGE IS
OF POOR QUALITY

A=13.200 RR= 72.0 TS=2.215 TP=1.100 TPAD=1.500 RO=13.750

LTPT

S O R T E D B U L K D A T A E C H O

CARD COUNT	. 1 ..	2 ..	3 ..	4 ..	5 .. 6 ..	7 ..	8 ..	9 ..	10
736-	GRID	347		70.142	11.800153.8434				
737-	GRID	348		70.142	12.116571.9383				
738-	GRID	349		70.142	12.22272.0000				
739-	GRID	350		70.142	.00000 17.0000				
740-	GRID	351		70.142	1.81285 16.8546				
741-	GRID	352		70.142	3.59645 16.4207				
742-	GRID	353		70.142	5.32178 15.7059				
743-	GRID	354		70.142	6.96035 14.7224				
744-	GRID	355		70.142	8.48453 13.4870				
745-	GRID	356		70.142	9.86794 12.0208				
746-	GRID	357		70.142	11.0859310.3489				
747-	GRID	358		70.142	12.116148.5000				
748-	GRID	359		70.142	12.939136.5056				
749-	GRID	360		70.142	13.538944.3999				
750-	GRID	361		70.142	13.903722.2189				
751-	GRID	362		70.142	14.02613.0000				
752-	GRID	363		70.142	.00000 20.5000				
753-	GRID	364		70.142	2.18625 20.3246				
754-	GRID	365		70.142	4.33819 19.8015				
755-	GRID	366		70.142	6.42165 18.9395				
756-	GRID	367		70.142	8.40282 17.7535				
757-	GRID	368		70.142	10.2485616.2637				
758-	GRID	369		70.142	11.9267814.4957				
759-	GRID	370		70.142	13.4070812.4796				
760-	GRID	371		70.142	14.6614810.2500				
761-	GRID	372		70.142	15.665227.8450				
762-	GRID	373		70.142	16.397805.3057				
763-	GRID	374		70.142	16.843752.6757				
764-	GRID	375		70.142	16.99349.0000				
765-	GRID	376		70.142	.00000 23.0000				
766-	GRID	377		70.142	2.45302 22.8032				
767-	GRID	378		70.142	4.86845 22.2163				
768-	GRID	379		70.142	7.20871 21.2492				
769-	GRID	380		70.142	9.43640 19.9186				
770-	GRID	381		70.142	11.5145218.2471				

ORIGINAL PAGE IS OF POOR QUALITY

A=13.200 RR= 72.0 TS=2.215 TP=1.100 TPAD=1.500 PD=13.750

LIPT

S O R T E D   B U L K   D A T A   E C H O

CARD COUNT	. 1 ..	2 ..	3 ..	4 ..	5 ..	6 ..	7 ..	8 ..	9 ..	10 .
771-	GRID	382		70.142	13.4068516.2634					
772-	GRID	383		70.142	15.0786514.0315					
773-	GRID	384		70.142	16.4975511.5000					
774-	GRID	385		70.142	17.634578.8017					
775-	GRID	386		70.142	18.465405.9528					
776-	GRID	387		70.142	18.971613.0020					
777-	GRID	388		70.142	19.14165.0000					
778-	GRID	411		73.858	.00000	13.2000				
779-	GRID	412		73.858	1.33672	13.0871				
780-	GRID	413		73.858	2.65126	12.7502				
781-	GRID	414		73.858	3.92176	12.1952				
782-	GRID	415		73.858	5.12686	11.4315				
783-	GRID	416		73.858	6.24611	10.4723				
784-	GRID	417		73.858	7.26021	9.3338				
785-	GRID	418		73.858	8.15144	8.0356				
786-	GRID	419		73.858	8.90393	6.6000				
787-	GRID	420		73.858	9.50408	5.0514				
788-	GRID	421		73.858	9.94091	3.4164				
789-	GRID	422		73.858	10.206311.7229					
790-	GRID	423		73.858	10.29533.0000					
791-	GRID	424		73.858	.00000	13.7500				
792-	GRID	425		73.858	1.39242	13.6324				
793-	GRID	426		73.858	2.76182	13.2815				
794-	GRID	427		73.858	4.08544	12.7033				
795-	GRID	428		73.858	5.34109	11.9078				
796-	GRID	429		73.858	6.50746	10.9086				
797-	GRID	430		73.858	7.56446	9.7227				
798-	GRID	431		73.858	8.49354	8.3704				
799-	GRID	432		73.858	9.27813	6.8750				
800-	GRID	433		73.858	9.90399	5.2619				
801-	GRID	434		73.858	10.359593.5587					
802-	GRID	435		73.858	10.636431.7947					
803-	GRID	436		73.858	10.72929.0000					
804-	GRID	437		73.858	.00000	14.8500				
805-	GRID	438		73.858	1.50384	14.7230				

PIPE AND BOTH PADS REINFORCED HOLE IN CYLINDRICAL SHELL JUNE 28, 1974 NASTRAN 2.

A=13.200 RR= 72.0 TS=2.215 TP=1.100 TPAD=1.500 PO=13.750

LTPI

S O R T E D B U L K D A T A E C H O

CARD COUNT	. 1 ..	2 ..	3 ..	4 ..	5 ..	6 ..	7 ..	8 ..	9 ..	10 .
806-	GRID	439		73.858	2.98296	14.3440				
307-	GRID	440		73.858	4.41289	13.7196				
808-	GRID	441		73.858	5.76977	12.8605				
809-	GRID	442		73.858	7.03059	11.7813				
810-	GRID	443		73.858	8.17360	10.5005				
811-	GRID	444		73.858	9.17867	9.0401				
812-	GRID	445		73.858	10.027767.4250					
813-	GRID	446		73.858	10.705305.6828					
814-	GRID	447		73.858	11.198663.8434					
815-	GRID	448		73.858	11.498501.9383					
816-	GRID	449		73.859	11.59909.0000					
817-	GRID	450		73.858	.00000	17.0000				
818-	GRID	451		73.858	1.72163	16.8546				
819-	GRID	452		73.858	3.41531	16.4207				
820-	GRID	453		73.858	5.05335	15.7059				
821-	GRID	454		73.858	6.60861	14.7224				
822-	GRID	455		73.858	8.05481	13.4870				
823-	GRID	456		73.858	9.36694	12.0208				
824-	GRID	457		73.858	10.5217210.3489					
825-	GRID	458		73.858	11.498108.5000					
826-	GRID	459		73.858	12.277806.5056					
827-	GRID	460		73.858	12.845904.3999					
828-	GRID	461		73.858	13.191322.2189					
829-	GRID	462		73.858	13.30722.0000					
830-	GRID	463		73.858	.00000	20.5000				
831-	GRID	464		73.858	2.07623	20.3246				
832-	GRID	465		73.858	4.11957	19.8015				
833-	GRID	466		73.858	6.09735	18.9395				
834-	GRID	467		73.858	7.97730	17.7535				
835-	GRID	468		73.858	9.72786	16.2637				
836-	GRID	469		73.858	11.3186614.4957					
837-	GRID	470		73.858	12.7210212.4796					
833-	GRID	471		73.858	13.9086810.2500					
839-	GRID	472		73.858	14.858527.8450					
840-	GRID	473		73.858	15.551445.3057					

A=13.200 RR= 72.0 TS=2.215 TP=1.100 TPAD=1.500 R0=13.750

LIPT

S O R T E D B U L K D A T A E C H O

CARD COUNT	. 1 ..	2 ..	3 ..	4 ..	5 ..	6 ..	7 ..	8 ..	9 ..	10 .
841-	GRID	474		73.858	15.973122.6757					
842-	GRID	475		73.858	16.11468.0000					
843-	GRID	476		73.858	.00000	23.0000				
844-	GRID	477		73.858	2.32956	22.8032				
845-	GRID	478		73.858	4.62299	22.2163				
846-	GRID	479		73.858	6.84430	21.2492				
847-	GRID	480		73.858	8.95770	19.9186				
848-	GRID	481		73.858	10.9279618.2471					
849-	GRID	482		73.858	12.7208016.2634					
850-	GRID	483		73.858	14.3035114.0015					
851-	GRID	484		73.858	15.6457711.5000					
852-	GRID	485		73.858	16.720638.8017					
853-	GRID	486		73.858	17.505595.9528					
854-	GRID	487		73.858	17.983653.0020					
855-	GRID	488		73.858	18.14421.0000					
856-	GRID	511		72.000	.00000	13.2000				
857-	GRID	512		72.000	1.37121	13.0871				
858-	GRID	513		72.000	2.71972	12.7502				
859-	GRID	514		72.000	4.02311	12.1952				
860-	GRID	515		72.000	5.25951	11.4315				
861-	GRID	516		72.000	6.40793	10.4723				
862-	GRID	517		72.000	7.44859	9.3338				
863-	GRID	518		72.000	8.36324	8.0356				
864-	GRID	519		72.000	9.13560	6.6000				
865-	GRID	520		72.000	9.75166	5.0514				
866-	GRID	521		72.000	10.200113.4164					
867-	GRID	522		72.000	10.472581.7229					
868-	GRID	523		72.000	10.56398.0000					
869-	GRID	524		72.000	.00000	13.7500				
870-	GRID	525		72.000	1.42836	13.6324				
871-	GRID	526		72.000	2.83313	13.2815				
872-	GRID	527		72.000	4.19103	12.7033				
873-	GRID	528		72.000	5.47931	11.9078				
874-	GRID	529		72.000	6.67612	10.9066				
875-	GRID	530		72.000	7.76082	9.7227				

A=13.200 RR= 72.0 TS=2.215 TP=1.100 TPAD=1.500 PO=13.750

LIPT

S O R T E D B U L K D A T A E C H O

CARD COUNT	. 1 ..	2 ..	3 ..	4 ..	5 ..	6 ..	7 ..	8 ..	9 ..	10 .
876-	GRID	531		72.000	8.71437	8.3704				
877-	GRID	532		72.000	9.51972	6.8750				
878-	GRID	533		72.000	10.16221	5.2619				
879-	GRID	534		72.000	10.62995	3.5587				
880-	GRID	535		72.000	10.91418	1.7947				
881-	GRID	536		72.000	11.0095	3.0000				
882-	GRID	537		72.000	.00000	14.8500				
883-	GRID	538		72.000	1.54265	14.7230				
884-	GRID	539		72.000	3.05999	14.3440				
885-	GRID	540		72.000	4.52699	13.7196				
886-	GRID	541		72.000	5.91916	12.8605				
887-	GRID	542		72.000	7.21294	11.7813				
888-	GRID	543		72.000	8.38599	10.5005				
889-	GRID	544		72.000	9.41762	9.0401				
890-	GRID	545		72.000	10.28927	7.4250				
891-	GRID	546		72.000	10.98490	5.6828				
892-	GRID	547		72.000	11.49149	3.8434				
893-	GRID	548		72.000	11.79939	1.9383				
894-	GRID	549		72.000	11.9026	8.0000				
895-	GRID	550		72.000	.00000	17.0000				
896-	GRID	551		72.000	1.76606	16.8546				
897-	GRID	552		72.000	3.50354	16.4207				
898-	GRID	553		72.000	5.18409	15.7059				
899-	GRID	554		72.000	6.77991	14.7224				
900-	GRID	555		72.000	8.26407	13.4870				
901-	GRID	556		72.000	9.61089	12.0208				
902-	GRID	557		72.000	10.79641	10.3489				
903-	GRID	558		72.000	11.79897	8.5000				
904-	GRID	559		72.000	12.59972	6.5056				
905-	GRID	560		72.000	13.18324	4.3999				
906-	GRID	561		72.000	13.53806	2.2189				
907-	GRID	562		72.000	13.6571	3.0000				
908-	GRID	563		72.000	.00000	20.5000				
909-	GRID	564		72.000	2.12982	20.3246				
910-	GRID	565		72.000	4.22605	19.8015				

A=13.200 RP= 72.0 TS=2.215 TP=1.100 TPAD=1.500 PO=13.750

LIPT

S O R T E D   B U L K   D A T A   E C H O

CARD COUNT	. 1 ..	2 ..	3 ..	4 ..	5 ..	6 ..	7 ..	8 ..	9 ..	10 .
911-	GRID	566		72.000	6.25529	18.9395				
912-	GRID	567		72.000	8.18451	17.7535				
913-	GRID	568		72.000	9.98139	16.2637				
914-	GRID	569		72.000	11.61471	14.4957				
915-	GRID	570		72.000	13.05497	12.4796				
916-	GRID	571		72.000	14.27505	10.2500				
917-	GRID	572		72.000	15.25108	7.8450				
918-	GRID	573		72.000	15.96325	5.3057				
919-	GRID	574		72.000	16.39672	2.6757				
920-	GRID	575		72.000	16.54225	.0000				
921-	GRID	576		72.000	.00000	23.0000				
922-	GRID	577		72.000	2.38970	22.8032				
923-	GRID	578		72.000	4.74254	22.2163				
924-	GRID	579		72.000	7.02176	21.2492				
925-	GRID	580		72.000	9.19079	19.9186				
926-	GRID	581		72.000	11.21352	18.2471				
927-	GRID	582		72.000	13.05473	16.2634				
928-	GRID	583		72.000	14.68074	14.0015				
929-	GRID	584		72.000	16.06021	11.5000				
930-	GRID	585		72.000	17.16524	8.8017				
931-	GRID	586		72.000	17.97246	5.9528				
932-	GRID	587		72.000	18.46418	3.0020				
933-	GRID	588		72.000	18.62933	.0000				
934-	GRID	589		72.000	.00000	25.0000				
935-	GRID	590		72.000	2.59763	24.7861				
936-	GRID	591		72.000	5.15601	24.1481				
937-	GRID	592		72.000	7.63585	23.0970				
938-	GRID	593		72.000	9.99786	21.6506				
939-	GRID	594		72.000	12.20300	19.8338				
940-	GRID	595		72.000	14.21278	17.6776				
941-	GRID	596		72.000	15.99005	15.2190				
942-	GRID	597		72.000	17.49987	12.4999				
943-	GRID	598		72.000	18.71082	9.5670				
944-	GRID	599		72.000	19.59633	6.4704				
945-	GRID	600		72.000	20.13613	3.2631				

PIPE AND BOTH PADS REINFORCED HOLE IN CYLINDRICAL SHELL JUNE 28, 1974 NASTRAN 2.

A=13.200 RR= 72.0 TS=2.215 TP=1.100 TPAD=1.500 PO=13.750

LTPT

S O R T E D B U L K D A T A E C H O

CARD COUNT	. 1 ..	2 ..	3 ..	4 ..	5 .. 6	7 ..	8 ..	9 ..	10
946-	GRID	601		72.000	20.31751.0000				
947-	GRID	602		72.000	.00000 27.0000				
948-	GRID	603		72.000	2.80560 26.7690				
949-	GRID	604		72.000	5.56975 26.0800				
950-	GRID	605		72.000	8.25081 24.9447				
951-	GRID	606		72.000	10.8069523.3827				
952-	GRID	607		72.000	13.1961821.4205				
953-	GRID	608		72.000	15.3767919.0918				
954-	GRID	609		72.000	17.3079916.4365				
955-	GRID	610		72.000	18.9510313.4999				
956-	GRID	611		72.000	20.2706510.3324				
957-	GRID	612		72.000	21.236756.9880				
958-	GRID	613		72.000	21.826183.5241				
959-	GRID	614		72.000	22.02431.0000				
960-	GRID	615		72.000	.00000 29.7000				
961-	GRID	616		72.000	3.08642 29.4459				
962-	GRID	617		72.000	6.12876 28.6880				
963-	GRID	618		72.000	9.08255 27.4392				
964-	GRID	619		72.000	11.9027125.7209				
965-	GRID	620		72.000	14.5434823.5626				
966-	GRID	621		72.000	16.9586921.0010				
967-	GRID	622		72.000	19.1024818.0802				
968-	GRID	623		72.000	20.9305514.8499				
969-	GRID	624		72.000	22.4018811.3656				
970-	GRID	625		72.000	23.480997.6868				
971-	GRID	626		72.000	24.140223.8765				
972-	GRID	627		72.000	24.36198.0000				
973-	GRID	628		72.000	18.3824023.1000				
974-	GRID	629		72.000	15.7563426.4000				
975-	GRID	630		72.000	21.0084519.8000				
976-	GRID	631		72.000	18.3824026.4000				
977-	GRID	632		72.000	21.0084523.1000				
978-	GRID	633		72.000	21.0084526.4000				
979-	GRID	634		72.000	23.634519.9000				
980-	GRID	635		72.000	23.6345113.2000				

LIPT

S O R T E D   B U L K   D A T A   E C H O

CARD COUNT	. 1 ..	2 ..	3 ..	4 ..	5 .. 6 ..	7 ..	8 ..	9 ..	10
981-	GRID	636		72.000	23.6345116.5000				
982-	GRID	637		72.000	23.6345119.8000				
983-	GRID	638		72.000	23.6345123.1000				
984-	GRID	639		72.000	23.6345126.4000				
985-	GRID	640		72.000	23.6345129.7000				
986-	GRID	641		72.000	21.0084529.7000				
987-	GRID	642		72.000	18.3824029.7000				
988-	GRID	643		72.000	15.7563429.7000				
989-	GRID	644		72.000	13.1302829.7000				
990-	GRID	645		72.000	10.5042329.7000				
991-	GRID	646		72.000	7.87817 29.7000				
992-	GRID	647		72.000	26.26057.0000				
993-	GRID	648		72.000	26.260573.3000				
994-	GRID	649		72.000	26.260576.6000				
995-	GRID	650		72.000	26.260579.9000				
996-	GRID	651		72.000	26.2605713.2000				
997-	GRID	652		72.000	26.2605716.5000				
998-	GRID	653		72.000	26.2605719.8000				
999-	GRID	654		72.000	26.2605723.1000				
1000-	GRID	655		72.000	26.2605726.4000				
1001-	GRID	656		72.000	26.2605729.7000				
1002-	GRID	657		72.000	26.2605733.0000				
1003-	GRID	658		72.000	23.6345133.0000				
1004-	GRID	659		72.000	21.0084533.0000				
1005-	GRID	660		72.000	18.3824033.0000				
1006-	GRID	661		72.000	15.7563433.0000				
1007-	GRID	662		72.000	13.1302833.0000				
1008-	GRID	663		72.000	10.5042333.0000				
1009-	GRID	664		72.000	7.87817 33.0000				
1010-	GRID	665		72.000	5.25211 33.0000				
1011-	GRID	666		72.000	2.62606 33.0000				
1012-	GRID	667		72.000	.00000 33.0000				
1013-	GRID	668		72.000	31.51268.0000				
1014-	GRID	669		72.000	31.512686.6000				
1015-	GRID	670		72.000	31.5126813.2000				

```
                                    S O R T E D   B U L K   D A T A   E C H O
          CARD
          COUNT        .   1  ..   2  ..   3  ..   4  ..   5  ..   6  ..   7  ..   8  ..   9  ..  10  .
          1016-        GRID    671             72.000  31.5126819.8000
          1017-        GRID    672             72.000  31.5126826.4000
          1018-        GRID    673             72.000  31.5126833.0000
          1019-        GRID    674             72.000  31.5126839.6000
          1020-        GRID    675             72.000  26.2605739.6000
          1021-        GRID    676             72.000  21.0084539.6000
          1022-        GRID    677             72.000  15.7563439.6000
          1023-        GRID    678             72.000  10.5042339.6000
          1024-        GRID    679             72.000  5.25211 39.6000
          1025-        GRID    680             72.000  .00000  39.6000
          1026-        GRID    681             72.000  42.01690.0000
          1027-        GRID    682             72.000  42.0169013.2000
          1028-        GRID    683             72.000  42.0169026.4000
          1029-        GRID    684             72.000  42.0169039.6000
          1030-        GRID    685             72.000  42.0169052.8000
          1031-        GRID    686             72.000  31.5126852.8000
          1032-        GRID    687             72.000  21.0084552.8000
          1033-        GRID    688             72.000  10.5042352.8000
          1034-        GRID    689             72.000  .00000  52.8000
          1035-        GRID    690             72.000  63.02536.0000
          1036-        GRID    691             72.000  63.0253626.4000
          1037-        GRID    692             72.000  63.0253652.8000
          1038-        GRID    693             72.000  63.0253679.2000
          1039-        GRID    694             72.000  42.0169079.2000
          1040-        GRID    695             72.000  21.0084579.2000
          1041-        GRID    696             72.000  .00000  79.2000
          1042-        GRID    697             72.000  57.09113.0000
          1043-        GRID    698             72.000  57.0911352.8000
          1044-        GRID    699             72.000  57.0911389.6000
          1045-        GRID    700             72.000  42.0169089.6000
          1046-        GRID    701             72.000  .00000  89.6000
          1047-        GRID    702             72.000  .00000  100.0000
          1048-        GRID    703             72.000  .00000  150.0000
          1049-        GRID    704             72.000  17.05230100.0000
          1050-        GRID    705             72.000  17.05230150.0000
```

A=13.200 RR= 72.0 TS=2.215 TP=1.100 TPAD=1.500 P0=13.750

LTPT

S O R T E D   B U L K   D A T A   E C H O

CARD COUNT	1	2	3	4	5	6	7	8	9	10
1051-	GRID	706		72.000	34.10460100.0000					
1052-	GRID	707		72.000	34.10460150.0000					
1053-	GRID	708		72.000	51.15690.0000					
1054-	GRID	709		72.000	51.1569050.0000					
1055-	GRID	710		72.000	51.15690100.0000					
1056-	GRID	711		72.000	51.15690150.0000					
1057-	GRID	712		72.000	58.83040.0000					
1058-	GRID	713		72.000	58.8304050.0000					
1059-	GRID	714		72.000	58.83040100.0000					
1060-	GRID	715		72.000	58.83040150.0000					
1061-	GRID	716		72.000	66.50390.0000					
1062-	GRID	717		72.000	66.5039050.0000					
1063-	GRID	718		72.000	66.50390100.0000					
1064-	GRID	719		72.000	66.50390150.0000					
1065-	GRID	720		72.000	74.17740.0000					
1066-	GRID	721		72.000	74.1774050.0000					
1067-	GRID	722		72.000	74.17740100.0000					
1068-	GRID	723		72.000	74.17740150.0000					
1069-	GRID	724		72.000	81.85090.0000					
1070-	GRID	725		72.000	81.8509050.0000					
1071-	GRID	726		72.000	81.85090100.0000					
1072-	GRID	727		72.000	81.85090150.0000					
1073-	GRID	728		72.000	90.00000.0000					
1074-	GRID	729		72.000	90.0000050.0000					
1075-	GRID	730		72.000	90.00000100.0000					
1076-	GRID	731		72.000	90.00000150.0000					
1077-	MAT1	47	29.0+6		.3					
1078-	MPC	30	263	6	1.0	525	6	-1.0		
1079-	MPC	30	264	6	1.0	526	6	-1.0		
1080-	MPC	30	265	6	1.0	527	6	-1.0		
1081-	MPC	30	266	6	1.0	528	6	-1.0		
1082-	MPC	30	267	6	1.0	529	6	-1.0		
1083-	MPC	30	268	6	1.0	530	6	-1.0		
1084-	MPC	30	269	6	1.0	531	6	-1.0		
1085-	MPC	30	270	6	1.0	532	6	-1.0		

A=13.200 RR= 72.0 TS=2.215 TP=1.100 TPAD=1.500 PO=13.750

LTPT

S O R T E D B U L K D A T A E C H O

CARD COUNT	. 1 ..	2 ..	3 ..	4 ..	5 ..	6 ..	7 ..	8 ..	9 ..	10
1086-	MPC	30	271	6	1.0	533	6	-1.0		
1087-	MPC	30	272	6	1.0	534	6	-1.0		
1088-	MPC	30	273	6	1.0	535	6	-1.0		
1089-	MPC	31	263	5	1.0	525	5	-1.0		
1090-	MPC	31	264	5	1.0	526	5	-1.0		
1091-	MPC	31	265	5	1.0	527	5	-1.0		
1092-	MPC	31	266	5	1.0	528	5	-1.0		
1093-	MPC	31	267	5	1.0	529	5	-1.0		
1094-	MPC	31	268	5	1.0	530	5	-1.0		
1095-	MPC	31	269	5	1.0	531	5	-1.0		
1096-	MPC	31	270	5	1.0	532	5	-1.0		
1097-	MPC	31	271	5	1.0	533	5	-1.0		
1098-	MPC	31	272	5	1.0	534	5	-1.0		
1099-	MPC	31	273	5	1.0	535	5	-1.0		
1100-	MPC	32	263	1	1.0	525	1	-1.0		
1101-	MPC	32	264	1	1.0	526	1	-1.0		
1102-	MPC	32	265	1	1.0	527	1	-1.0		
1103-	MPC	32	266	1	1.0	528	1	-1.0		
1104-	MPC	32	267	1	1.0	529	1	-1.0		
1105-	MPC	32	268	1	1.0	530	1	-1.0		
1106-	MPC	32	269	1	1.0	531	1	-1.0		
1107-	MPC	32	270	1	1.0	532	1	-1.0		
1108-	MPC	32	271	1	1.0	533	1	-1.0		
1109-	MPC	32	272	1	1.0	534	1	-1.0		
1110-	MPC	32	273	1	1.0	535	1	-1.0		
1111-	MPC	34	263	2	1.0	525	2	-1.0		+JR1
1112-	+JR1		525	6	-2.6077					
1113-	MPC	34	264	2	1.0	526	2	-1.0		+JR2
1114-	+JR2		526	6	-2.6077					
1115-	MPC	34	265	2	1.0	527	2	-1.0		+JR3
1116-	+JR3		527	6	-2.6077					
1117-	MPC	34	266	2	1.0	528	2	-1.0		+JR4
1118-	+JR4		528	6	-2.6077					
1119-	MPC	34	267	2	1.0	529	2	-1.0		+JR5
1120-	+JR5		529	6	-2.6077					

PIPE AND BOTH PADS REINFORCED HOLE IN CYLINDRICAL SHELL JUNE 28, 1974 NASTRAN 2.

A=13.203 RR= 72.0 TS=2.215 TP=1.100 TPAD=1.500 PO=13.750

LTPT

S O R T E D   B U L K   D A T A   E C H O

CARD COUNT	. 1 ..	2 ..	3 ..	4 ..	5 ..	6 ..	7 ..	8 ..	9 ..	10 .
1121-	MPC	34	268	2	1.0	530	2	-1.0		+JR6
1122-	+JR6		530	6	-2.6077					
1123-	MPC	34	269	2	1.0	531	2	-1.0		+JR7
1124-	+JR7		531	6	-2.6077					
1125-	MPC	34	270	2	1.0	532	2	-1.0		+JR8
1126-	+JR8		532	6	-2.6077					
1127-	MPC	34	271	2	1.0	533	2	-1.0		+JR9
1128-	+JR9		533	6	-2.6077					
1129-	MPC	34	272	2	1.0	534	2	-1.0		+JR10
1130-	+JR10		534	6	-2.6077					
1131-	MPC	34	273	2	1.0	535	2	-1.0		+JR11
1132-	+JR11		535	6	-2.6077					
1133-	MPC	35	263	3	1.0	525	3	-1.0		+JR12
1134-	+JR12		525	5	2.6077					
1135-	MPC	35	264	3	1.0	526	3	-1.0		+JR13
1136-	+JR13		526	5	2.6077					
1137-	MPC	35	265	3	1.0	527	3	-1.0		+JR14
1138-	+JR14		527	5	2.6077					
1139-	MPC	35	266	3	1.0	528	3	-1.0		+JR15
1140-	+JR15		528	5	2.6077					
1141-	MPC	35	267	3	1.0	529	3	-1.0		+JR16
1142-	+JR16		529	5	2.6077					
1143-	MPC	35	268	3	1.0	530	3	-1.0		+JR17
1144-	+JR17		530	5	2.6077					
1145-	MPC	35	269	3	1.0	531	3	-1.0		+JR18
1146-	+JR18		531	5	2.6077					
1147-	MPC	35	270	3	1.0	532	3	-1.0		+JR19
1148-	+JR19		532	5	2.6077					
1149-	MPC	35	271	3	1.0	533	3	-1.0		+JR20
1150-	+JR20		533	5	2.6077					
1151-	MPC	35	272	3	1.0	534	3	-1.0		+JR21
1152-	+JR21		534	5	2.6077					
1153-	MPC	35	273	3	1.0	535	3	-1.0		+JR22
1154-	+JR22		535	5	2.6077					
1155-	MPC	37	262	1	1.0	524	1	-1.0		

A=13.200 RR= 72.0 TS=2.215 TP=1.100 TPAD=1.500 PO=13.750

LIPT

S O R T E D   B U L K   D A T A   E C H O

CARD COUNT	. 1 ..	2 ..	3 ..	4 ..	5 ..	6 ..	7 ..	8 ..	9 ..	10 .
1156-	MPC	37	262	3	1.0	524	3	-1.0		+JR23
1157-	+JR23		524	5	2.6077					
1158-	MPC	37	262	5	1.0	524	5	-1.0		
1159-	MPC	37	274	1	1.0	536	1	-1.0		
1160-	MPC	37	274	2	1.0	536	2	-1.0		+JR24
1161-	+JR24		536	6	-2.6077					
1162-	MPC	37	274	6	1.0	536	6	-1.0		
1163-	MPC	60	312	1	1.0	512	1	-1.0		
1164-	MPC	60	313	1	1.0	513	1	-1.0		
1165-	MPC	60	314	1	1.0	514	1	-1.0		
1166-	MPC	60	315	1	1.0	515	1	-1.0		
1167-	MPC	60	316	1	1.0	516	1	-1.0		
1168-	MPC	60	317	1	1.0	517	1	-1.0		
1169-	MPC	60	318	1	1.0	518	1	-1.0		
1170-	MPC	60	319	1	1.0	519	1	-1.0		
1171-	MPC	60	320	1	1.0	520	1	-1.0		
1172-	MPC	60	321	1	1.0	521	1	-1.0		
1173-	MPC	60	322	1	1.0	522	1	-1.0		
1174-	MPC	60	377	1	1.0	577	1	-1.0		
1175-	MPC	60	378	1	1.0	578	1	-1.0		
1176-	MPC	60	379	1	1.0	579	1	-1.0		
1177-	MPC	60	380	1	1.0	580	1	-1.0		
1178-	MPC	60	381	1	1.0	581	1	-1.0		
1179-	MPC	60	382	1	1.0	582	1	-1.0		
1180-	MPC	60	383	1	1.0	583	1	-1.0		
1181-	MPC	60	384	1	1.0	584	1	-1.0		
1182-	MPC	60	385	1	1.0	585	1	-1.0		
1183-	MPC	60	386	1	1.0	586	1	-1.0		
1184-	MPC	60	387	1	1.0	587	1	-1.0		
1185-	MPC	60	412	1	1.0	512	1	-1.0		
1186-	MPC	60	413	1	1.0	513	1	-1.0		
1187-	MPC	60	414	1	1.0	514	1	-1.0		
1188-	MPC	60	415	1	1.0	515	1	-1.0		
1189-	MPC	60	416	1	1.0	516	1	-1.0		
1190-	MPC	60	417	1	1.0	517	1	-1.0		

A=13.200 RR= 72.0 TS=2.215 TP=1.100 TPAD=1.500 PO=13.750

LTPT

S O R T E D B U L K D A T A E C H O

CARD COUNT	. 1 ..	2 ..	3 ..	4 ..	5 ..	6 ..	7 ..	8 ..	9 ..	10 .
1191-	MPC	60	418	1	1.0	518	1	-1.0		
1192-	MPC	60	419	1	1.0	519	1	-1.0		
1193-	MPC	60	420	1	1.0	520	1	-1.0		
1194-	MPC	60	421	1	1.0	521	1	-1.0		
1195-	MPC	60	422	1	1.0	522	1	-1.0		
1196-	MPC	60	477	1	1.0	577	1	-1.0		
1197-	MPC	60	478	1	1.0	578	1	-1.0		
1198-	MPC	60	479	1	1.0	579	1	-1.0		
1199-	MPC	60	480	1	1.0	580	1	-1.0		
1200-	MPC	60	481	1	1.0	581	1	-1.0		
1201-	MPC	60	482	1	1.0	582	1	-1.0		
1202-	MPC	60	483	1	1.0	583	1	-1.0		
1203-	MPC	60	484	1	1.0	584	1	-1.0		
1204-	MPC	60	485	1	1.0	585	1	-1.0		
1205-	MPC	60	486	1	1.0	586	1	-1.0		
1206-	MPC	60	487	1	1.0	587	1	-1.0		
1207-	MPC	61	312	5	1.0	512	5	-1.0		
1208-	MPC	61	313	5	1.0	513	5	-1.0		
1209-	MPC	61	314	5	1.0	514	5	-1.0		
1210-	MPC	61	315	5	1.0	515	5	-1.0		
1211-	MPC	61	316	5	1.0	516	5	-1.0		
1212-	MPC	61	317	5	1.0	517	5	-1.0		
1213-	MPC	61	318	5	1.0	518	5	-1.0		
1214-	MPC	61	319	5	1.0	519	5	-1.0		
1215-	MPC	61	320	5	1.0	520	5	-1.0		
1216-	MPC	61	321	5	1.0	521	5	-1.0		
1217-	MPC	61	322	5	1.0	522	5	-1.0		
1218-	MPC	61	377	5	1.0	577	5	-1.0		
1219-	MPC	61	378	5	1.0	578	5	-1.0		
1220-	MPC	61	379	5	1.0	579	5	-1.0		
1221-	MPC	61	380	5	1.0	580	5	-1.0		
1222-	MPC	61	381	5	1.0	581	5	-1.0		
1223-	MPC	61	382	5	1.0	582	5	-1.0		
1224-	MPC	61	383	5	1.0	583	5	-1.0		
1225-	MPC	61	384	5	1.0	584	5	-1.0		

ORIGINAL PAGE IS OF POOR QUALITY

A=13.200 RR=, 72.0 TS=2.215 TP=1.100 TPAD=1.500 P0=13.750

LTPT

S O R T E D   B U L K   D A T A   E C H O

CARD COUNT	. 1 ..	2 ..	3 ..	4 ..	5 ..	6 ..	7 ..	8 ..	9 ..	10 .
1226-	MPC	61	385	5	1.0	585	5	-1.0		
1227-	MPC	61	386	5	1.0	586	5	-1.0		
1228-	MPC	61	387	5	1.0	587	5	-1.0		
1229-	MPC	61	412	5	1.0	512	5	-1.0		
1230-	MPC	61	413	5	1.0	513	5	-1.0		
1231-	MPC	61	414	5	1.0	514	5	-1.0		
1232-	MPC	61	415	5	1.0	515	5	-1.0		
1233-	MPC	61	416	5	1.0	516	5	-1.0		
1234-	MPC	61	417	5	1.0	517	5	-1.0		
1235-	MPC	61	418	5	1.0	518	5	-1.0		
1236-	MPC	61	419	5	1.0	519	5	-1.0		
1237-	MPC	61	420	5	1.0	520	5	-1.0		
1238-	MPC	61	421	5	1.0	521	5	-1.0		
1239-	MPC	61	422	5	1.0	522	5	-1.0		
1240-	MPC	61	477	5	1.0	577	5	-1.0		
1241-	MPC	61	478	5	1.0	578	5	-1.0		
1242-	MPC	61	479	5	1.0	579	5	-1.0		
1243-	MPC	61	480	5	1.0	580	5	-1.0		
1244-	MPC	61	481	5	1.0	581	5	-1.0		
1245-	MPC	61	482	5	1.0	582	5	-1.0		
1246-	MPC	61	483	5	1.0	583	5	-1.0		
1247-	MPC	61	484	5	1.0	584	5	-1.0		
1248-	MPC	61	485	5	1.0	585	5	-1.0		
1249-	MPC	61	486	5	1.0	586	5	-1.0		
1250-	MPC	61	487	5	1.0	587	5	-1.0		
1251-	MPC	62	312	6	1.0	512	6	-1.0		
1252-	MPC	62	313	6	1.0	513	6	-1.0		
1253-	MPC	62	314	6	1.0	514	6	-1.0		
1254-	MPC	62	315	6	1.0	515	6	-1.0		
1255-	MPC	62	316	6	1.0	516	6	-1.0		
1256-	MPC	62	317	6	1.0	517	6	-1.0		
1257-	MPC	62	318	6	1.0	518	6	-1.0		
1258-	MPC	62	319	6	1.0	519	6	-1.0		
1259-	MPC	62	320	6	1.0	520	6	-1.0		
1260-	MPC	62	321	6	1.0	521	6	-1.0		

A=13.200 BR= 72.0 TS=2.215 TP=1.100 TPAD=1.500 PD=13.750

LTPT

S O R T E D   B U L K   D A T A   E C H O

CARD COUNT	1	2	3	4	5	6	7	8	9	10
1261-	MPC	62	322	6	1.0	522	6	-1.0		
1262-	MPC	62	377	6	1.0	577	6	-1.0		
1263-	MPC	62	378	6	1.0	578	6	-1.0		
1264-	MPC	62	379	6	1.0	579	6	-1.0		
1265-	MPC	62	380	6	1.0	580	6	-1.0		
1266-	MPC	62	381	6	1.0	581	6	-1.0		
1267-	MPC	62	382	6	1.0	582	6	-1.0		
1268-	MPC	62	383	6	1.0	583	6	-1.0		
1269-	MPC	62	384	6	1.0	584	6	-1.0		
1270-	MPC	62	385	6	1.0	585	6	-1.0		
1271-	MPC	62	386	6	1.0	586	6	-1.0		
1272-	MPC	62	387	6	1.0	587	6	-1.0		
1273-	MPC	62	412	6	1.0	512	6	-1.0		
1274-	MPC	62	413	6	1.0	513	6	-1.0		
1275-	MPC	62	414	6	1.0	514	6	-1.0		
1276-	MPC	62	415	6	1.0	515	6	-1.0		
1277-	MPC	62	416	6	1.0	516	6	-1.0		
1278-	MPC	62	417	6	1.0	517	6	-1.0		
1279-	MPC	62	418	6	1.0	518	6	-1.0		
1280-	MPC	62	419	6	1.0	519	6	-1.0		
1281-	MPC	62	420	6	1.0	520	6	-1.0		
1282-	MPC	62	421	6	1.0	521	6	-1.0		
1283-	MPC	62	422	6	1.0	522	6	-1.0		
1284-	MPC	62	477	6	1.0	577	6	-1.0		
1285-	MPC	62	478	6	1.0	578	6	-1.0		
1286-	MPC	62	479	6	1.0	579	6	-1.0		
1287-	MPC	62	480	6	1.0	580	6	-1.0		
1288-	MPC	62	481	6	1.0	581	6	-1.0		
1289-	MPC	62	482	6	1.0	582	6	-1.0		
1290-	MPC	62	483	6	1.0	583	6	-1.0		
1291-	MPC	62	484	6	1.0	584	6	-1.0		
1292-	MPC	62	485	6	1.0	585	6	-1.0		
1293-	MPC	62	486	6	1.0	586	6	-1.0		
1294-	MPC	62	487	6	1.0	587	6	-1.0		
1295-	MPC	64	312	2	1.0	512	2	-1.0		+R2

A=13.200 RP= 72.0 TS=2.215 TP=1.100 TPAD=1.500 P0=13.750

LIPT

S O R T E D B U L K D A T A E C H O

CARD COUNT	. 1 ..	2 ..	3 ..	4 ..	5 ..	6 ..	7 ..	8 ..	9 ..	10
1296-	+R2		512	6	1.8577					
1297-	MPC	64	313	2	1.0	513	2	-1.0		+R3
1298-	+R3		513	6	1.8577					
1299-	MPC	64	314	2	1.0	514	2	-1.0		+R4
1300-	+R4		514	6	1.8577					
1301-	MPC	64	315	2	1.0	515	2	-1.0		+R5
1302-	+R5		515	6	1.8577					
1303-	MPC	64	316	2	1.0	516	2	-1.0		+R6
1304-	+R6		516	6	1.8577					
1305-	MPC	64	317	2	1.0	517	2	-1.0		+R7
1306-	+R7		517	6	1.8577					
1307-	MPC	64	318	2	1.0	518	2	-1.0		+R8
1308-	+R8		518	6	1.8577					
1309-	MPC	64	319	2	1.0	519	2	-1.0		+R9
1310-	+R9		519	6	1.8577					
1311-	MPC	64	320	2	1.0	520	2	-1.0		+R10
1312-	+R10		520	6	1.8577					
1313-	MPC	64	321	2	1.0	521	2	-1.0		+R11
1314-	+R11		521	6	1.8577					
1315-	MPC	64	322	2	1.0	522	2	-1.0		+R12
1316-	+R12		522	6	1.8577					
1317-	MPC	64	377	2	1.0	577	2	-1.0		+R24
1318-	+R24		577	6	1.8577					
1319-	MPC	64	378	2	1.0	578	2	-1.0		+R25
1320-	+R25		578	6	1.8577					
1321-	MPC	64	379	2	1.0	579	2	-1.0		+R26
1322-	+R26		579	6	1.8577					
1323-	MPC	64	380	2	1.0	580	2	-1.0		+R27
1324-	+R27		580	6	1.8577					
1325-	MPC	64	381	2	1.0	581	2	-1.0		+R28
1326-	+R28		581	6	1.8577					
1327-	MPC	64	382	2	1.0	582	2	-1.0		+R29
1328-	+R29		582	6	1.8577					
1329-	MPC	64	383	2	1.0	583	2	-1.0		+R30
1330-	+R30		583	6	1.8577					

PIPE AND BOTH PADS REINFORCED HOLE IN CYLINDRICAL SHELL JUNE 28, 1974 NASTRAN 2/

A=13.200 RR= 72.0 TS=2.215 TP=1.100 TPAD=1.500 PO=13.750

LTPT

S O R T E D   B U L K   D A T A   E C H O

CARD COUNT	. 1 ..	2 ..	3 ..	4 ..	5 ..	6 ..	7 ..	8 ..	9 ..	10
1331-	MPC	64	384	2	1.0	584	2	-1.0		+R31
1332-	+R31		584	6	1.8577					
1333-	MPC	64	385	2	1.0	585	2	-1.0		+R32
1334-	+R32		585	6	1.8577					
1335-	MPC	64	386	2	1.0	586	2	-1.0		+R33
1336-	+R33		586	6	1.8577					
1337-	MPC	64	387	2	1.0	587	2	-1.0		+R34
1338-	+R34		587	6	1.8577					
1339-	MPC	64	412	2	1.0	512	2	-1.0		+R13
1340-	+R13		512	6	-1.8577					
1341-	MPC	64	413	2	1.0	513	2	-1.0		+R14
1342-	+R14		513	6	-1.8577					
1343-	MPC	64	414	2	1.0	514	2	-1.0		+R15
1344-	+R15		514	6	-1.8577					
1345-	MPC	64	415	2	1.0	515	2	-1.0		+R16
1346-	+R16		515	6	-1.8577					
1347-	MPC	64	416	2	1.0	516	2	-1.0		+R17
1348-	+R17		516	6	-1.8577					
1349-	MPC	64	417	2	1.0	517	2	-1.0		+R18
1350-	+R18		517	6	-1.8577					
1351-	MPC	64	418	2	1.0	518	2	-1.0		+R19
1352-	+R19		518	6	-1.8577					
1353-	MPC	64	419	2	1.0	519	2	-1.0		+R20
1354-	+R20		519	6	-1.8577					
1355-	MPC	64	421	2	1.0	520	2	-1.0		+R21
1356-	+R21		520	6	-1.8577					
1357-	MPC	64	421	2	1.0	521	2	-1.0		+R22
1358-	+R22		521	6	-1.8577					
1359-	MPC	64	422	2	1.0	522	2	-1.0		+R23
1360-	+R23		522	6	-1.8577					
1361-	MPC	64	477	2	1.0	577	2	-1.0		+R35
1362-	+R35		577	6	-1.8577					
1363-	MPC	64	478	2	1.0	578	2	-1.0		+R36
1364-	+R36		578	6	-1.8577					
1365-	MPC	64	479	2	1.0	579	2	-1.0		+R37

A=13.200 RP= 72.0 TS=2.215 TP=1.100 TPAD=1.500 PO=13.750

LTPT

S O R T E D B U L K D A T A E C H O

CARD COUNT	. 1 ..	2 ..	3 ..	4 ..	5 ..	6 ..	7 ..	8 ..	9 ..	10 .
1366-	+R37		579	6	-1.8577					
1367-	MPC	64	480	2	1.0	580	2	-1.0		+R38
1368-	+R38		580	6	-1.8577					
1369-	MPC	64	481	2	1.0	581	2	-1.0		+R39
1370-	+R39		581	6	-1.8577					
1371-	MPC	64	482	2	1.0	582	2	-1.0		+R40
1372-	+R40		582	6	-1.8577					
1373-	MPC	64	483	2	1.0	583	2	-1.0		+R41
1374-	+R41		583	6	-1.8577					
1375-	MPC	64	484	2	1.0	584	2	-1.0		+R42
1376-	+R42		584	6	-1.8577					
1377-	MPC	64	485	2	1.0	585	2	-1.0		+R43
1378-	+R43		585	6	-1.8577					
1379-	MPC	64	486	2	1.0	586	2	-1.0		+R44
1380-	+R44		586	6	-1.8577					
1381-	MPC	64	487	2	1.0	587	2	-1.0		+R45
1382-	+R45		587	6	-1.8577					
1383-	MPC	65	312	3	1.0	512	3	-1.0		+R46
1384-	+R46		512	5	-1.8577					
1385-	MPC	65	313	3	1.0	513	3	-1.0		+R47
1386-	+R47		513	5	-1.8577					
1387-	MPC	65	314	3	1.0	514	3	-1.0		+R48
1388-	+R48		514	5	-1.8577					
1389-	MPC	65	315	3	1.0	515	3	-1.0		+R49
1390-	+R49		515	5	-1.8577					
1391-	MPC	65	316	3	1.0	516	3	-1.0		+R50
1392-	+R50		516	5	-1.8577					
1393-	MPC	65	317	3	1.0	517	3	-1.0		+R51
1394-	+R51		517	5	-1.8577					
1395-	MPC	65	318	3	1.0	518	3	-1.0		+R52
1396-	+R52		518	5	-1.8577					
1397-	MPC	65	319	3	1.0	519	3	-1.0		+R53
1398-	+R53		519	5	-1.8577					
1399-	MPC	65	320	3	1.0	520	3	-1.0		+R54
1400-	+R54		520	5	-1.8577					

ORIGINAL PAGE IS OF POOR QUALITY

A=13.200 RR= 72.0 TS=2.215 TP=1.100 TPAD=1.500 PO=13.750

LIPT

S O R T E D B U L K D A T A E C H O

CARD COUNT	. 1 ..	2 ..	3 ..	4 ..	5 ..	6 ..	7 ..	8 ..	9 ..	10 .
1401-	MPC	65	321	3	1.0	521	3	-1.0		+R55
1402-	+R55		521	5	-1.8577					
1403-	MPC	65	322	3	1.0	522	3	-1.0		+R56
1404-	+R56		522	5	-1.8577					
1405-	MPC	65	377	3	1.0	577	3	-1.0		+R68
1406-	+R68		577	5	-1.8577					
1407-	MPC	65	378	3	1.0	578	3	-1.0		+R69
1408-	+R69		578	5	-1.8577					
1409-	MPC	65	379	3	1.0	579	3	-1.0		+R70
1410-	+R70		579	5	-1.8577					
1411-	MPC	65	380	3	1.0	580	3	-1.0		+R71
1412-	+R71		580	5	-1.8577					
1413-	MPC	65	381	3	1.0	581	3	-1.0		+R72
1414-	+R72		581	5	-1.8577					
1415-	MPC	65	382	3	1.0	582	3	-1.0		+R73
1416-	+R73		582	5	-1.8577					
1417-	MPC	65	383	3	1.0	583	3	-1.0		+R74
1418-	+R74		583	5	-1.8577					
1419-	MPC	65	384	3	1.0	584	3	-1.0		+R75
1420-	+R75		584	5	-1.8577					
1421-	MPC	65	385	3	1.0	585	3	-1.0		+R76
1422-	+R76		585	5	-1.8577					
1423-	MPC	65	386	3	1.0	586	3	-1.0		+R77
1424-	+R77		586	5	-1.8577					
1425-	MPC	65	387	3	1.0	587	3	-1.0		+R78
1426-	+R78		587	5	-1.8577					
1427-	MPC	65	412	3	1.0	512	3	-1.0		+R57
1428-	+R57		512	5	1.8577					
1429-	MPC	65	413	3	1.0	513	3	-1.0		+R58
1430-	+R58		513	5	1.8577					
1431-	MPC	65	414	3	1.0	514	3	-1.0		+R59
1432-	+R59		514	5	1.8577					
1433-	MPC	65	415	3	1.0	515	3	-1.0		+R60
1434-	+R60		515	5	1.8577					
1435-	MPC	65	416	3	1.0	516	3	-1.0		+R61

A=13.200 RB= 72.0 TS=2.215 TP=1.100 TPAD=1.500 PO=13.750

1IPT

S O R T E D B U L K D A T A E C H O

CARD COUNT	. 1 ..	2 ..	3 ..	4 ..	5 ..	6 ..	7 ..	8 ..	9 ..	10
1436-	+R61		516	5	1.8577					
1437-	MPC	65	417	3	1.0	517	3	-1.0		+R62
1438-	+R62		517	5	1.8577					
1439-	MPC	65	418	3	1.0	518	3	-1.0		+R63
1440-	+R63		518	5	1.8577					
1441-	MPC	65	419	3	1.0	519	3	-1.0		+R64
1442-	+R64		519	5	1.8577					
1443-	MPC	65	420	3	1.0	520	3	-1.0		+R65
1444-	+R65		520	5	1.8577					
1445-	MPC	65	421	3	1.0	521	3	-1.0		+R66
1446-	+R66		521	5	1.8577					
1447-	MPC	65	422	3	1.0	522	3	-1.0		+R67
1448-	+R67		522	5	1.8577					
1449-	MPC	65	477	3	1.0	577	3	-1.0		+R79
1450-	+R79		577	5	1.8577					
1451-	MPC	65	478	3	1.0	578	3	-1.0		+R80
1452-	+R80		578	5	1.8577					
1453-	MPC	65	479	3	1.0	579	3	-1.0		+R81
1454-	+R81		579	5	1.8577					
1455-	MPC	65	480	3	1.0	580	3	-1.0		+R82
1456-	+R82		580	5	1.8577					
1457-	MPC	65	481	3	1.0	581	3	-1.0		+R83
1458-	+R83		581	5	1.8577					
1459-	MPC	65	482	3	1.0	582	3	-1.0		+R84
1460-	+R84		582	5	1.8577					
1461-	MPC	65	483	3	1.0	583	3	-1.0		+R85
1462-	+R85		583	5	1.8577					
1463-	MPC	65	484	3	1.0	584	3	-1.0		+R86
1464-	+R86		584	5	1.8577					
1465-	MPC	65	485	3	1.0	585	3	-1.0		+R87
1466-	+R87		585	5	1.8577					
1467-	MPC	65	486	3	1.0	586	3	-1.0		+R88
1468-	+R88		586	5	1.8577					
1469-	MPC	65	487	3	1.0	587	3	-1.0		+R89
1470-	+R89		587	5	1.8577					

A=13.200 RR= 72.0 TS=2.215 TP=1.100 TPAD=1.500 PO=13.750

LTPT

S O R T E D B U L K D A T A E C H O

CARD COUNT	. 1 ..	2 ..	3 ..	4 ..	5 ..	6 ..	7 ..	8 ..	9 ..	10
1471-	MPC	66	311	1	1.0	511	1	-1.0		
1472-	MPC	66	311	3	1.0	511	3	-1.0		+R90
1473-	+R90		511	5	-1.8577					
1474-	MPC	66	311	5	1.0	511	5	-1.0		
1475-	MPC	66	323	1	1.0	523	1	-1.0		
1476-	MPC	66	323	2	1.0	523	2	-1.0		+R94
1477-	+R94		523	6	1.8577					
1478-	MPC	66	323	6	1.0	523	6	-1.0		
1479-	MPC	66	376	1	1.0	576	1	-1.0		
1480-	MPC	66	376	3	1.0	576	3	-1.0		+R92
1481-	+R92		576	5	-1.8577					
1482-	MPC	66	376	5	1.0	576	5	-1.0		
1483-	MPC	66	388	1	1.0	588	1	-1.0		
1484-	MPC	66	388	2	1.0	588	2	-1.0		+R96
1485-	+R96		588	6	1.8577					
1486-	MPC	66	388	6	1.0	588	6	-1.0		
1487-	MPC	66	411	1	1.0	511	1	-1.0		
1488-	MPC	66	411	3	1.0	511	3	-1.0		+R91
1489-	+R91		511	5	1.8577					
1490-	MPC	66	411	5	1.0	511	5	-1.0		
1491-	MPC	66	423	1	1.0	523	1	-1.0		
1492-	MPC	66	423	2	1.0	523	2	-1.0		+R95
1493-	+R95		523	6	-1.8577					
1494-	MPC	66	423	6	1.0	523	6	-1.0		
1495-	MPC	66	476	1	1.0	576	1	-1.0		
1496-	MPC	66	476	3	1.0	576	3	-1.0		+R93
1497-	+R93		576	5	1.8577					
1498-	MPC	66	476	5	1.0	576	5	-1.0		
1499-	MPC	66	488	1	1.0	588	1	-1.0		
1500-	MPC	66	488	2	1.0	588	2	-1.0		+R97
1501-	+R97		588	6	-1.8577					
1502-	MPC	66	488	6	1.0	588	6	-1.0		
1503-	MPCADD	36	30	31	32	66	34	35	37	+R1
1504-	+R1	50	61	62	64	65				
1505-	PLOAD2	6	100.	576	THRU	587				

A=13.200 RR= 72.0 TS=2.215 TP=1.100 TPAD=1.500 PO=13.750

LTPT

S O R T E D   B U L K   D A T A   E C H O

CARD COUNT	. 1 ..	2 ..	3 ..	4 ..	5 ..	6 ..	7 ..	8 ..	9 ..	10
1506-	PLOAD2	6	100.	589	THRU	600				
1507-	PLOAD2	6	100.	602	THRU	613				
1508-	PLOAD2	6	100.	615	THRU	666				
1509-	PLOAD2	6	100.	668	THRU	679				
1510-	PLOAD2	6	100.	681	THRU	702				
1511-	PLOAD2	6	100.	708	THRU	710				
1512-	PLOAD2	6	100.	712	THRU	714				
1513-	PLOAD2	6	100.	716	THRU	718				
1514-	PLOAD2	6	100.	720	THRU	722				
1515-	PLOAD2	6	100.	724	THRU	726				
1516-	PLOAD2	6	100.	1615	1616	1618	1619	1620	1622	
1517-	PLOAD2	6	100.	1623	1624	1625	1626	1627	1629	
1518-	PLOAD2	6	100.	1630	1648	1650	1652	1654	1656	
1519-	PLOAD2	6	100.	1657	1658	1660	1662	1664	1666	
1520-	PLOAD2	6	100.	1669	1671	1673	1674	1675	1677	
1521-	PLOAD2	6	100.	1679	1682	1684	1685	1687	1698	
1522-	PLOAD2	6	100.	1693	1695					
1523-	PLOAD2	6	100.	1699	1700	2619	2623	2625	2627	
1524-	PLOAD2	6	100.	2629	2630	2700	704	706	1691	
1525-	PLOAD2	6	100.0	311	THRU	322				
1526-	PLOAD2	6	100.0	324	THRU	335				
1527-	PLOAD2	6	100.0	337	THRU	348				
1528-	PLOAD2	6	100.0	350	THRU	361				
1529-	PLOAD2	6	100.0	363	THRU	374				
1530-	PLOAD2	6	100.0	3311	THRU	3322				
1531-	PLOAD2	6	100.0	3324	THRU	3335				
1532-	PLOAD2	6	100.0	3337	THRU	3348				
1533-	PLOAD2	6	100.0	3350	THRU	3361				
1534-	PLOAD2	6	100.0	3363	THRU	3374				
1535-	PLOAD2	6	100.0	3576	THRU	3587				
1536-	PLOAD2	6	100.0	3589	THRU	3600				
1537-	PLOAD2	6	100.0	3602	THRU	3613				
1538-	PLOAD2	6	-100.0	227	THRU	229				
1539-	PLOAD2	6	-100.0	231	THRU	233				
1540-	PLOAD2	6	-100.0	235	THRU	237				

A=13.200 RR= 72.0 TS=2.215 TP=1.100 TPAD=1.500 PO=13.750

1TPT

S O R T E D B U L K D A T A E C H O

CARD COUNT	. 1 ..	2 ..	3 ..	4 ..	5 ..	6 ..	7 ..	8 ..	9 ..	10 .
1541-	PLOAD2	6	-100.0	239	THRU	241				
1542-	PLOAD2	6	-100.0	243	THRU	245				
1543-	PLOAD2	6	-100.0	247	THRU	249				
1544-	PLOAD2	6	-100.0	251	THRU	253				
1545-	PLOAD2	6	-100.0	255	THRU	260				
1546-	PLOAD2	6	-100.0	262	THRU	273				
1547-	PLOAD2	6	-100.0	1256	1258	1260				
1548-	PLOAD2	6	-100.0	1263	1265	1267	1269	1271	1273	
1549-	PQUAD2	41	47	2.21538						
1550-	PQUAD2	43	47	1.50000						
1551-	PQUAD2	44	47	1.50000						
1552-	PQUAD2	51	47	1.10000						
1553-	PQUAD2	75	47	.75000						
1554-	PTRIA2	41	47	2.21538						
1555-	PTRIA2	43	47	1.50000						
1556-	PTRIA2	44	47	1.50000						
1557-	PTRIA2	51	47	1.10000						
1558-	PTRIA2	75	47	.75000						
1559-	SPC1	1	26	511	524	537	550	563	576	+K1
1560-	+K1	589	602	615	667	680	689	696	701	+K2
1561-	+K2	702	311	324	337	350	363	376	411	+K3
1562-	+K3	424	437	450	463	476				
1563-	SPC1	2	35	523	536	549	562	575	588	+L1
1564-	+L1	601	614	627	647	668	681	690	697	+L2
1565-	+L2	708	712	716	720	724	323	336	349	+L3
1566-	+L3	362	375	388	423	436	449	462	475	+L4
1567-	+L4	488								
1568-	SPC1	3	5	705	707	711	715	719	723	+M1
1569-	+M1	727								
1570-	SPC1	4	26	729	730					
1571-	SPC1	6	2356	728						
1572-	SPC1	8	256	703	731					
1573-	SPC1	9	246	223	227	231	235	239	243	+P1
1574-	+P1	262	247	251	255					
1575-	SPC1	10	345	226	230	234	238	242	246	+P2

```
A=13.200 RR=  72.0 TS=2.215 TP=1.100 TPAD=1.500 P0=13.750

 LTPT

                              S O R T E D   B U L K   D A T A   E C H O

      CARD
      COUNT      .  1  ..  2  ..  3  ..  4  ..  5  ..  6  ..  7  ..  8  ..  9  ..  10
      1576-      +P2     274     250     254     261
      1577-      SPCADD  5       1       2       3       4       6       8       9       +P3
      1578-      +P3     10
                 ENDDATA

     **NO ERRORS FOUND - EXECUTE NASTRAN PROGRAM**
                                 METHOD 2 NT,NBR PASSES =   1,EST. TIME =     14.6
                                 METHOD 2 T ,NBR PASSES =   1,EST. TIME =      9.7
                                 METHOD 2 T ,NBR PASSES =   1,EST. TIME =     38.0

*** USER INFORMATION MESSAGE 3023,        B =    71
                                          C =   183
                                          R =    70

*** USER INFORMATION MESSAGE 3027, SYMMETRIC REAL S.P. TIME ESTIMATE IS    640 SECONDS.
                                 METHOD 2 T ,NBR PASSES =   1,EST. TIME =       .2
                                 METHOD 2 NT,NBR PASSES =   1,EST. TIME =      1.1
                                 METHOD 1 NT,NBR PASSES =   1,EST. TIME =      5.1

*** USER INFORMATION MESSAGE 3035

FOR LOAD     1 EPSILON SUB E =-23.2524127E-14
                                 METHOD 2 NT,NBR PASSES =   1,EST. TIME =       .4
                                 METHOD 1 T ,NBR PASSES =   1,EST. TIME =      1.6
                                 METHOD 2 NT,NBR PASSES =   1,EST. TIME =       .2

*** SYSTEM WARNING MESSAGE 3022

    DATA BLOCK PLTPAR   IS REQUIRED AS INPUT AND IS NOT OUTPUT BY A PREVIOUS MODULE IN THE CURRENT DMAP ROU

*** SYSTEM WARNING MESSAGE 3022

    DATA BLOCK GPSETS   IS REQUIRED AS INPUT AND IS NOT OUTPUT BY A PREVIOUS MODULE IN THE CURRENT DMAP ROU
```

ORIGINAL PAGE IS OF POOR QUALITY

PIPE AND BOTH PADS REINFORCED HOLE IN CYLINDRICAL SHELL   JUNE 28, 1974

A=13.200 RR= 72.0 TS=2.215 TP=1.100 TPAD=1.500 P0=13.750

LTPT

S T R E S S E S   I N   G E N E R A L   T R I A N G U L A R   E L E M E N T S

ELEMENT ID.	FIBRE DISTANCE	STRESSES IN ELEMENT COORD SYSTEM NORMAL-X	NORMAL-Y	SHEAR-XY	PRINCIPAL STRESSES ANGLE	MAJOR
267	-55.000000E-02	36.626921E+02	15.282235E+02	16.874622E+01	4.4925	36.759504E+02
	55.000000E-02	27.996382E+02	79.493408E+00	-12.236078E+01	-2.5704	28.051313E+02
268	-55.000000E-02	17.455225E+02	10.201016E+02	-31.448518E+00	-2.4777	17.468833E+02
	55.000000E-02	37.184511E+02	34.966212E+01	30.306191E+01	5.0999	37.454979E+02
269	-55.000000E-02	28.478904E+02	10.733020E+02	21.705942E+01	6.8732	28.740544E+02
	55.000000E-02	19.551830E+02	-30.799750E+01	-63.394563E+00	-1.6033	19.569574E+02
270	-55.000000E-02	12.970949E+02	64.832626E+01	17.810507E+00	1.5714	12.975834E+02
	55.000000E-02	26.851675E+02	-10.364289E+01	22.019174E+01	4.4868	27.024457E+02
271	-55.000000E-02	21.905377E+02	64.843281E+01	82.812711E+00	3.0651	21.949721E+02
	55.000000E-02	13.357490E+02	-65.177969E+01	38.476868E+00	1.1086	13.364936E+02
272	-55.000000E-02	13.067414E+02	37.872258E+01	-57.859562E+00	-3.5539	13.103348E+02
	55.000000E-02	17.634289E+02	-51.761951E+01	16.233038E+01	4.0502	17.749232E+02
273	-55.000000E-02	16.595845E+02	40.629698E+01	47.376145E+00	2.1618	16.613728E+02
	55.000000E-02	12.291916E+02	-71.326576E+01	-27.871346E+00	-.8219	12.295915E+02
					Peak Stress	Answer
311	-37.500000E-02	63.524534E+02	69.873755E+01	-21.898232E+01	-2.2148	$\boxed{63.609224E+02}$
	37.500000E-02	59.054469E+02	44.554233E+01	-20.918724E+01	-2.1909	59.134498E+02
312	-37.500000E-02	60.296639E+02	72.081228E+01	-23.693549E+01	-2.5500	60.402347E+02
	37.500000E-02	56.980266E+02	52.815005E+01	-23.783955E+01	-2.6285	57.089453E+02
313	-37.500000E-02	58.169284E+02	74.174435E+01	-13.888619E+01	-1.5664	58.207263E+02
	37.500000E-02	52.382165E+02	28.458522E+01	-16.351277E+01	-1.8885	52.436080E+02
314	-37.500000E-02	53.494800E+02	86.723580E+01	-89.961737E+00	-1.1493	53.512848E+02
	37.500000E-02	48.072939E+02	18.989494E+01	-13.207812E+01	-1.6371	48.110689E+02

APPENDIX B

NASTRAN SUMMARY SHEETS

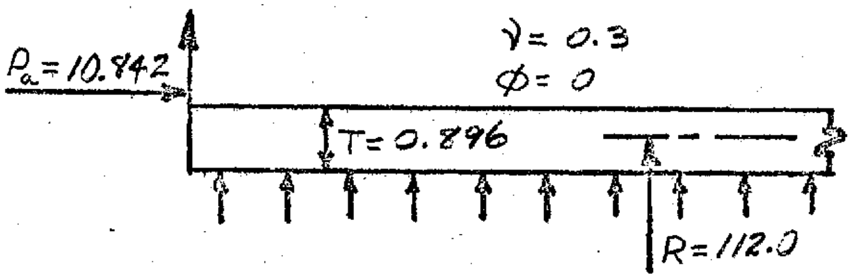

P/P_a	I/s SCF	O/s SCF
1.000	5.406	3.575
1.033	5.147	3.282
1.224	3.550	1.939
1.416	2.630	1.284
1.607	1.971	0.936
1.832	1.634	0.777
2.120	1.283	0.656
2.409	1.121	0.676

FORCE

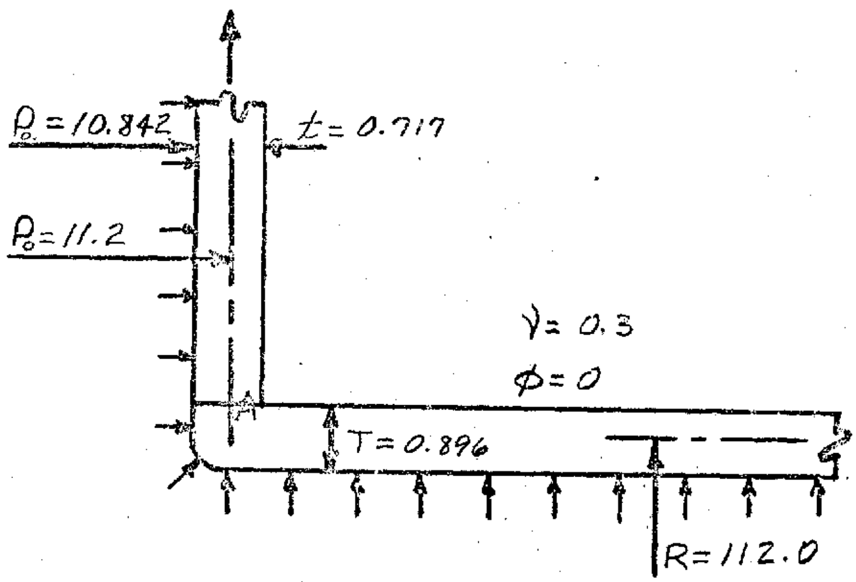

P/P_0	I/S SCF	O/S SCF
1.000 @ A	1.975	2.547
SHELL @ $\phi = 0$		
0.968	2.812	2.398
1.000	2.509	2.524
1.185	1.857	2.099
1.371	1.566	1.720
1.556	1.343	1.423
1.773	1.264	1.277
2.052	1.093	1.079
2.332	1.006	1.001

PIPE

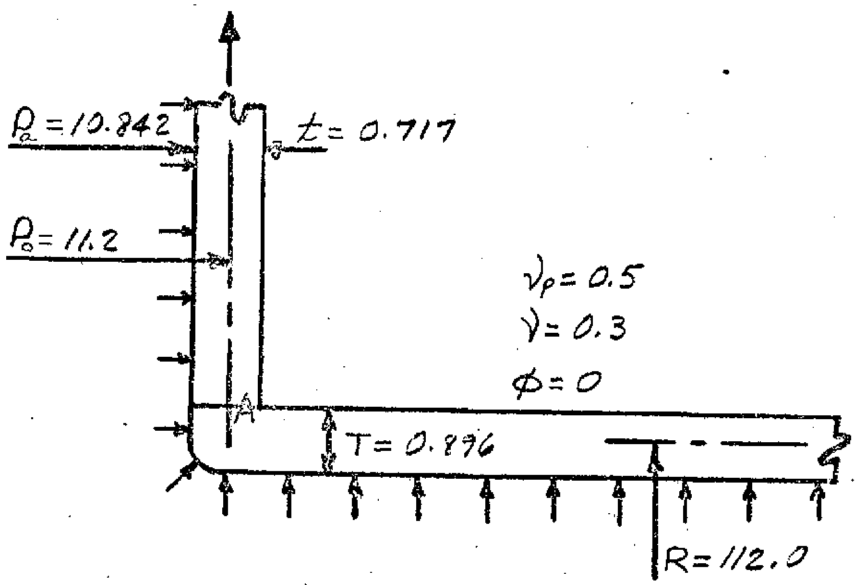

P/P_o	I/s SCF	O/s SCF
1.000 @ A	2.009	2.910
SHELL @ $\phi = 0$		
0.968	3.061	2.598
1.000	2.685	2.630
1.185	1.869	2.143
1.371	1.559	1.717
1.556	1.368	1.420
1.773	1.209	1.203
2.052	1.083	1.048
2.332	1.019	0.976

PIPE

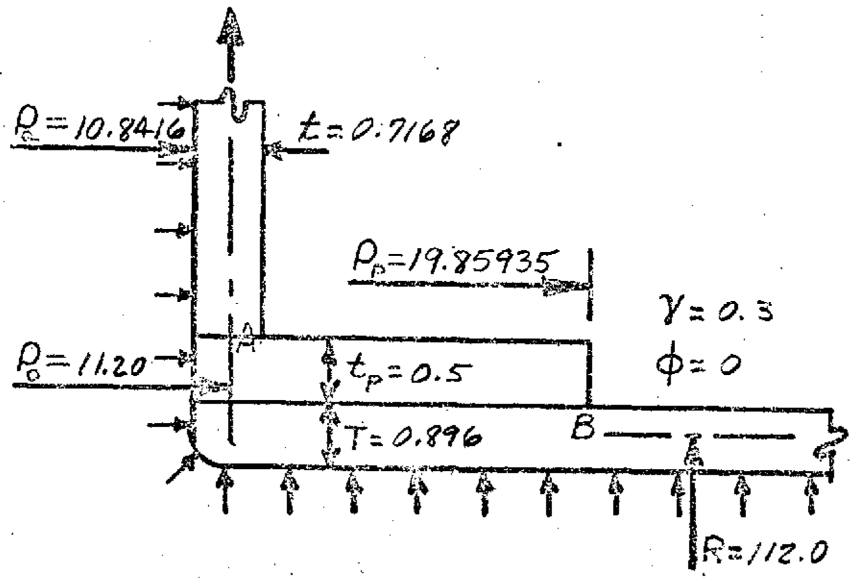

P/P_o	I/S SCF	O/S SCF
1.000 @ A	1.538	1.695
1.773 @ B	0.601	1.400
SHELL @ $\phi = 0$		
0.968	2.403	1.698
1.000	2.005	1.878
1.134	1.528	1.473
1.383	1.358	1.114
1.631	1.282	0.800
1.773	1.195	0.843
1.844	1.127	0.868
1.915	1.092	0.881

PIPE AND PAD

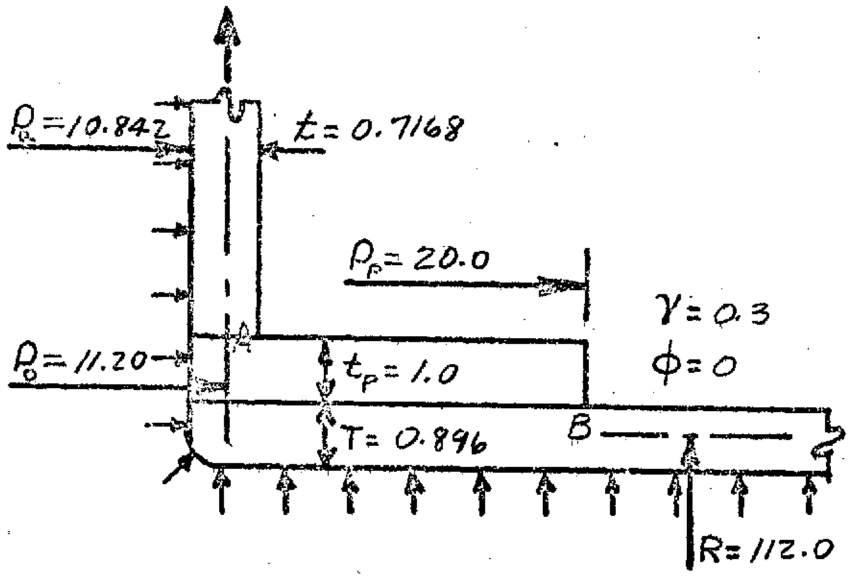

P/P_o	I/S SCF	O/S SCF
1.000 @ A	1.242	0.808
1.786 @ B	0.593	1.473
SHELL @ $\phi = 0$		
0.968	1.945	1.494
1.000	1.648	1.552
1.071	1.546	1.382
1.250	1.382	1.072
1.518	1.305	0.726
1.786	1.173	0.713
2.052	1.160	0.811
2.332	1.129	0.848

PIPE AND PAD

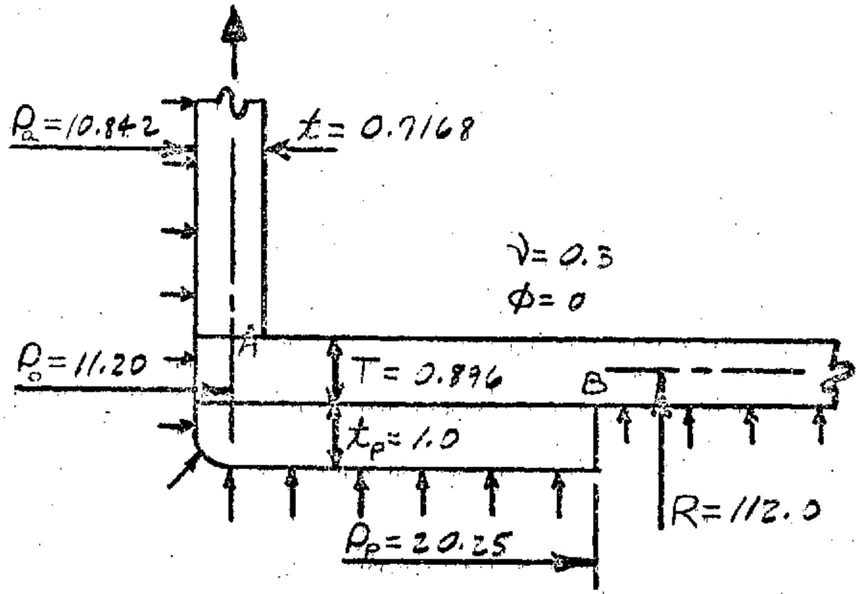

P/P_o	I/S SCF	O/S SCF
1.000 @ A	1.327	1.635
1.808 @ B	1.356	0.789
SHELL @ $\phi = 0$		
0.968	1.779	1.529
1.000	1.413	1.751
1.071	1.392	1.531
1.250	1.178	1.283
1.518	0.865	1.188
1.808	0.894	0.977
2.052	0.813	0.975
2.332	0.796	0.994

PIPE AND PAD

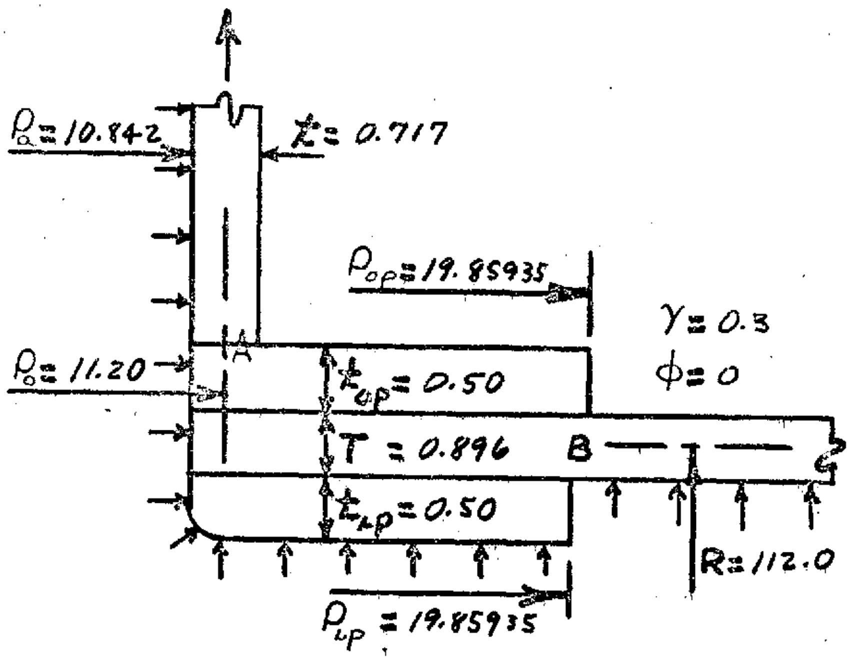

P/R_o	I/S SCF	O/S SCF
1.000 @ A	1.257	1.467
1.773 @ B	1.105	1.080
INNER PAD @ $\phi = 0$		
0.968	1.967	1.402
1.000	1.693	1.520
1.185	1.154	1.285
1.371	0.948	1.048
1.556	0.923	0.706
1.773	0.866	0.700
2.053	0.869	0.824
2.332	0.882	0.896

PIPE AND PADS

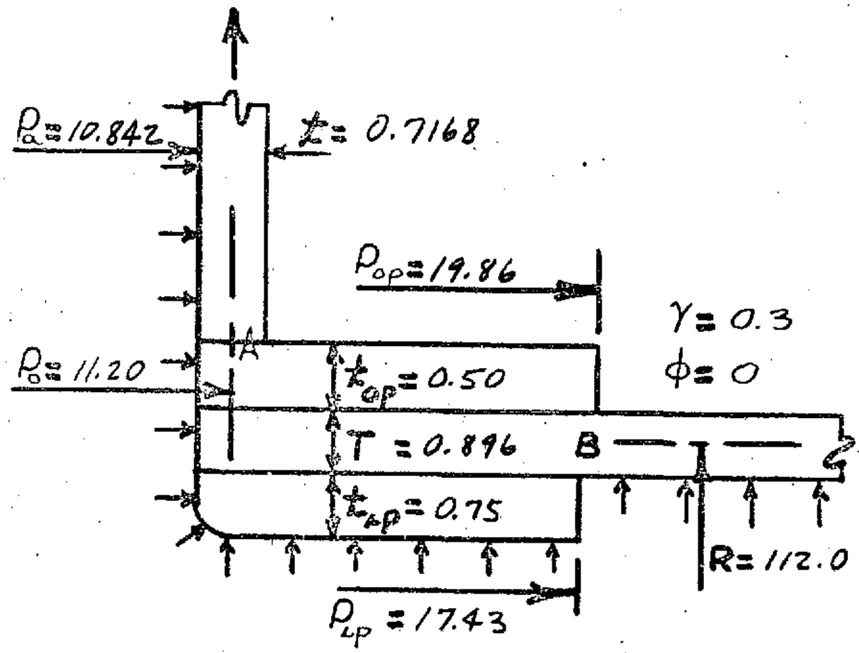

P/P_o	I/S SCF	O/S SCF
1.000 @ A	1.215	1.512
1.556 @ B	1.467	0.571
SHELL @ $\phi = 0$		
0.968	1.855	1.237
1.000	1.484	1.470
1.185	1.091	1.134
1.371	0.858	0.951
1.556	1.202	0.617
1.773	0.866	0.719
2.053	0.894	0.855
2.332	0.911	0.920

PIPE AND PADS

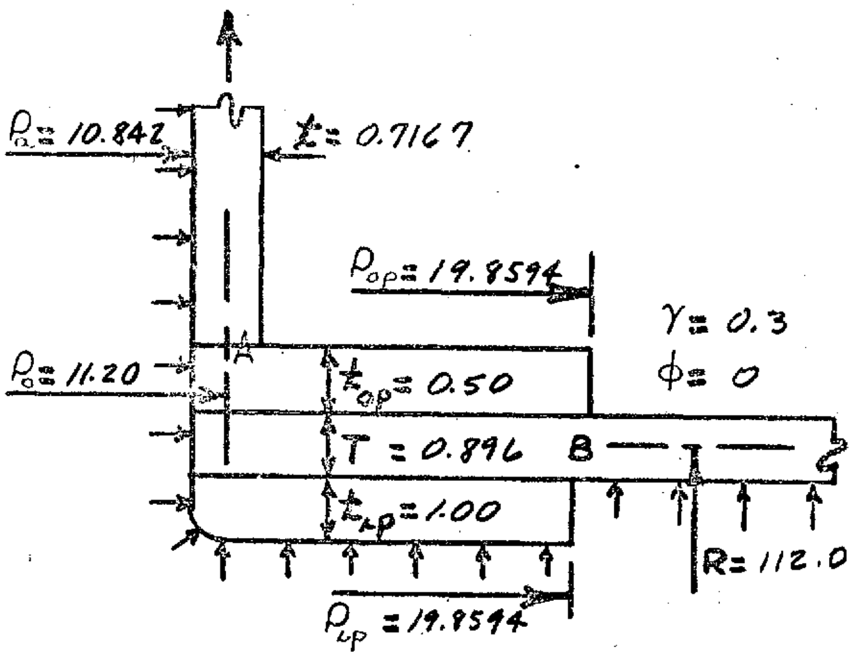

P/P_o	I/S SCF	O/S SCF
1.000 @ A	1.125	1.436
1.773 @ B	1.187	0.965
SHELL @ $\phi = 0$		
0.968	1.653	1.098
1.000	1.315	1.322
1.185	0.992	0.986
1.371	0.809	0.802
1.556	0.640	0.735
1.773	0.939	0.641
2.052	0.772	0.781
2.332	0.799	0.879

PIPE AND PADS

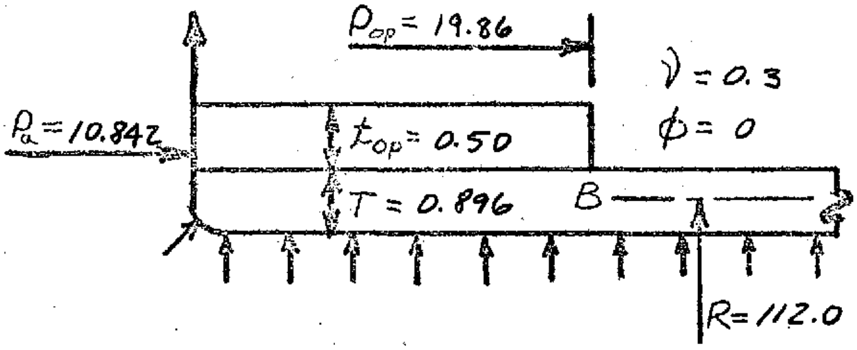

ρ/ρ_a	I/S SCF	O/S SCF
1.832 @ B	0.158	1.686
SHELL @ $\phi = 0$		
1.000	4.655	3.689
1.033	5.174	2.426
1.224	3.645	1.143
1.416	2.854	5.663
1.607	2.335	0.295
1.832	2.014	-0.005
2.120	1.752	0.060
2.409	1.625	0.160

FORCE AND PAD

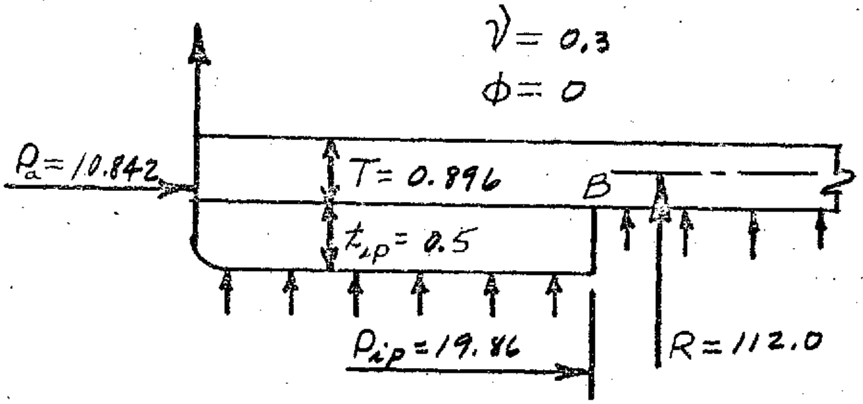

P/P_a	I/S SCF	O/S SCF
1.832 @ B	1.475	1.245
PAD @ $\phi = 0$		
1.000	3.810	3.221
1.033	3.077	3.108
1.224	1.702	1.942
1.416	1.031	1.367
1.607	0.784	0.877
1.832	1.027	1.044
2.120	0.740	0.942
2.409	0.712	0.945

FORCE AND PAD

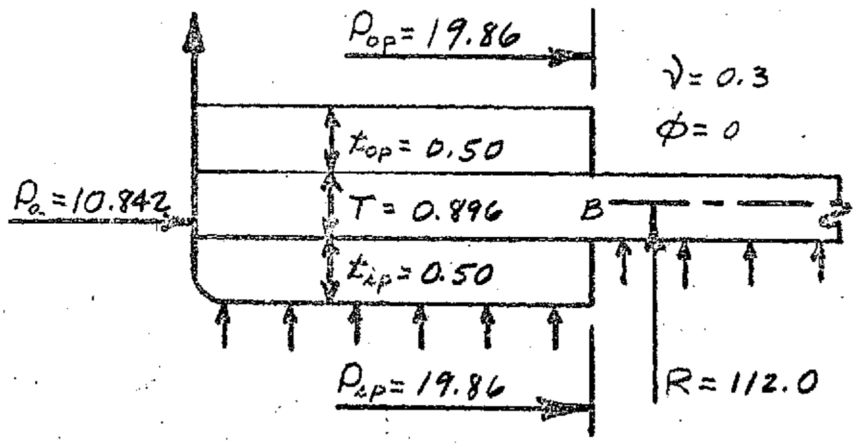

P/P_a	I/S SCF	O/S SCF
1.832 @ B	1.316	0.941
INNER PAD @ φ = 0		
1.000	3.364	2.704
1.033	2.899	2.544
1.224	1.816	1.660
1.416	1.300	1.228
1.607	1.071	0.846
1.832	0.945	0.410
2.120	0.853	0.571
—	—	—

FORCE AND PADS

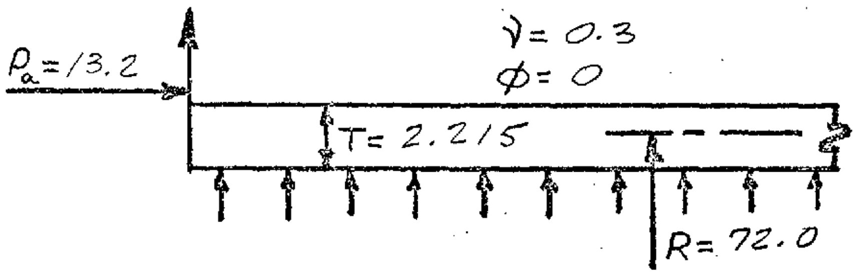

P/P_a	I/S SCF	O/S SCF
1.000	5.233	3.592
1.042	4.699	3.268
1.125	4.083	2.550
1.288	3.134	1.717
1.553	2.244	1.006
1.742	1.857	0.770
1.894	1.622	0.675
2.045	1.440	0.634

FORCE

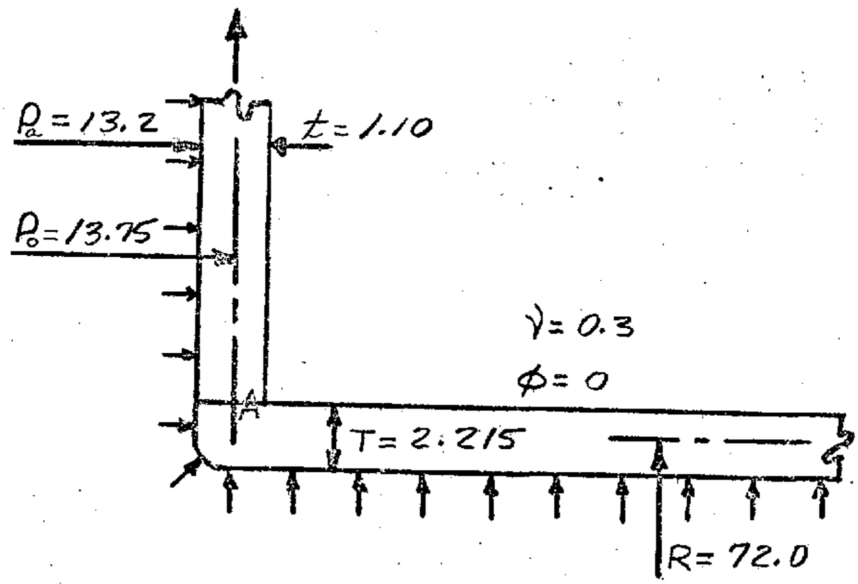

P/P_o	I/S SCF	O/S SCF
1.000 @ A	2.149	2.257
SHELL @ $\phi = 0$		
0.960	2.809	2.407
1.000	2.652	2.141
1.080	2.478	1.755
1.236	2.227	1.279
1.491	2.021	0.797
1.673	1.922	0.596
1.818	1.851	0.488
1.964	1.785	0.419

PIPE

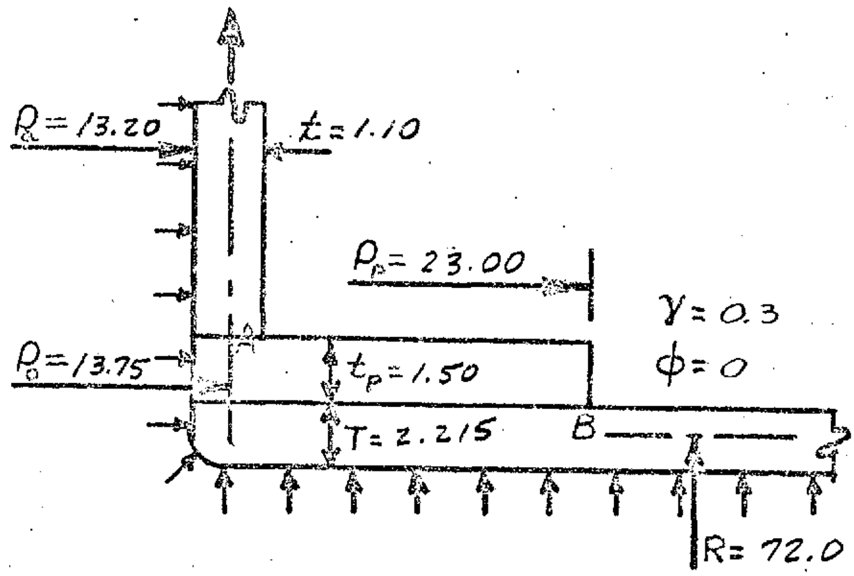

P/P_o	I/S SCF	O/S SCF
1.000 @ A	1.842	2.168
1.673 @ B	0.059	2.662
SHELL @ $\phi = 0$		
0.960	2.783	2.394
1.000	2.163	2.487
1.080	1.901	2.089
1.236	1.564	1.553
1.491	1.300	1.017
1.673	1.015	1.113
1.818	0.942	1.164
1.964	0.891	1.180

PIPE AND PAD

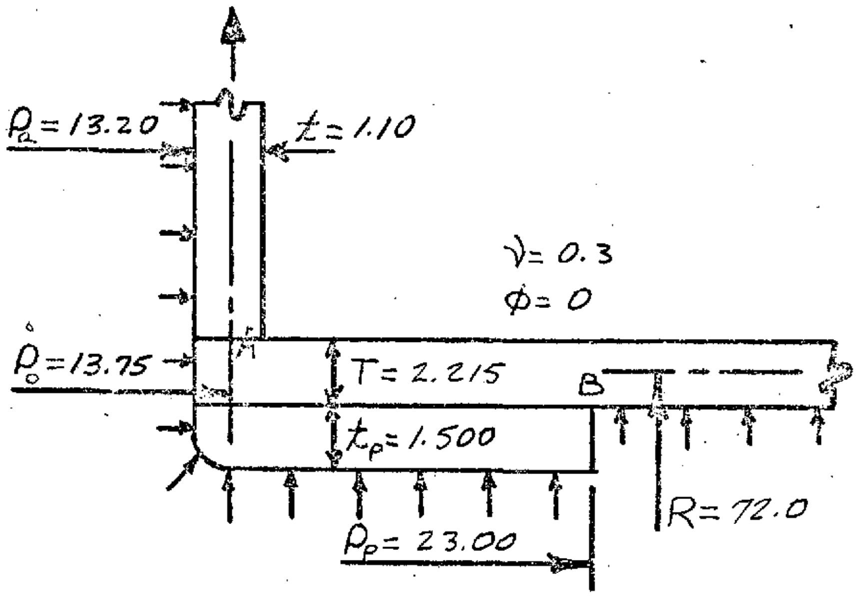

P/P_o	I/S SCF	O/S SCF
1.000 @ A	0.552	3.019
1.673 @ B	1.483	1.010
SHELL @ $\phi = 0$		
0.960	2.303	2.193
1.000	1.900	2.244
1.164	1.518	1.757
1.336	1.200	1.467
1.509	0.906	1.344
1.673	1.146	1.052
1.836	0.986	0.964
2.000	0.903	0.933

PIPE AND PAD

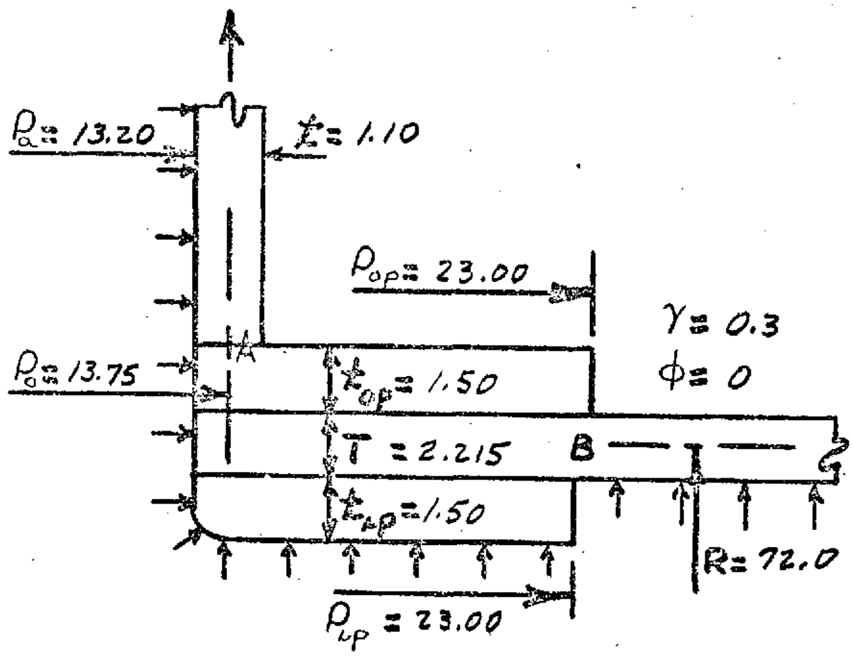

ρ/ρ_o	I/S SCF	O/S SCF
1.000 @ A	1.317	1.493
1.673 @ B	1.204	1.015
INNER PAD @ $\phi = 0$		
0.960	1.957	1.819
1.000	1.790	1.654
1.080	1.520	1.443
1.236	1.210	1.131
1.491	0.964	0.786
1.673	1.020	0.625
1.818	0.947	0.690
1.964	0.931	0.744

PIPE AND PADS

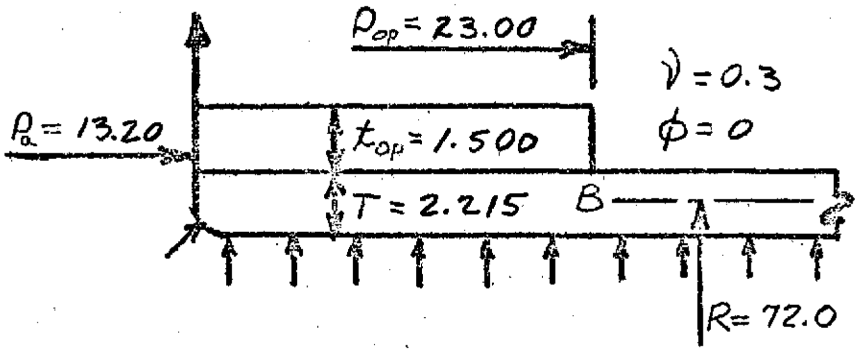

ρ/ρ_a	I/S SCF	O/S SCF
1.742 @ B	0.319	1.499
SHELL @ $\phi = 0$		
1.000	3.649	2.933
1.042	3.912	1.931
1.125	3.476	1.422
1.288	2.846	0.857
1.553	2.259	0.442
1.742	2.034	0.299
1.894	1.881	0.278
2.045	1.757	0.295

FORCE AND PAD